Supporting Information

Evans Enolates: Structures and Mechanisms Underlying the Aldol Addition of Oxazolidinone-Derived Boron Enolates

Zirong Zhang and David B. Collum*

Department of Chemistry and Chemical Biology
Baker Laboratory, Cornell University
Ithaca, New York 14853–1301

1. IR Spectra

2. MCV Study

3. Complexation

6. Aldol Addition Kinetics

7. ^{11}B NMR Spectra

8. ^{19}F NMR Spectra

9. 1-d_1 Synthesis

10. Computation Study

11. References

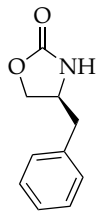

1S

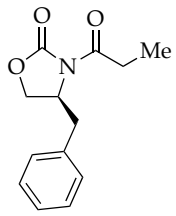

1

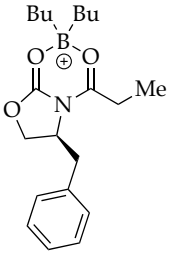

3

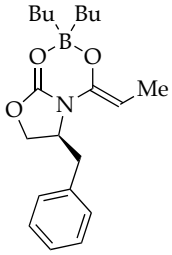

4

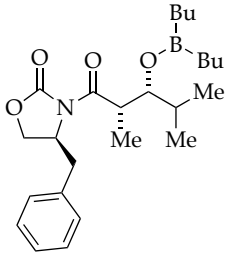

6

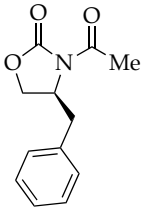

7

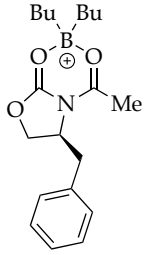

7a

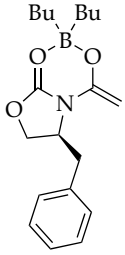

7b

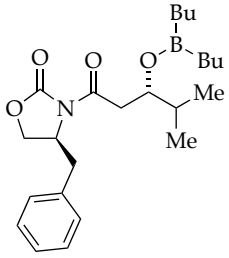

7c

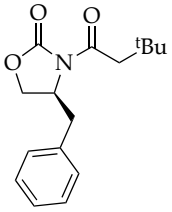

8

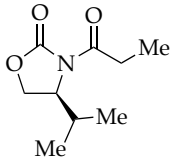

9

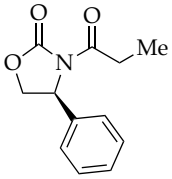

10

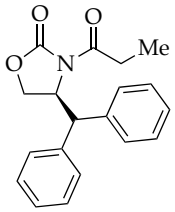

11

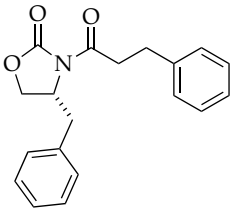

12

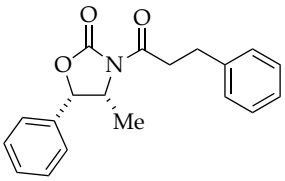

13

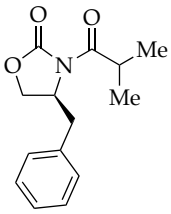

20

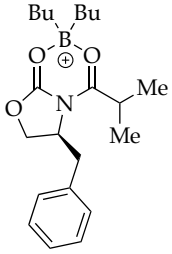

21

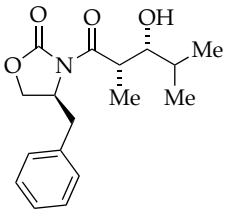

2

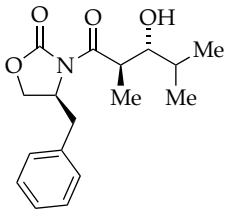

23

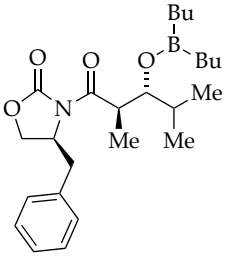

24

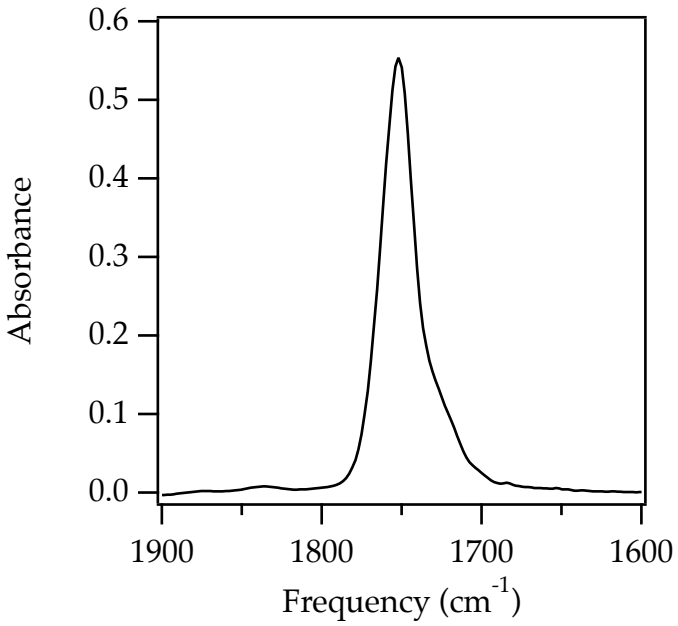

Figure S1. IR spectrum of 0.30 M **1S** in $CHCl_3$ recorded at –60 °C.

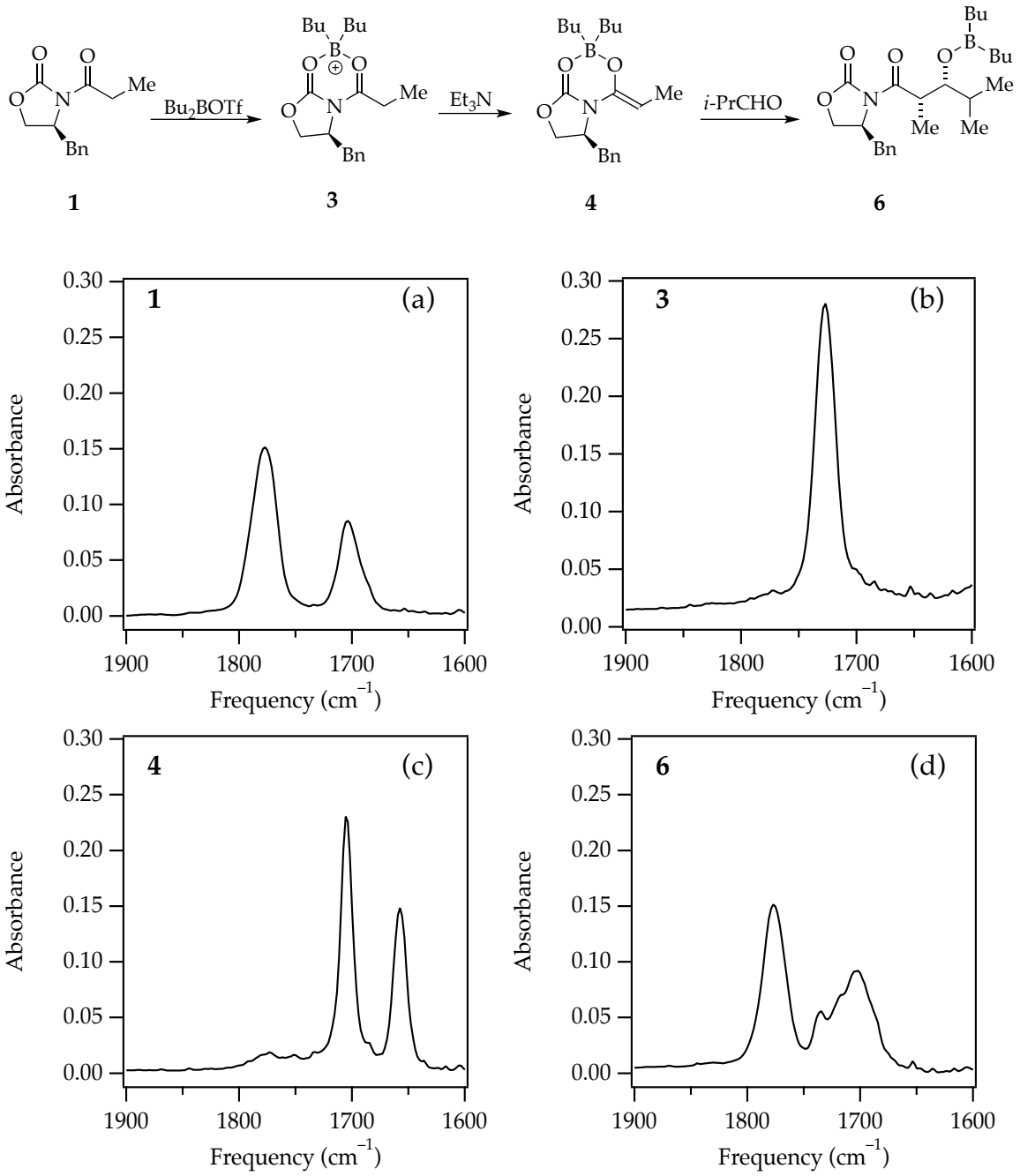

Figure S2. IR spectra in $CHCl_3$ recorded at –60 °C: (a) 0.10 M **1**; (b) 0.10 M **1** and 0.11 M Bu_2BOTf; (c) 0.10 M **1**, 0.11 M Bu_2BOTf, and 0.12 M Et_3N; (d) 0.10 M **1**, 0.11 M Bu_2BOTf, 0.12 M Et_3N, and 0.13 M isobutyraldehyde.

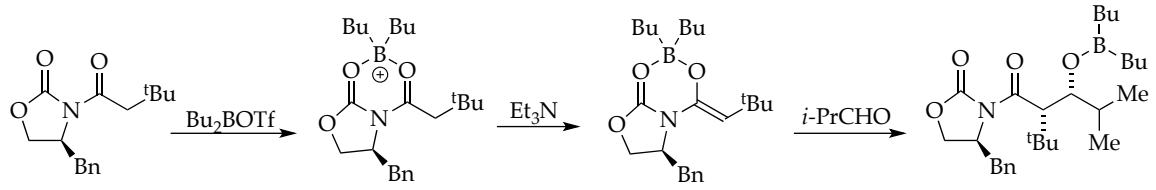
Bu2BOTf
Et3N
i-PrCHO
tBu
Bn
Me
Bu

8 **8a** **8b** **8c**

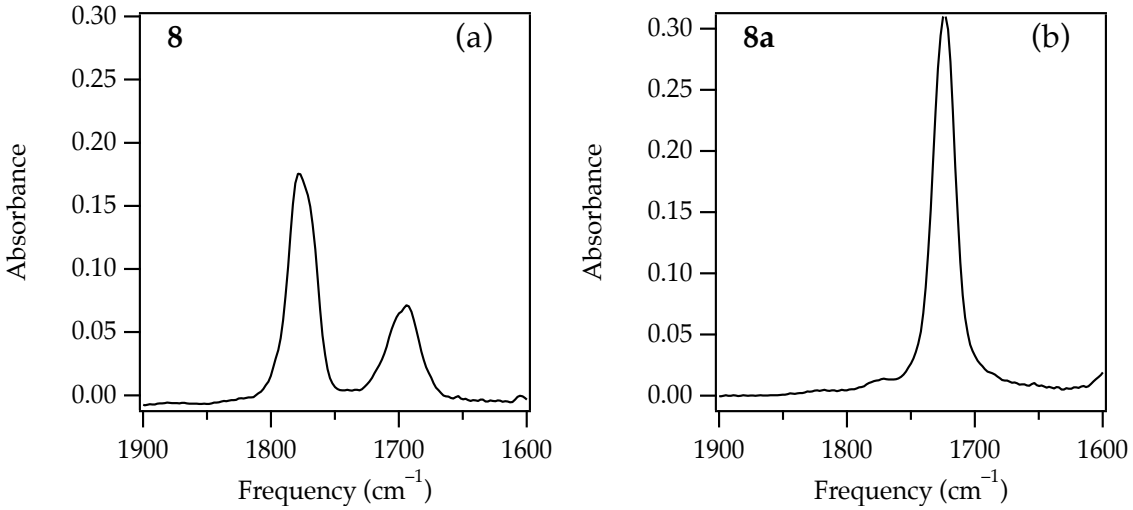
8
(a)
8a
(b)
Absorbance
Frequency (cm−1)
0.00
0.05
0.10
0.15
0.20
0.25
0.30
1900
1800
1700
1600

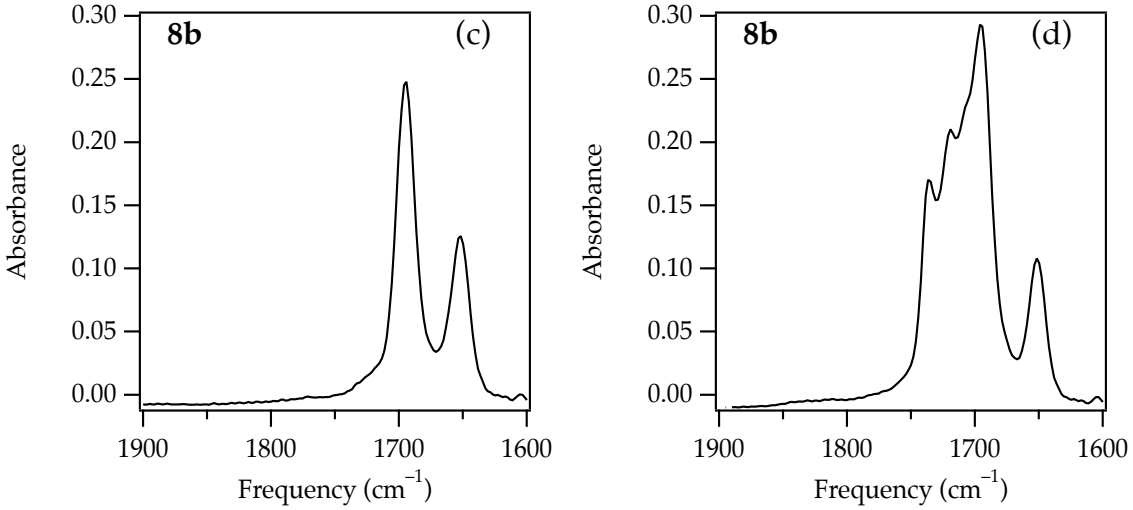
8b
(c)
8b
(d)
Absorbance
Frequency (cm−1)
0.00
0.05
0.10
0.15
0.20
0.25
0.30
1900
1800
1700
1600

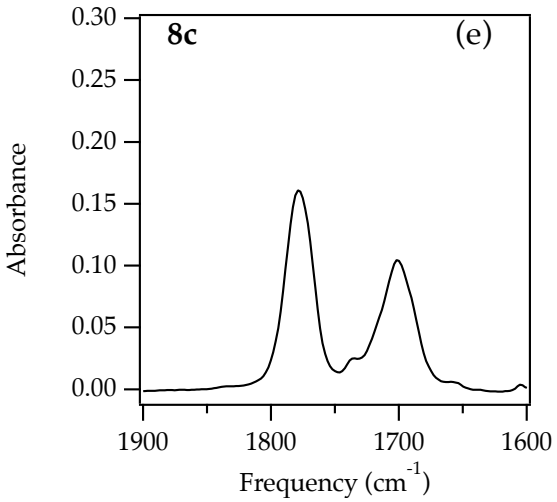

Figure S3. IR spectra in $CHCl_3$ recorded at –60 °C: (a) 0.10 M **8**; (b) 0.10 M **8** and 0.11 M Bu_2BOTf; (c) 0.10 M **8**, 0.11 M Bu_2BOTf, and 0.12 M Et_3N; (d) 0.10 M **8**, 0.11 M Bu_2BOTf, 0.12 M Et_3N, and 0.13 M isobutyraldehyde; (e) 0.10 M **8**, 0.11 M Bu_2BOTf, 0.12 M Et_3N, and 0.13 M isobutyraldehyde recorded at 0 °C.

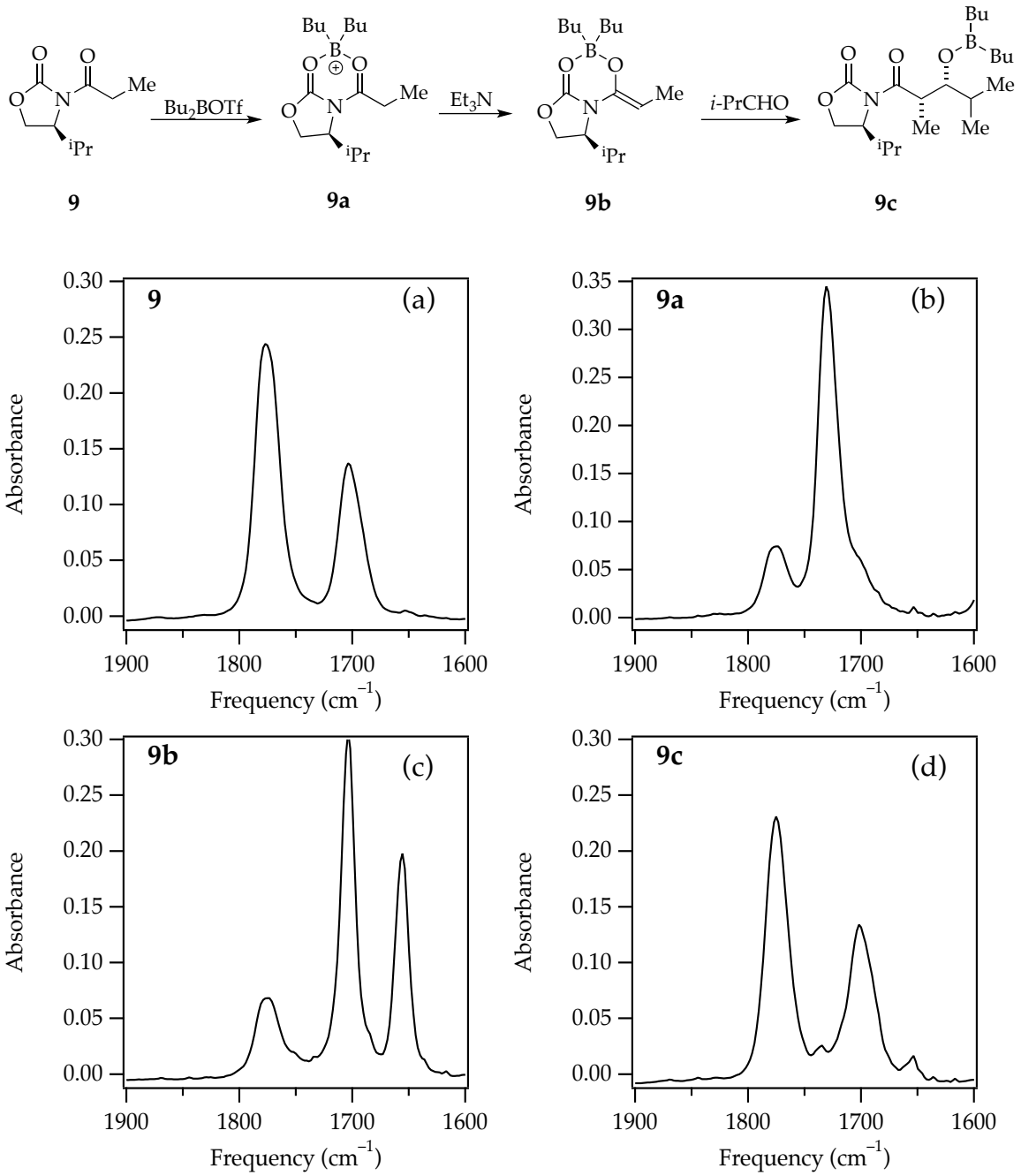

Figure S4. IR spectra in $CHCl_3$ recorded at –60 °C: (a) 0.10 M **9**; (b) 0.10 M **9** and 0.11 M Bu_2BOTf; (c) 0.10 M **9**, 0.11 M Bu_2BOTf, and 0.12 M Et_3N; (d) 0.10 M **9**, 0.11 M Bu_2BOTf, 0.12 M Et_3N, and 0.13 M isobutyraldehyde.

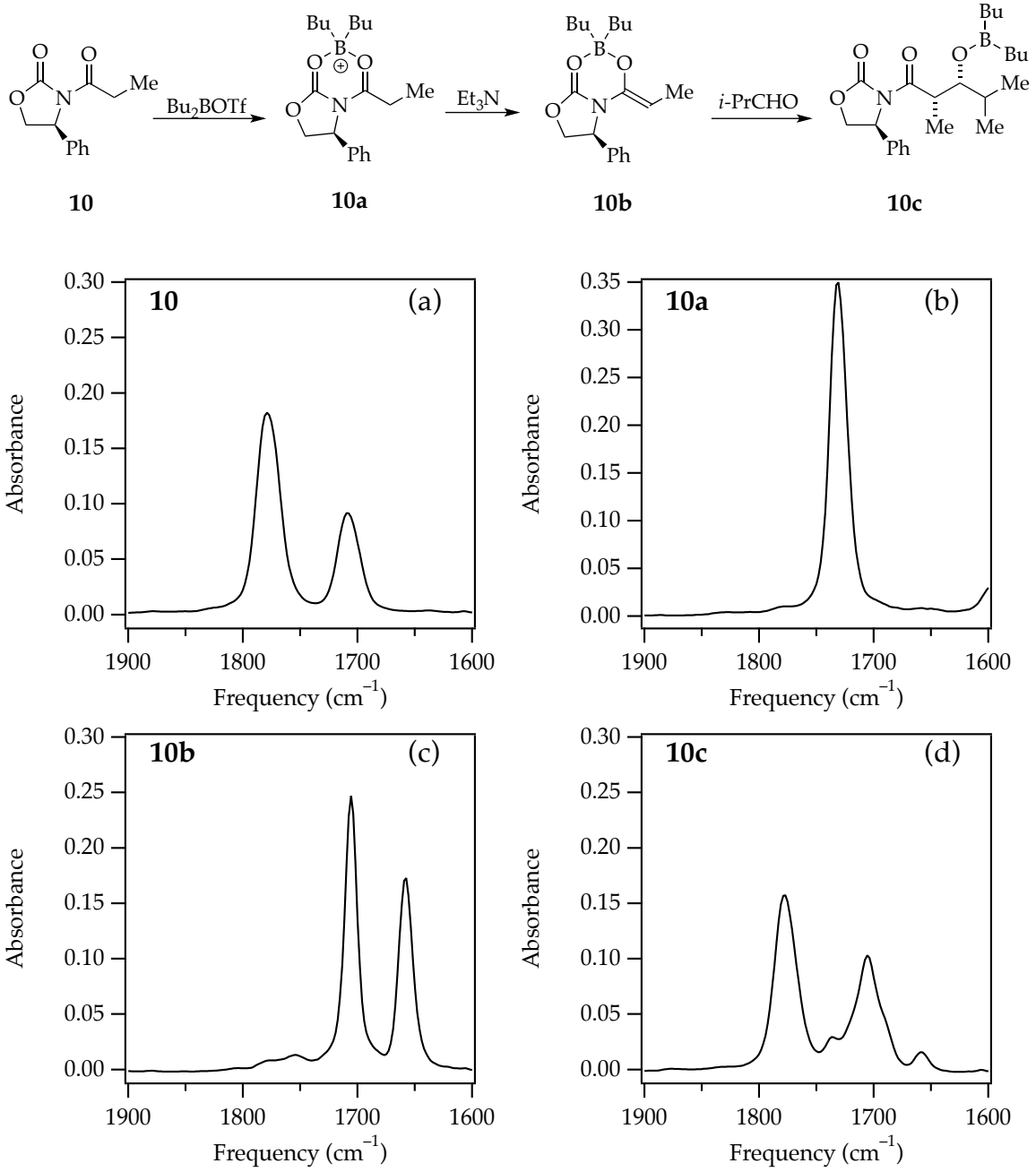

Figure S5. IR spectra in $CHCl_3$ recorded at –60 °C: (a) 0.10 M **10**; (b) 0.10 M **10** and 0.11 M Bu_2BOTf; (c) 0.10 M **10**, 0.11 M Bu_2BOTf, and 0.12 M Et_3N; (d) 0.10 M **10**, 0.11 M Bu_2BOTf, 0.12 M Et_3N, and 0.13 M isobutyraldehyde.

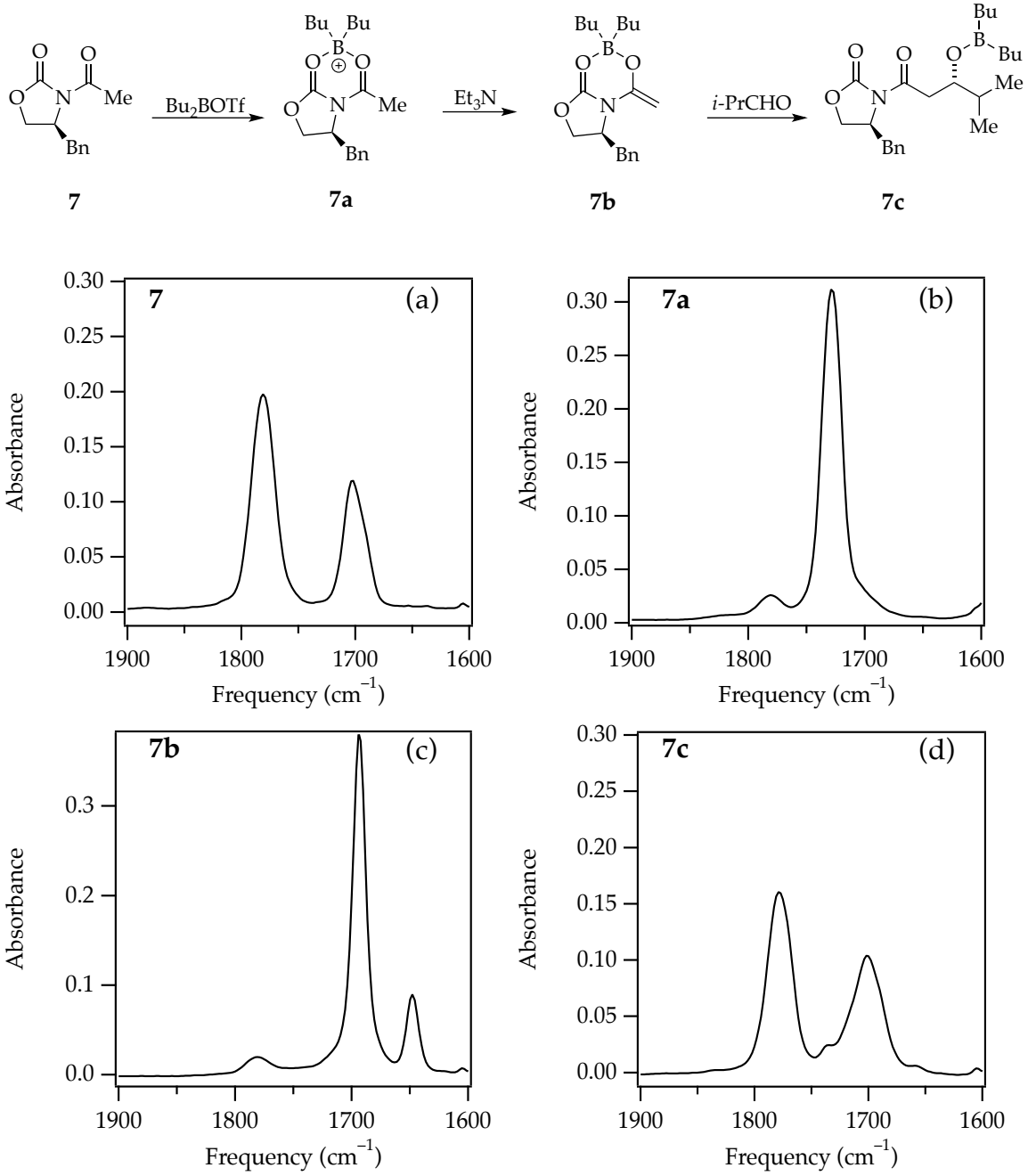

Figure S6. IR spectra in $CHCl_3$ recorded at –60 °C: (a) 0.10 M **7**; (b) 0.10 M **7** and 0.11 M Bu_2BOTf; (c) 0.10 M **7**, 0.11 M Bu_2BOTf, and 0.12 M Et_3N; (d) 0.10 M **7**, 0.11 M Bu_2BOTf, 0.12 M Et_3N, and 0.13 M isobutyraldehyde.

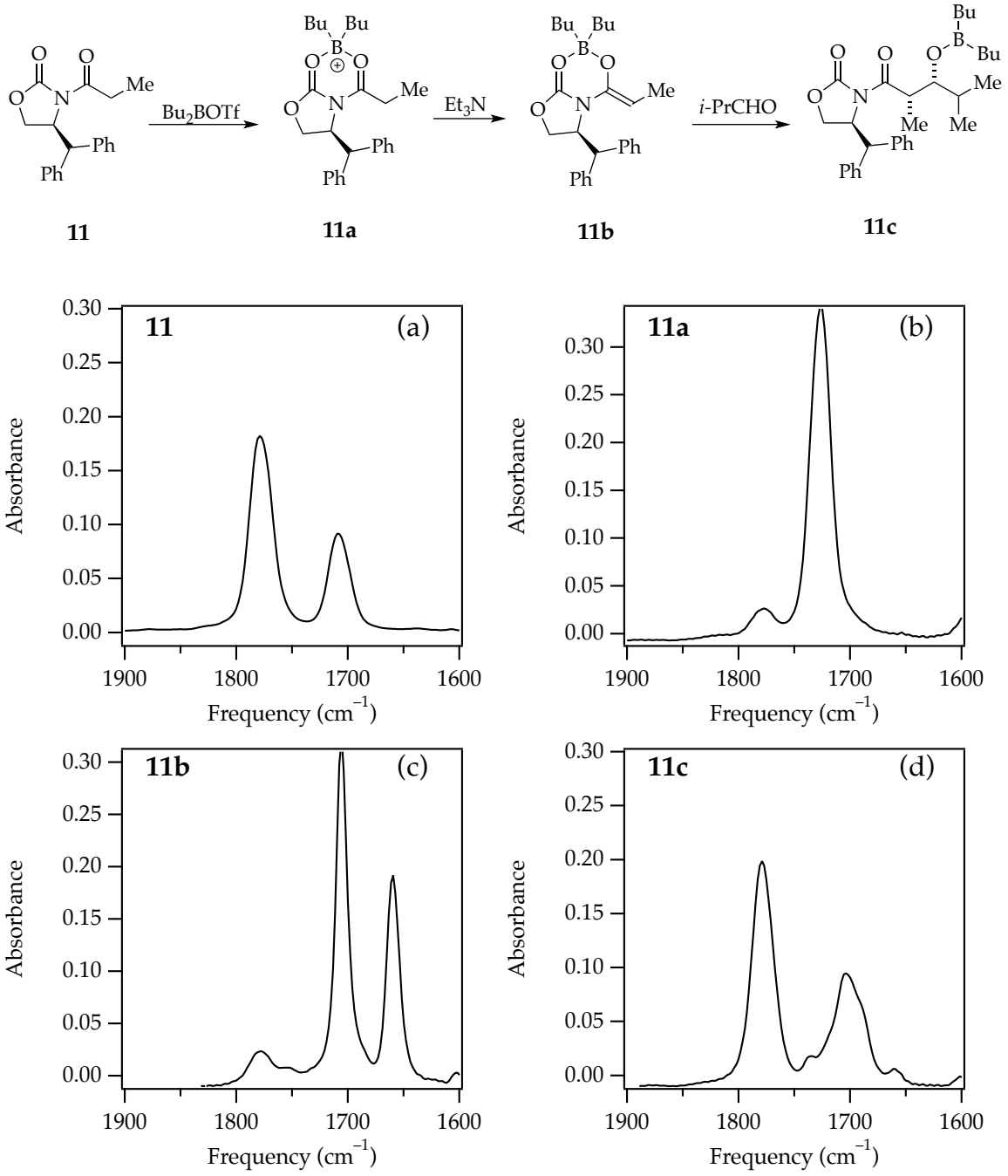

Figure S7. IR spectra in $CHCl_3$ recorded at –60 °C: (a) 0.10 M **11**; (b) 0.10 M **11** and 0.11 M Bu_2BOTf; (c) 0.10 M **11**, 0.11 M Bu_2BOTf, and 0.12 M Et_3N; (d) 0.10 M **11**, 0.11 M Bu_2BOTf, 0.12 M Et_3N, and 0.13 M isobutyraldehyde.

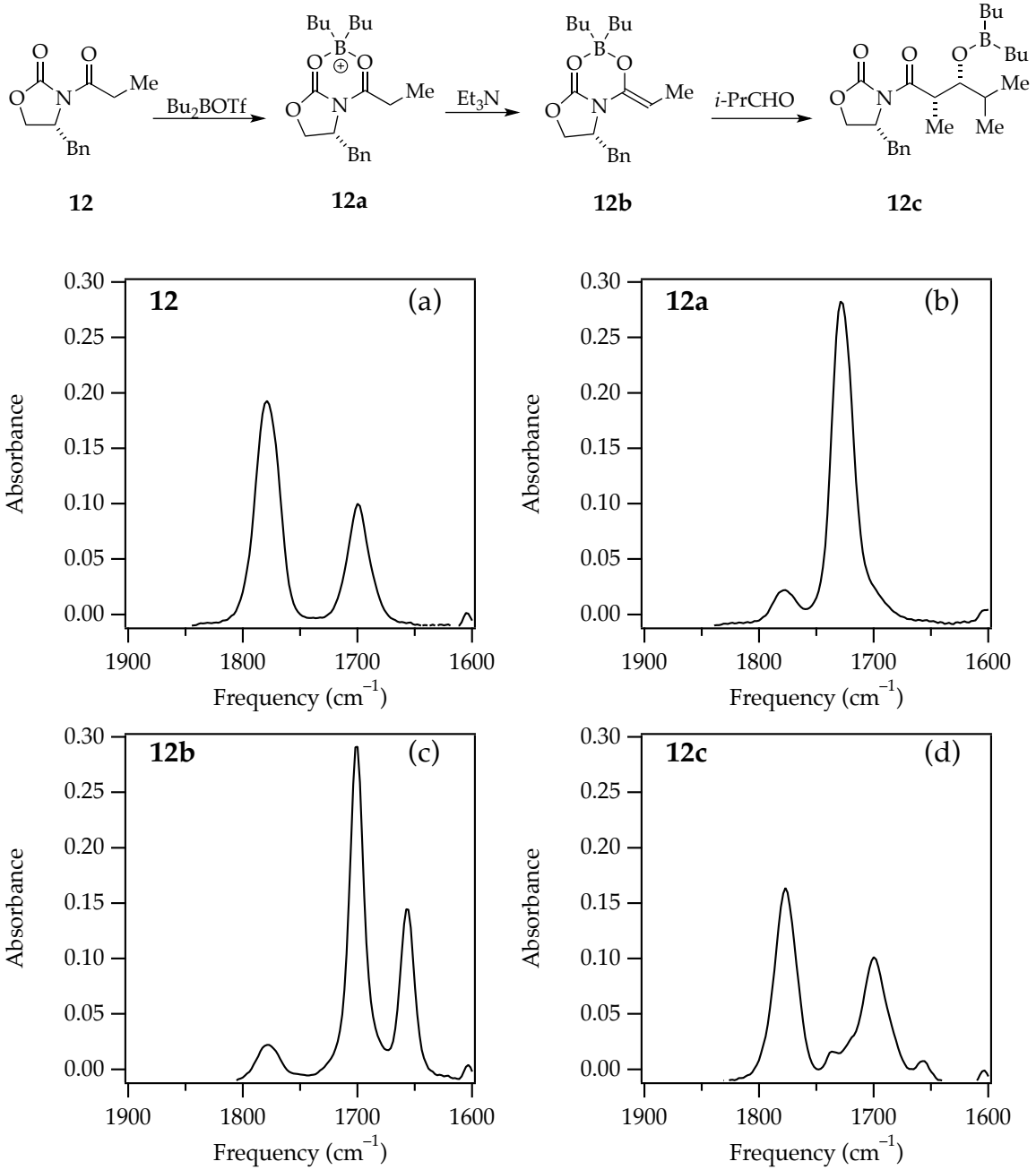

Figure S8. IR spectra in $CHCl_3$ recorded at –60 °C: (a) 0.10 M **12**; (b) 0.10 M **12** and 0.11 M Bu_2BOTf; (c) 0.10 M **12**, 0.11 M Bu_2BOTf, and 0.12 M Et_3N; (d) 0.10 M **12**, 0.11 M Bu_2BOTf, 0.12 M Et_3N, and 0.13 M isobutyraldehyde.

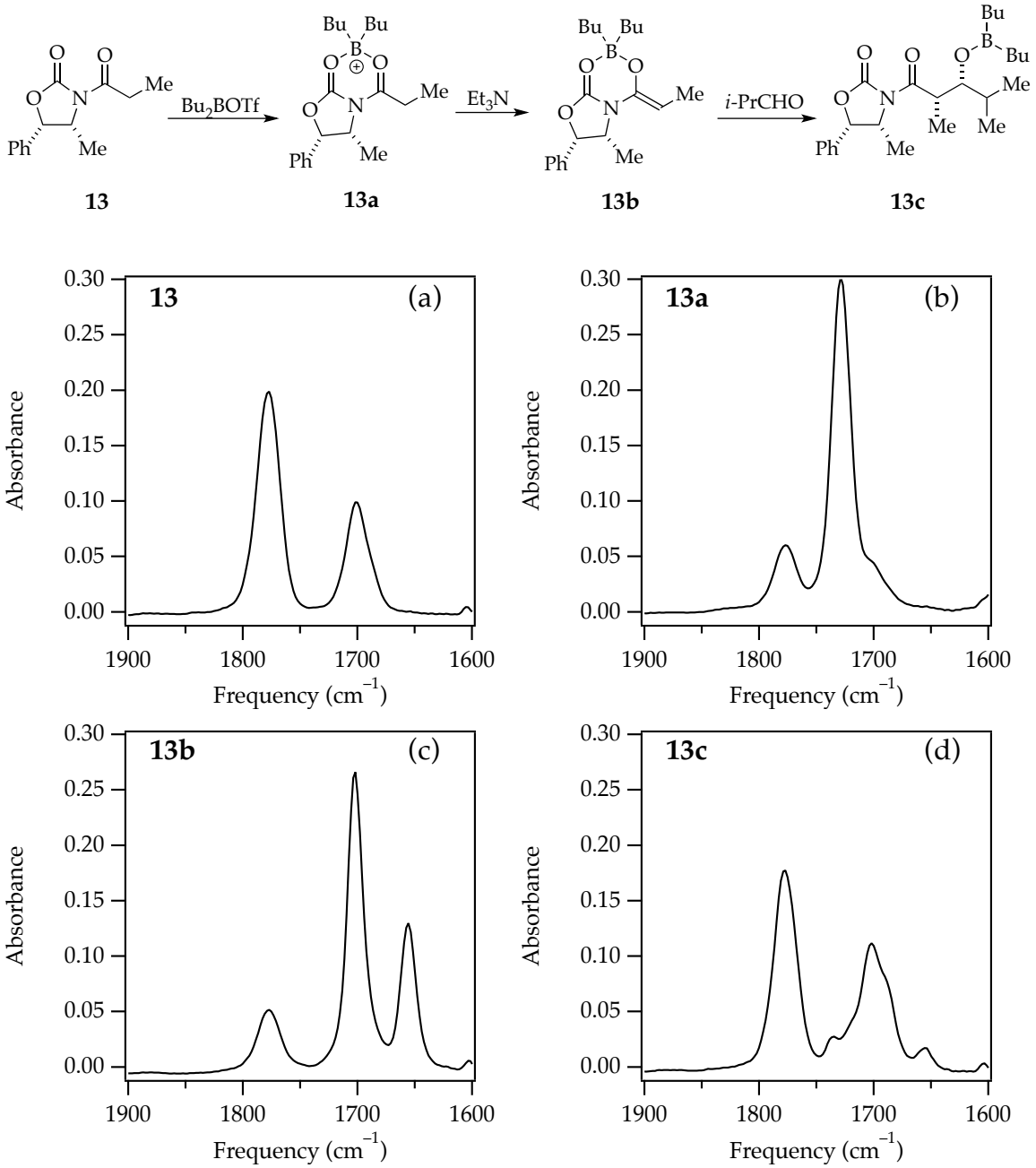

Figure S9. IR spectra in $CHCl_3$ recorded at –60 °C: (a) 0.10 M **13**; (b) 0.10 M **13** and 0.11 M Bu_2BOTf; (c) 0.10 M **13**, 0.11 M Bu_2BOTf, and 0.12 M Et_3N; (d) 0.10 M **13**, 0.11 M Bu_2BOTf, 0.12 M Et_3N, and 0.13 M isobutyraldehyde.

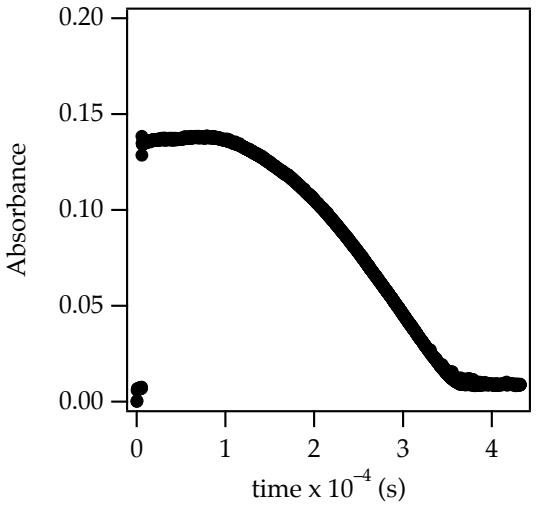

Figure S10. IR spectra of 0.10 M **1**, 0.11 M Bu_2BOTf, and 0.12 M Et_3N in $CHCl_3$ at rt, following decomposition of **4**.

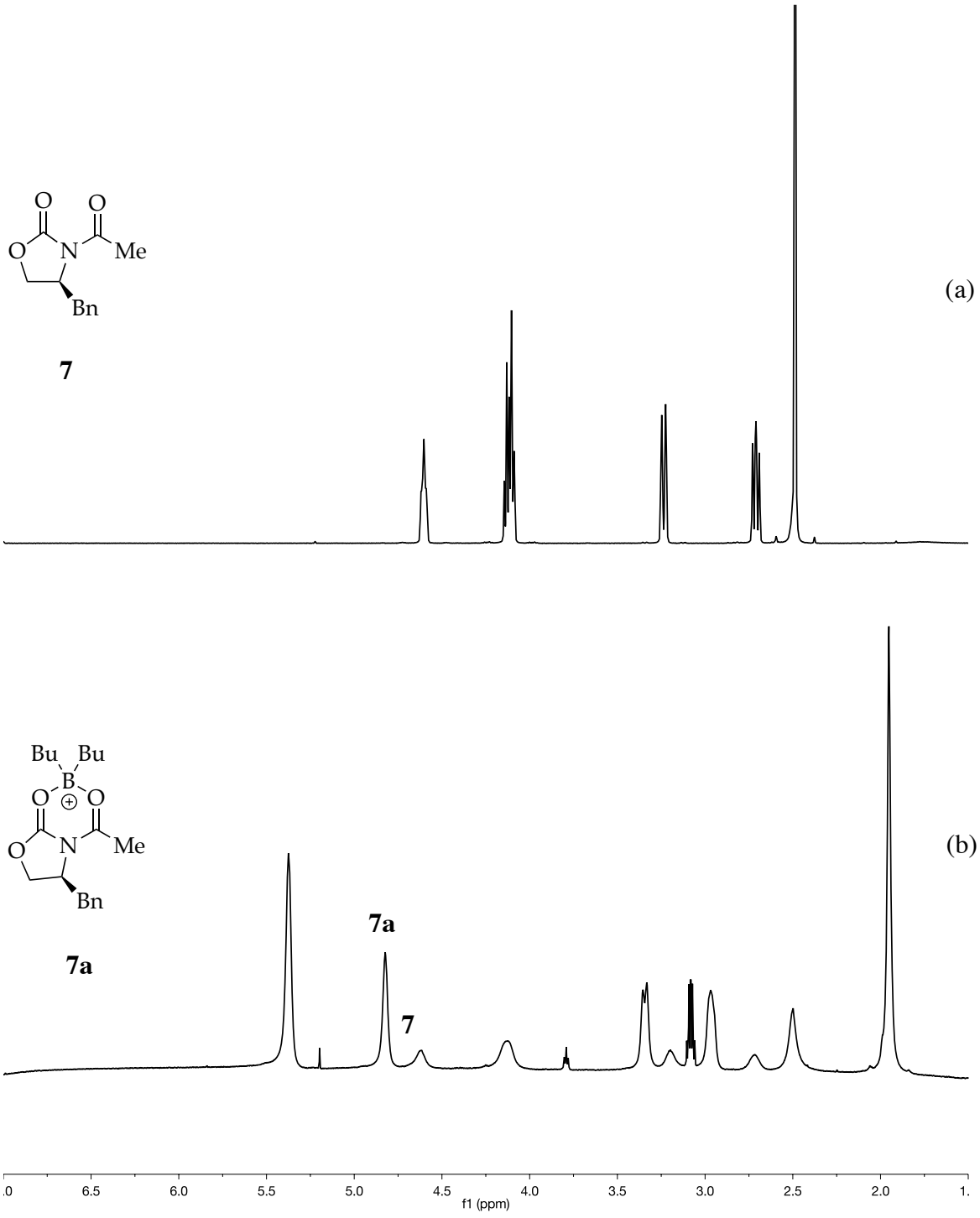

Figure S11. ^{1}H NMR spectra in $CDCl_3$ at rt: (a) 0.10 M **7**; (b) 0.10 M **7** and 0.25 M Bu_2BOTf.

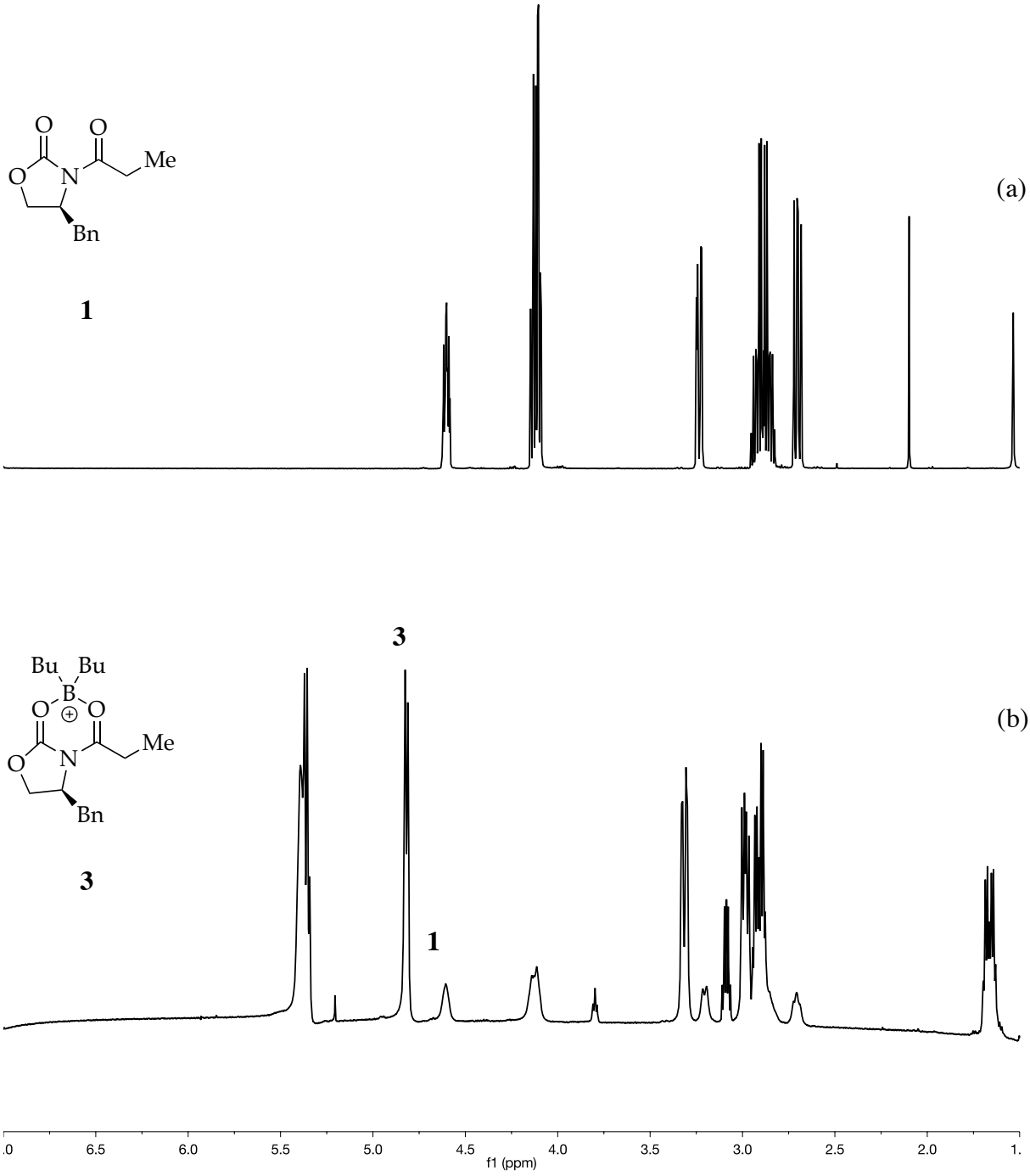

Figure S12. ^{1}H NMR spectra in $CDCl_3$ at rt: (a) 0.10 M **1**; (b) 0.10 M **1** and 0.25 M Bu_2BOTf.

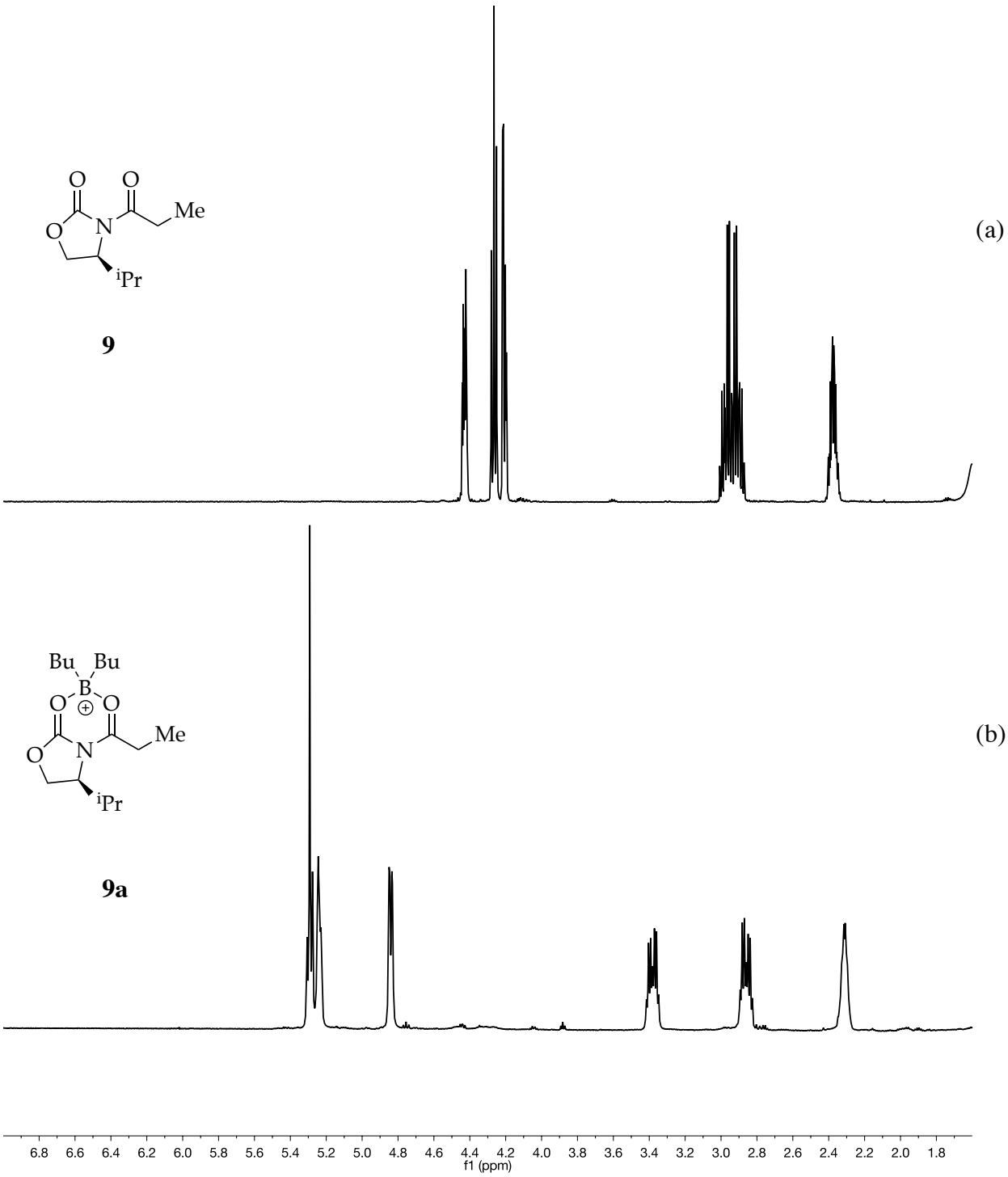

Figure S13. ^{1}H NMR spectra in $CDCl_3$ at rt: (a) 0.10 M **9**; (b) 0.10 M **9** and 0.25 M Bu_2BOTf.

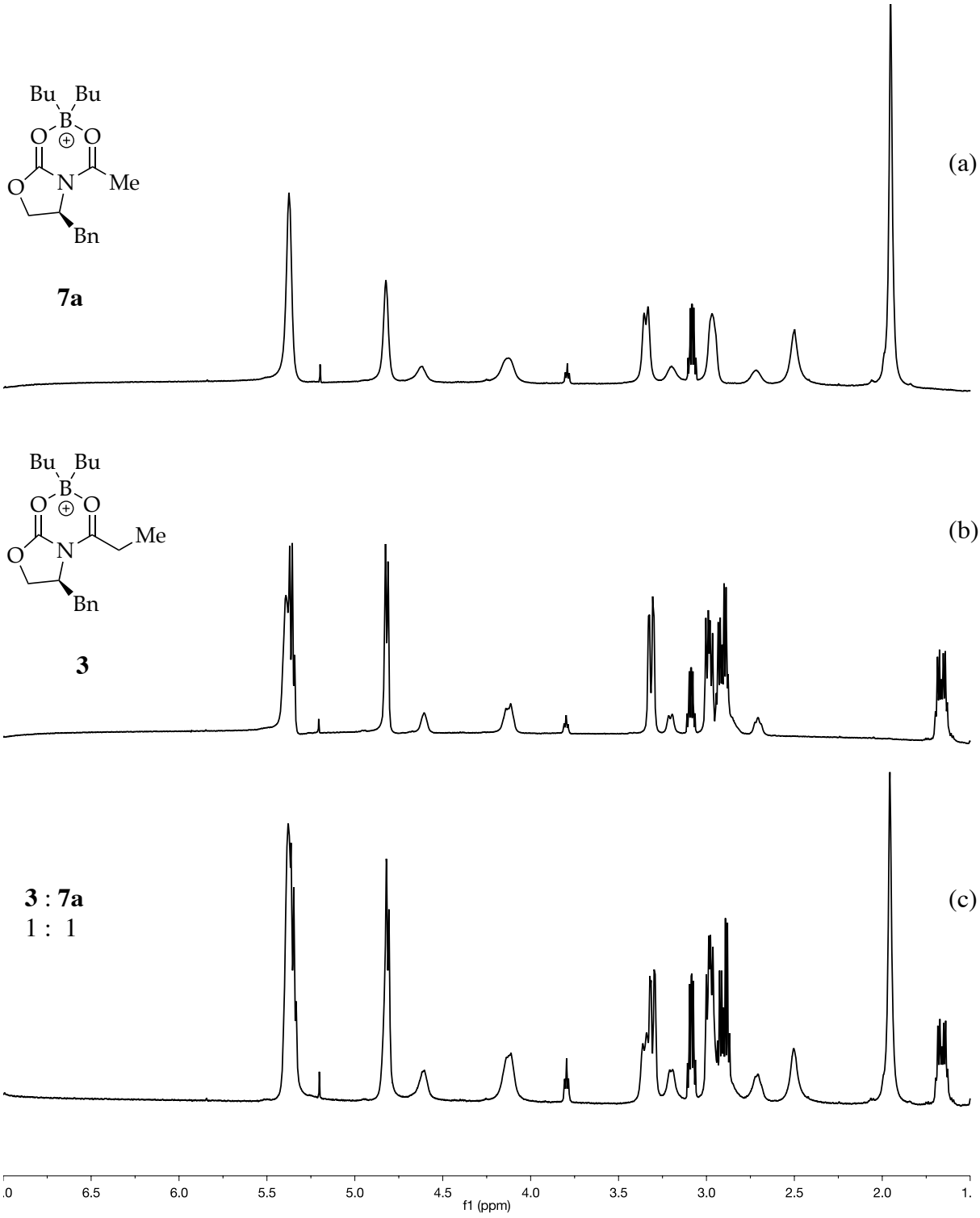

Figure S14. ^{1}H NMR spectra in $CDCl_3$ at rt: (a) 0.10 M **7** and 0.25 M Bu_2BOTf; (b) 0.10 M **1** and 0.25 M Bu_2BOTf; (c) 0.050 M **7**, 0.050 M **1**, and 0.25 M Bu_2BOTf.

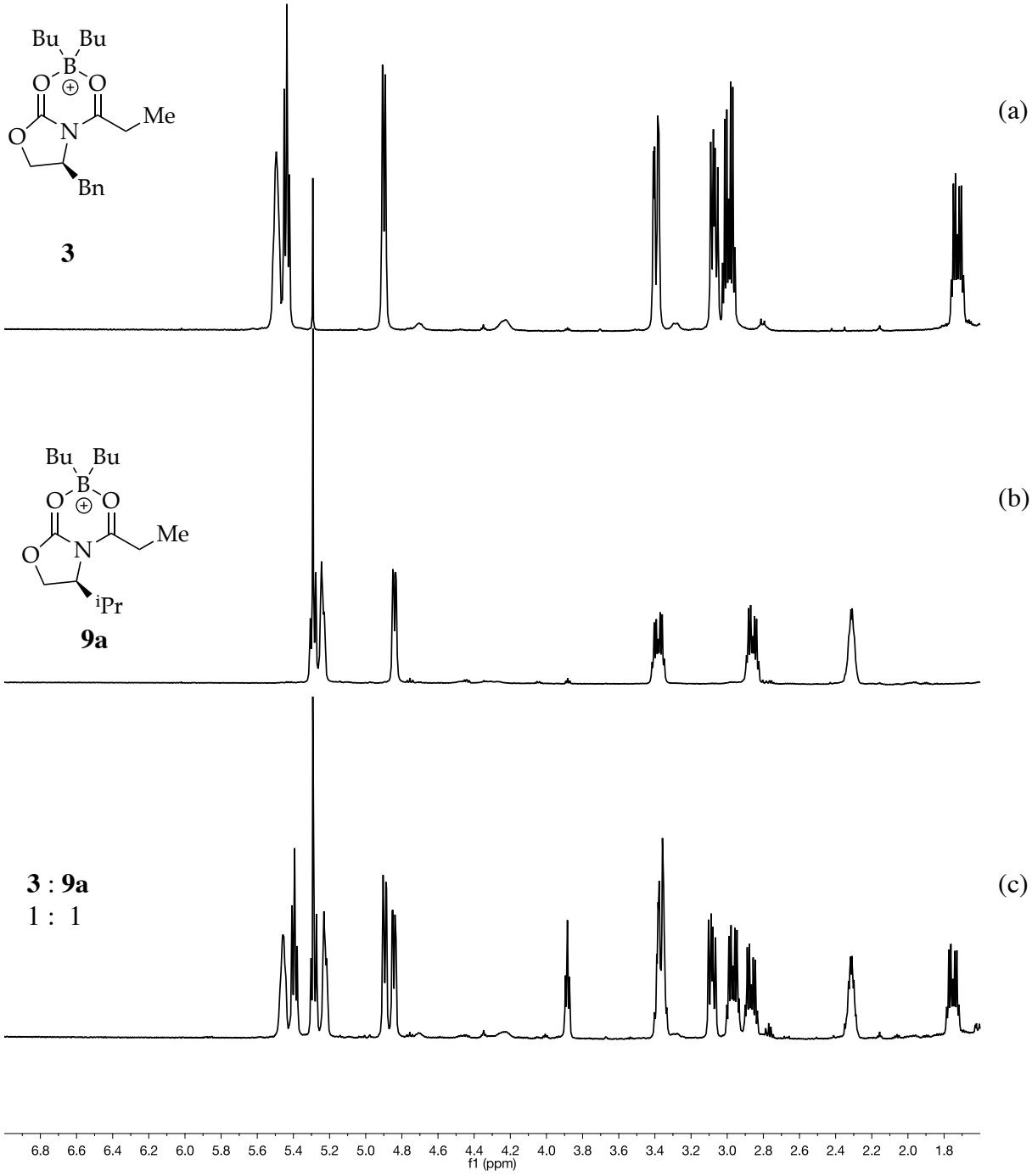

Figure S15. ^{1}H NMR spectra in $CDCl_3$ at rt: (a) 0.10 M **1** and 0.25 M Bu_2BOTf; (b) 0.10 M **9** and 0.25 M Bu_2BOTf; (c) 0.050 M **1**, 0.050 M **9**, and 0.25 M Bu_2BOTf.

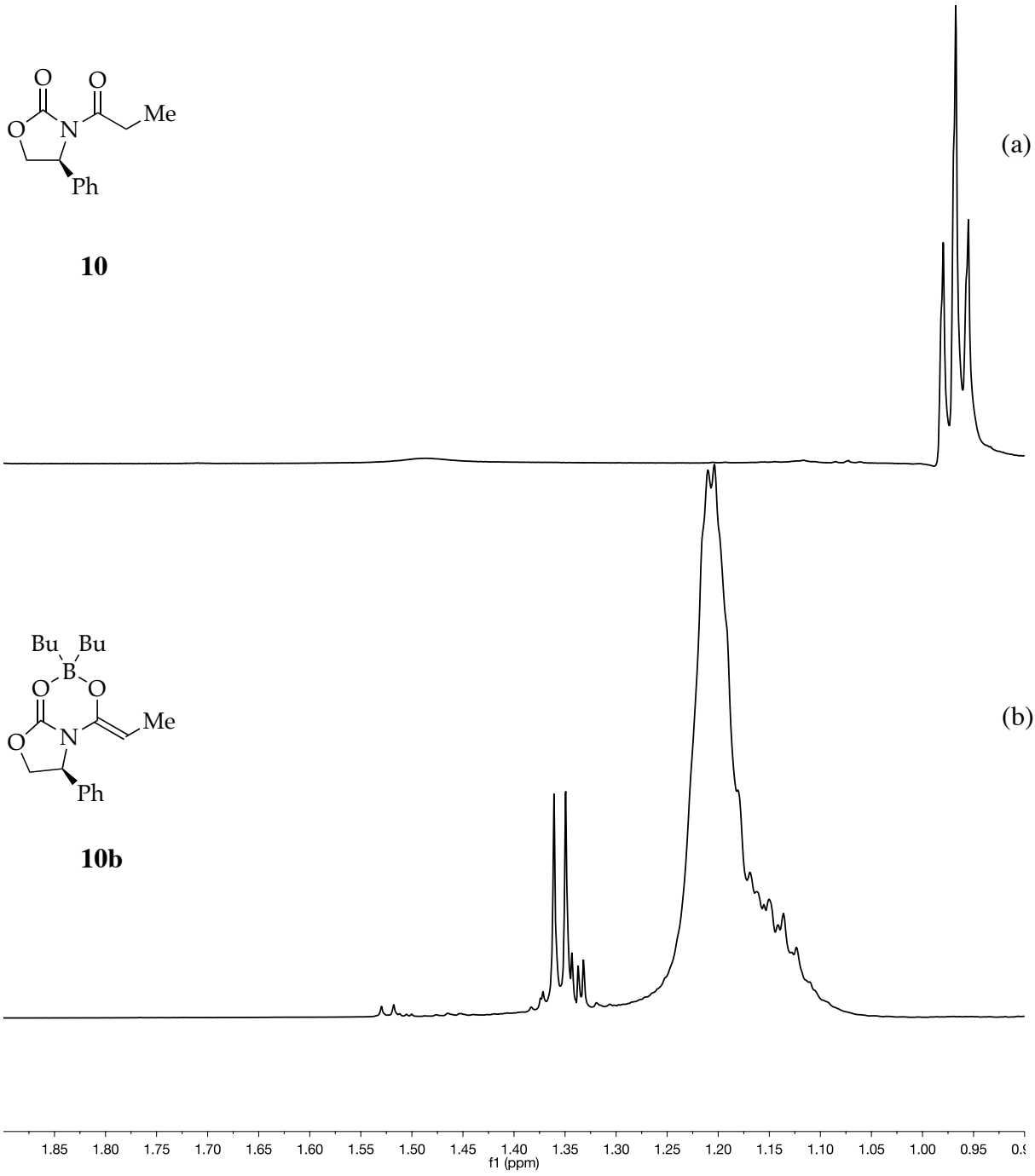

Figure S16. ^{1}H NMR spectra in $CDCl_3$ at rt: (a) 0.10 M **10**; (b) 0.10 M **10**, 0.11 M Bu_2BOTf, and 0.12 M Et_3N.

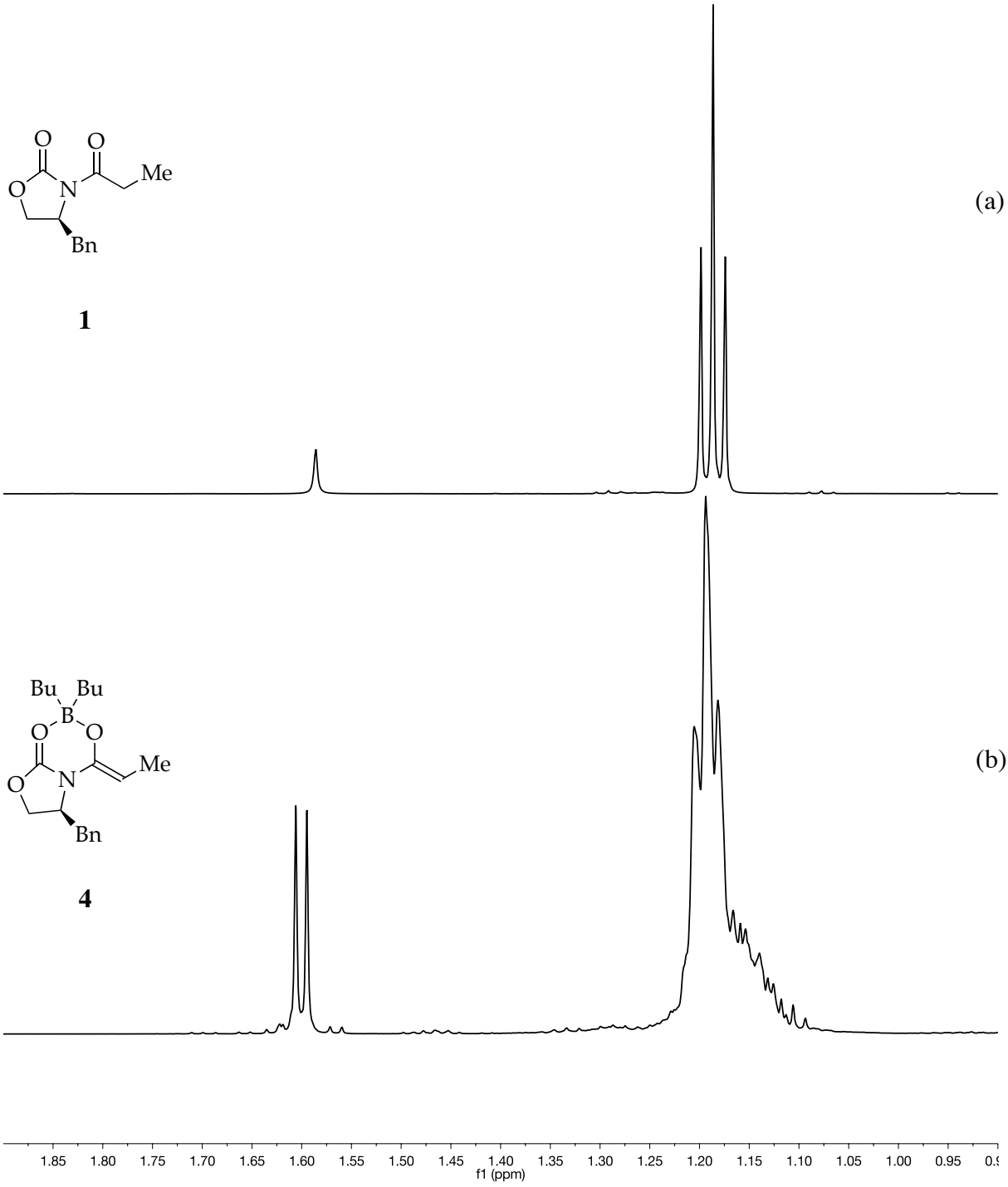

Figure S17. ^{1}H NMR spectra in $CDCl_3$ at rt: (a) 0.10 M **1**; (b) 0.10 M **1**, 0.11 M Bu_2BOTf, and 0.12 M Et_3N.

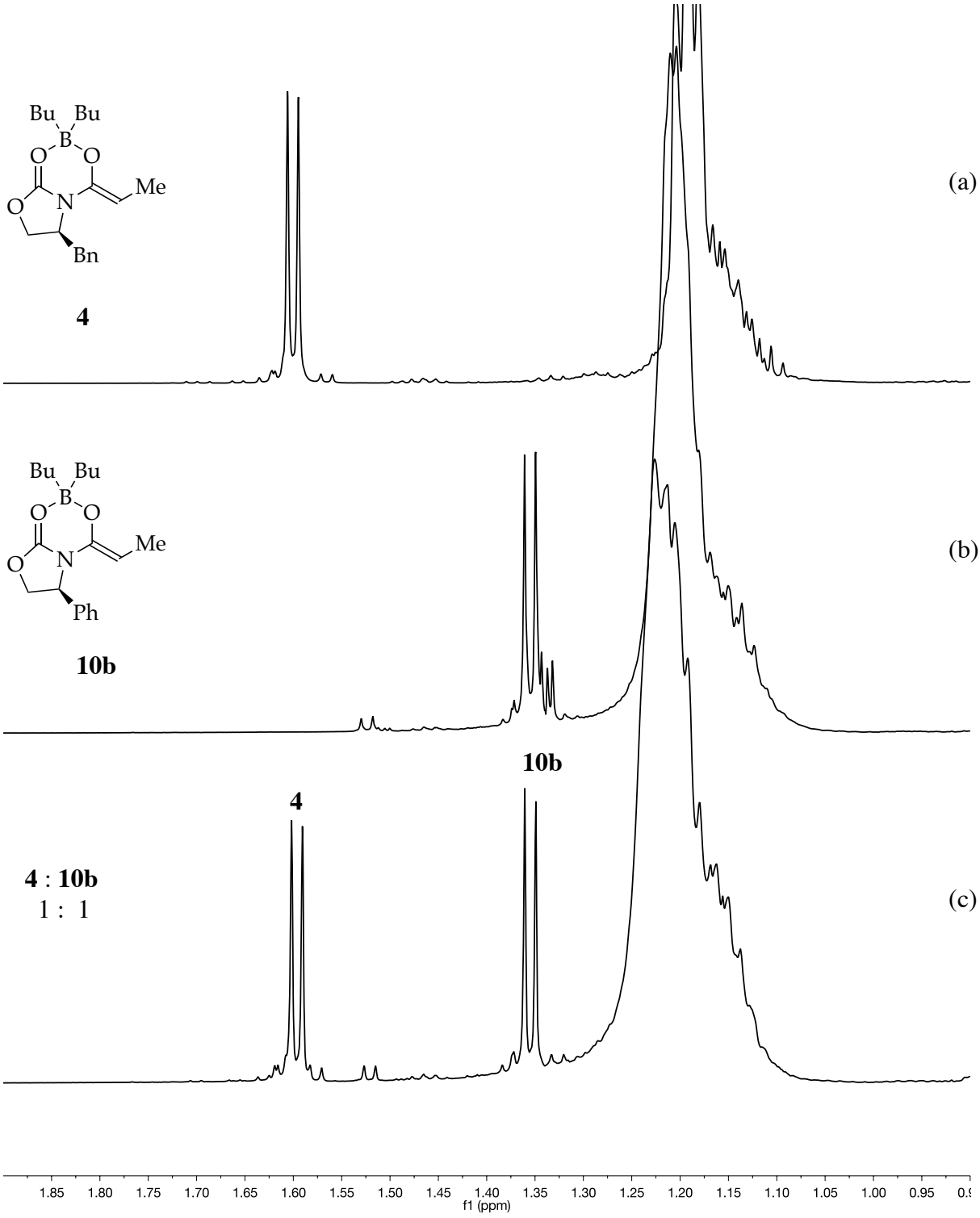

Figure S18. ^{1}H NMR spectra in $CDCl_3$ at rt: (a) 0.10 M **1**, 0.11 M Bu_2BOTf, and 0.12 M Et_3N; (b) 0.10 M **10**, 0.11 M Bu_2BOTf, and 0.12 M Et_3N; (c) 0.050 M **1**, 0.050 M **10**, 0.11 M Bu_2BOTf, and 0.12 M Et_3N.

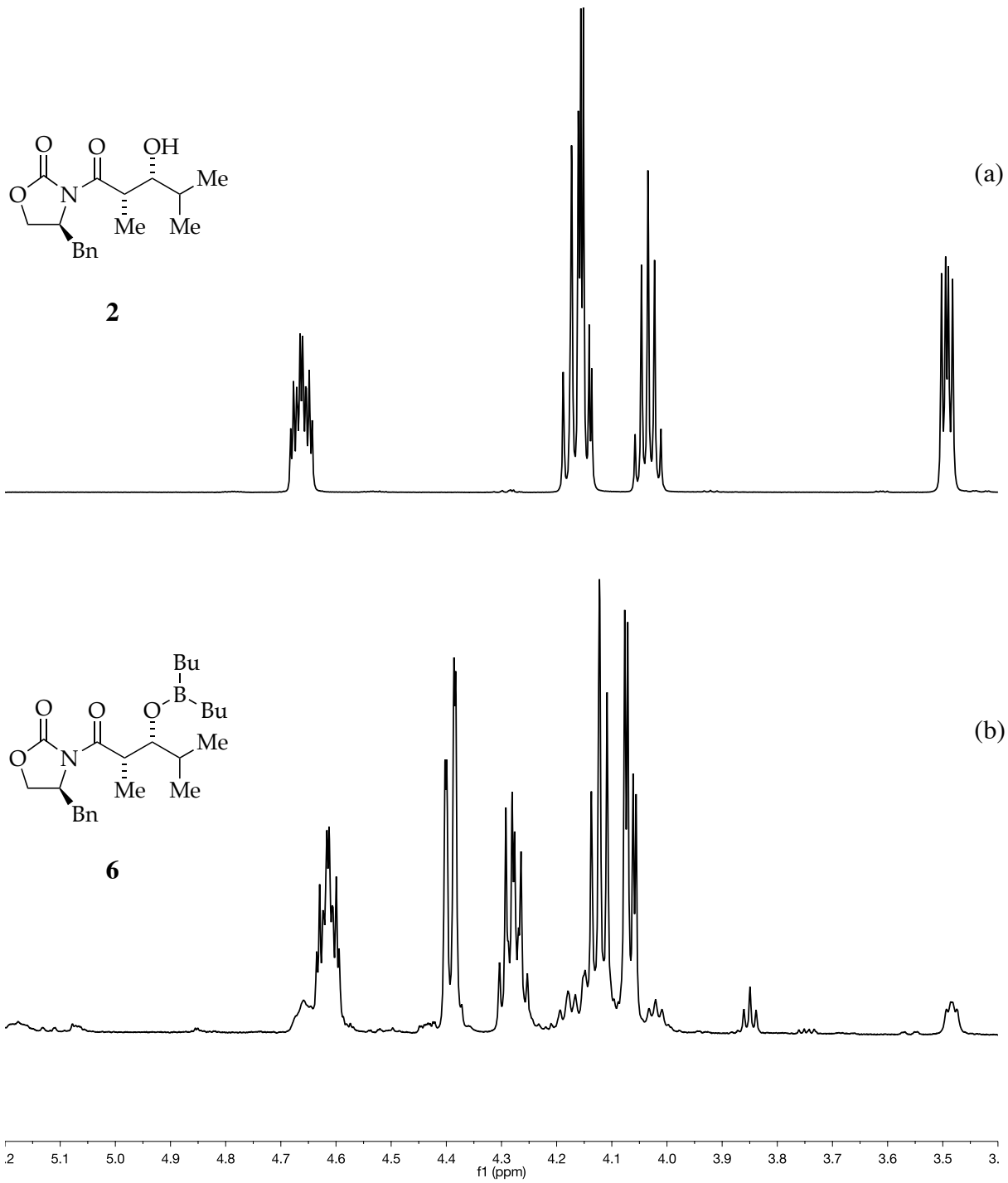

Figure S19. ^{1}H NMR spectra in $CDCl_3$ at rt: (a) 0.10 M **2**; (b) 0.10 M **2**, 0.11 M Bu_2BOTf, and 0.12 M Et_3N.

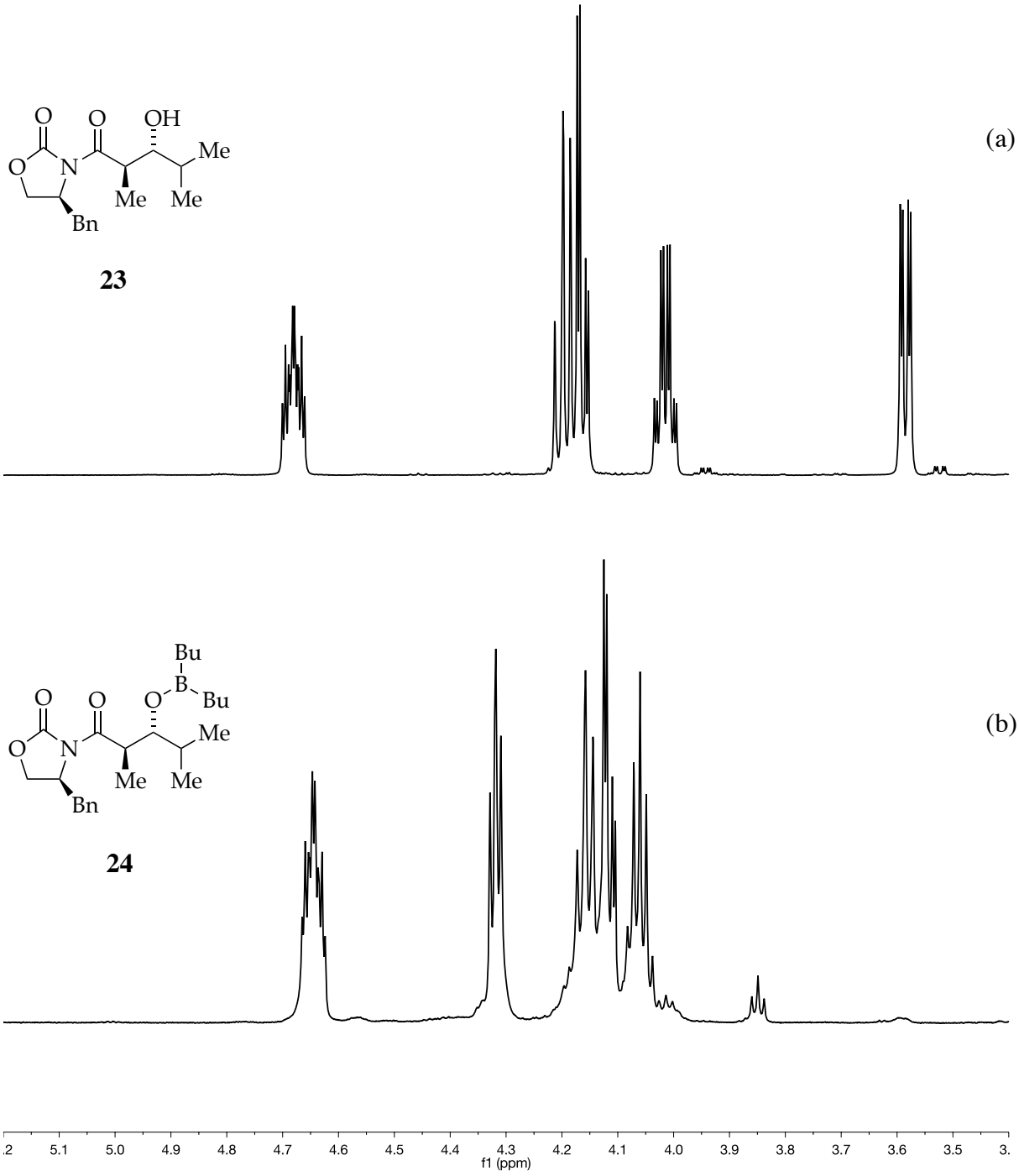

Figure S20. ^{1}H NMR spectra in $CDCl_3$ at rt: (a) 0.10 M **23**; (b) 0.10 M **23**, 0.11 M Bu_2BOTf, and 0.12 M Et_3N.

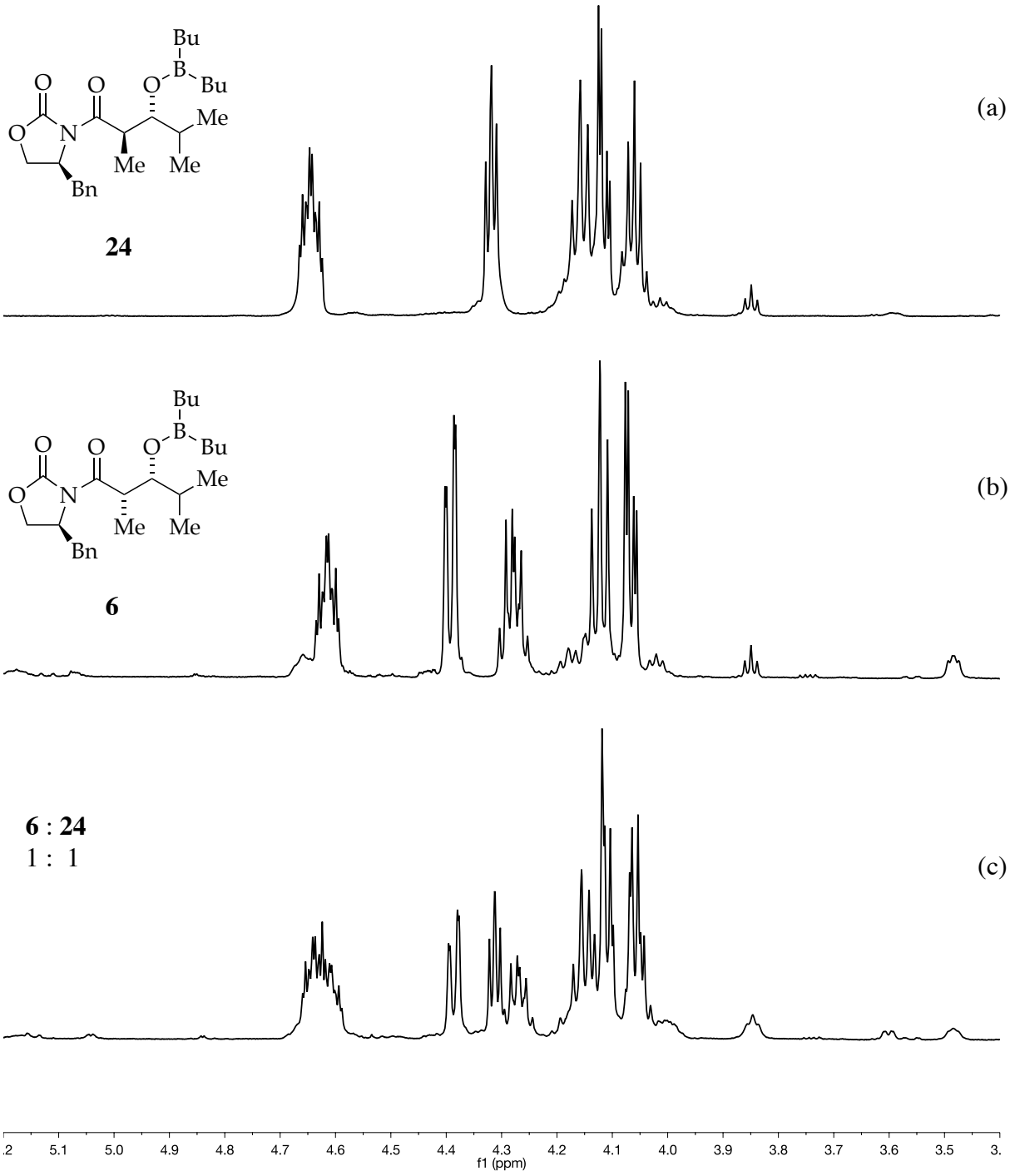

Figure S21. ^{1}H NMR spectra in $CDCl_3$ at rt: (a) 0.10 M **2**, 0.11 M Bu_2BOTf, and 0.12 M Et_3N; (b) 0.10 M **23**, 0.11 M Bu_2BOTf, and 0.12 M Et_3N; (c) 0.050 M **2**, 0.050 M **23**, 0.11 M Bu_2BOTf, and 0.12 M Et_3N.

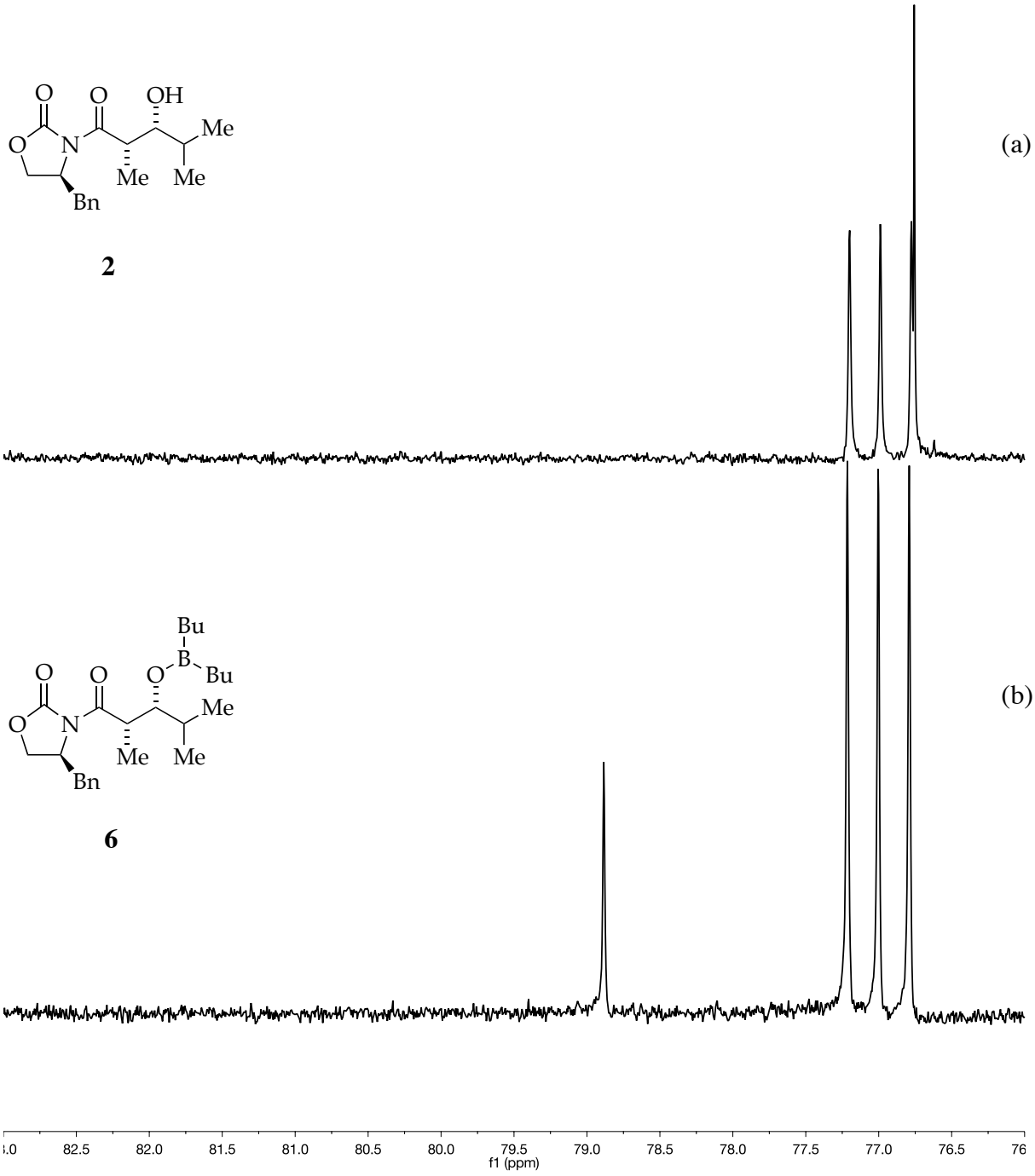

Figure S22. ^{13}C NMR spectra in $CDCl_3$ at rt: (a) 0.10 M **2**; (b) 0.10 M **2**, 0.11 M Bu_2BOTf, and 0.12 M Et_3N.

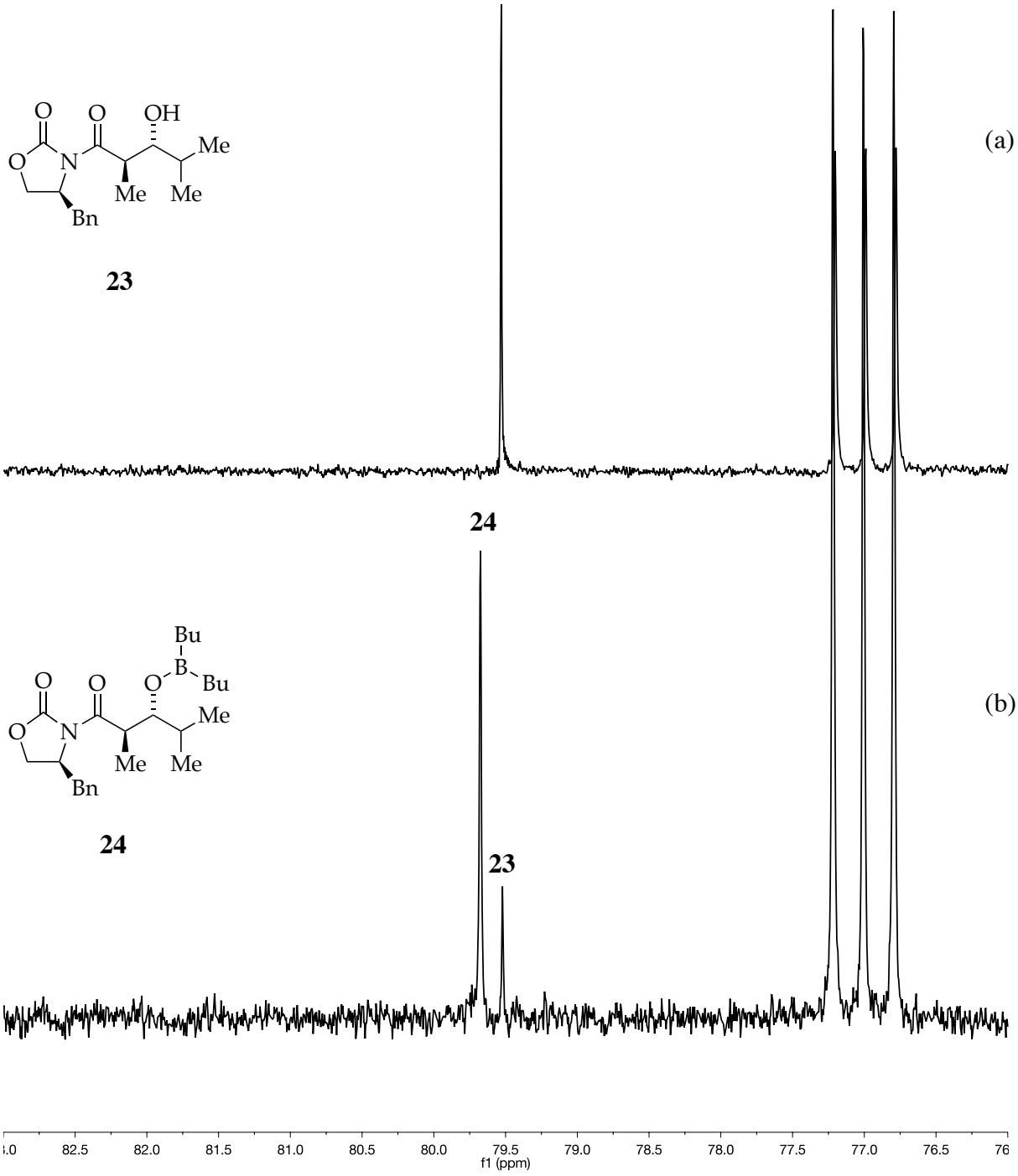

Figure S23. ^{13}C NMR spectra in $CDCl_3$ at rt: (a) 0.10 M **23**; (b) 0.10 M **23**, 0.11 M Bu_2BOTf, and 0.12 M Et_3N.

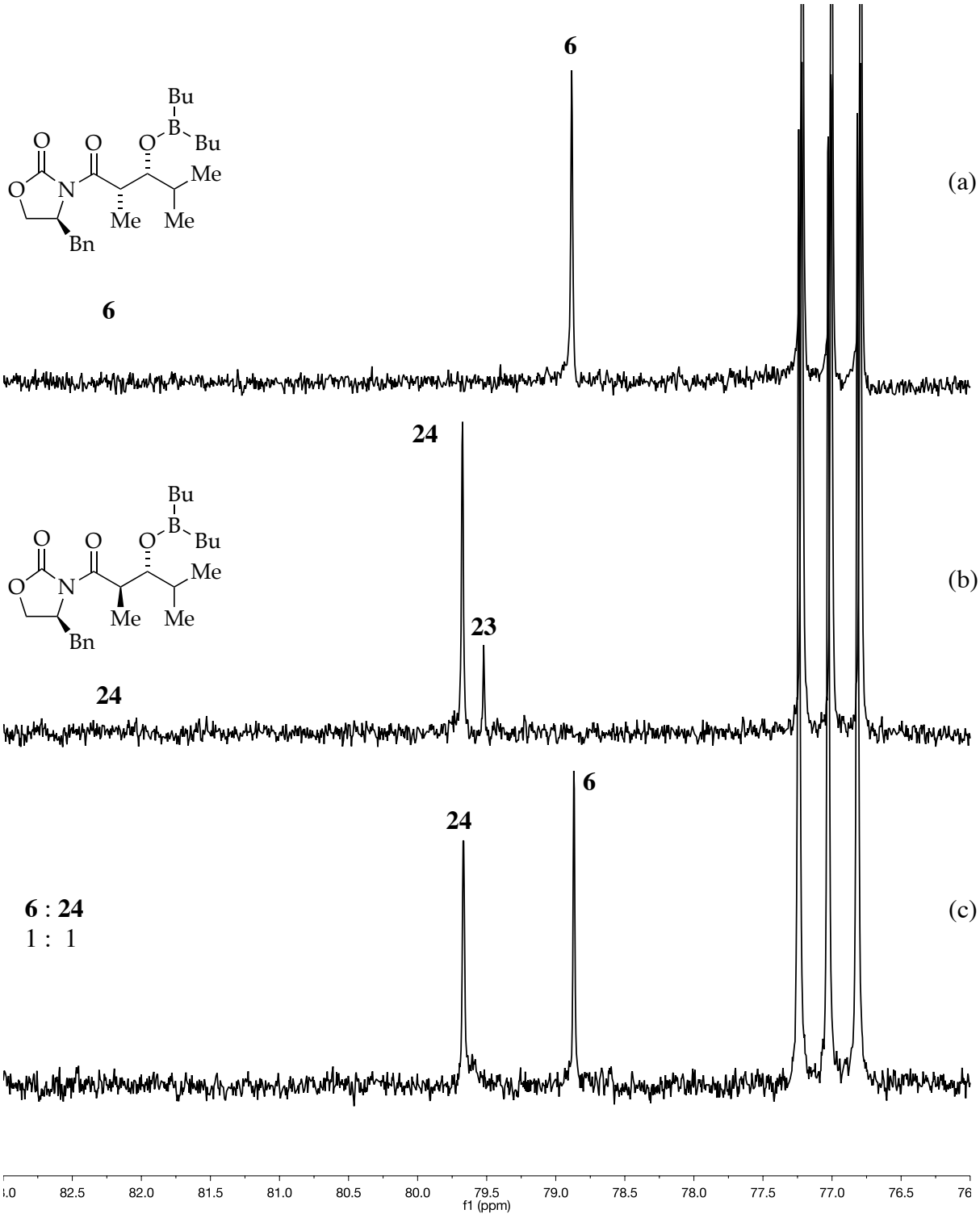

Figure S24. ^{13}C NMR spectra in $CDCl_3$ at rt: (a) 0.10 M **2**, 0.11 M Bu_2BOTf, and 0.12 M Et_3N; (b) 0.10 M **23**, 0.11 M Bu_2BOTf, and 0.12 M Et_3N; (c) 0.050 M **2**, 0.050 M **23**, 0.11 M Bu_2BOTf, and 0.12 M Et_3N in $CDCl_3$.

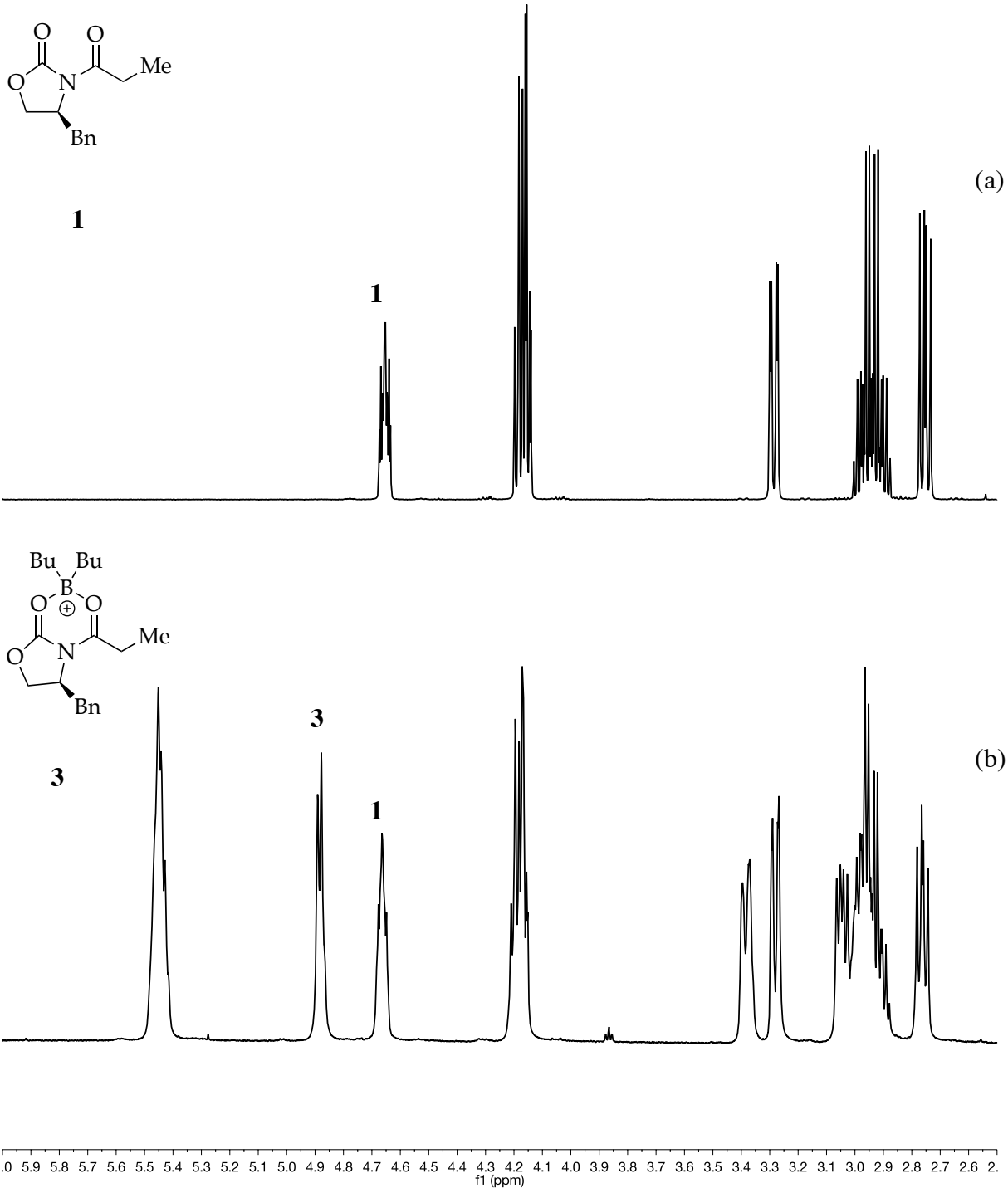

Figure S25. ^{1}H NMR spectra in $CDCl_3$ at rt: (a) 0.10 M **1**; (b) 0.10 M **1** and 0.11 M Bu_2BOTf.

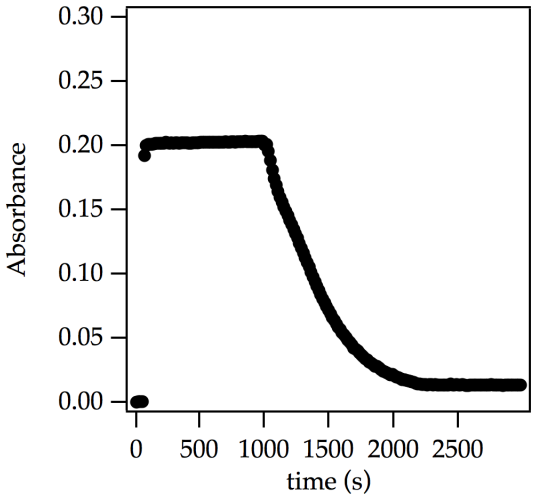

Figure S26. IR spectra of injecting 3.3 equivalents of Bu_2BOTf over 33 minutes into 0.10 M **1** in $CHCl_3$, following loss of **1**. The curvature indicates soft equilibrium of complexation at room temperature.

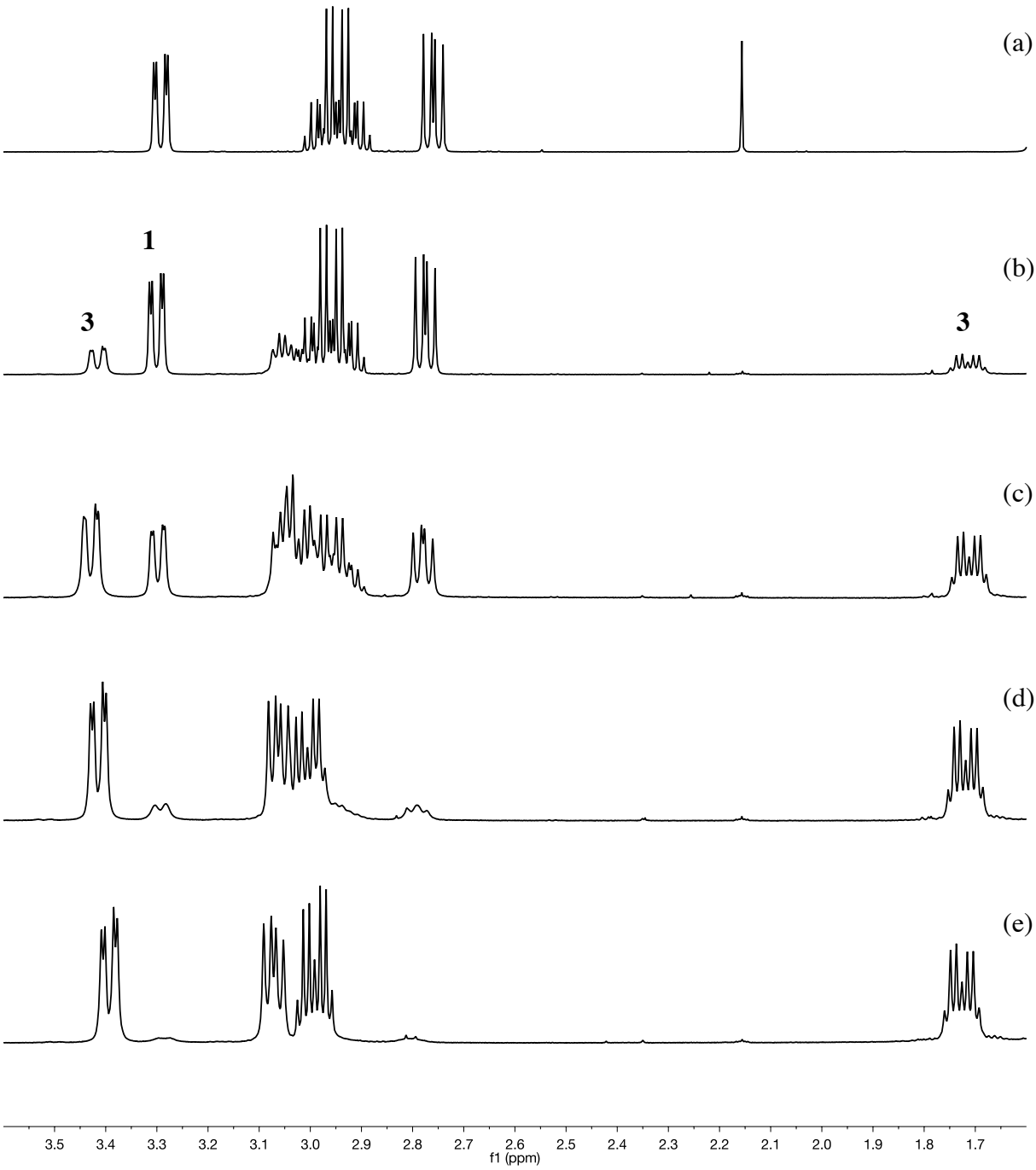

Figure S27. ^{1}H NMR spectra in $CDCl_3$ recorded at rt: (a) 0.10 M **1**; (b) 0.10 M **1** and 0.05 M Bu_2BOTf; (c) 0.10 M **1** and 0.10 M Bu_2BOTf; (d) 0.10 M **1** and 0.20 M Bu_2BOTf; (e) 0.10 M **1** and 0.30 M Bu_2BOTf.

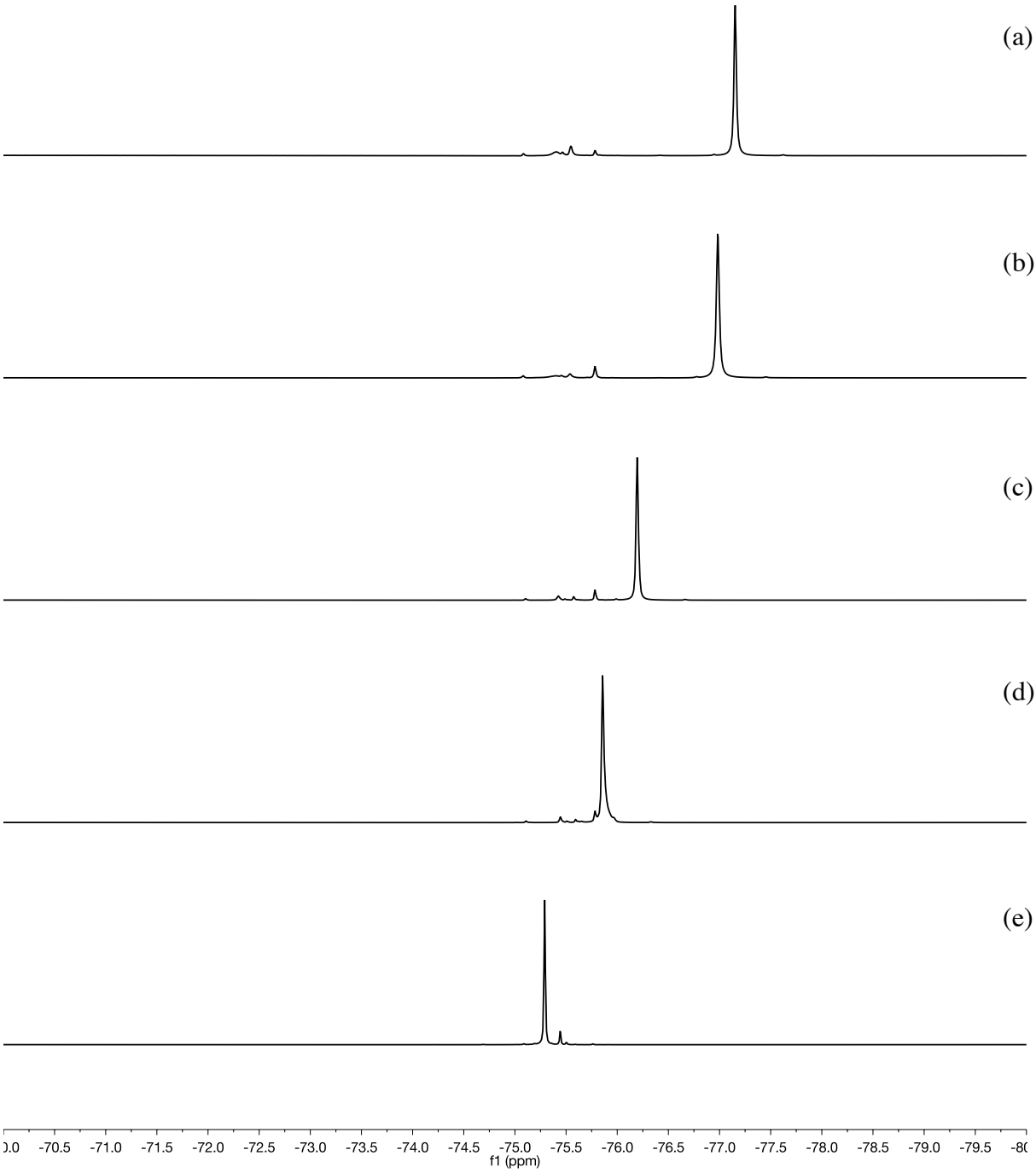

Figure S28. ^{19}F NMR spectra in $CDCl_3$ recorded at –60 °C: (a) 0.10 M **1** and 0.05 M Bu_2BOTf; (b) 0.10 M **1** and 0.10 M Bu_2BOTf; (c) 0.10 M **1** and 0.20 M Bu_2BOTf; (d) 0.10 M **1** and 0.30 M Bu_2BOTf; (e) 0.10 M Bu_2BOTf.

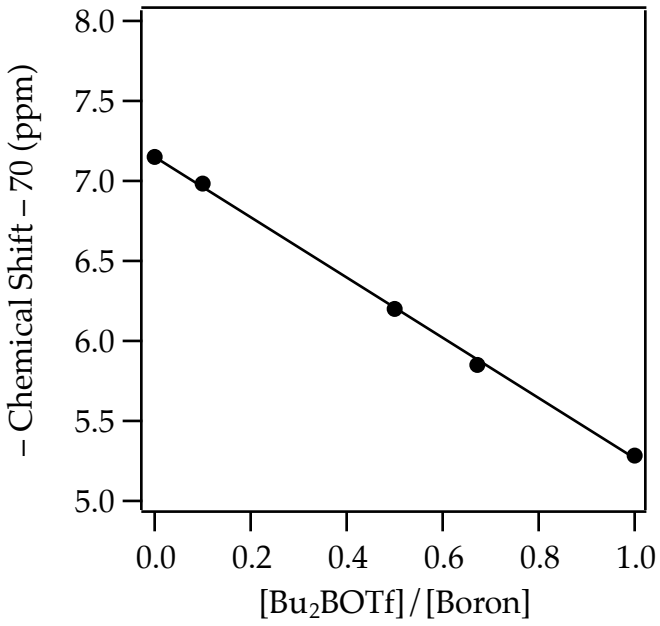

Figure S29. Plot of ^{19}F NMR chemical shift vs. [Bu_2BOTf]/[Boron] for titrating **1** with Bu_2BOTf in $CDCl_3$ at –60 °C. $y = ax + b$, $a = -1.89 \pm 0.03$, $b = 7.15 \pm 0.02$.

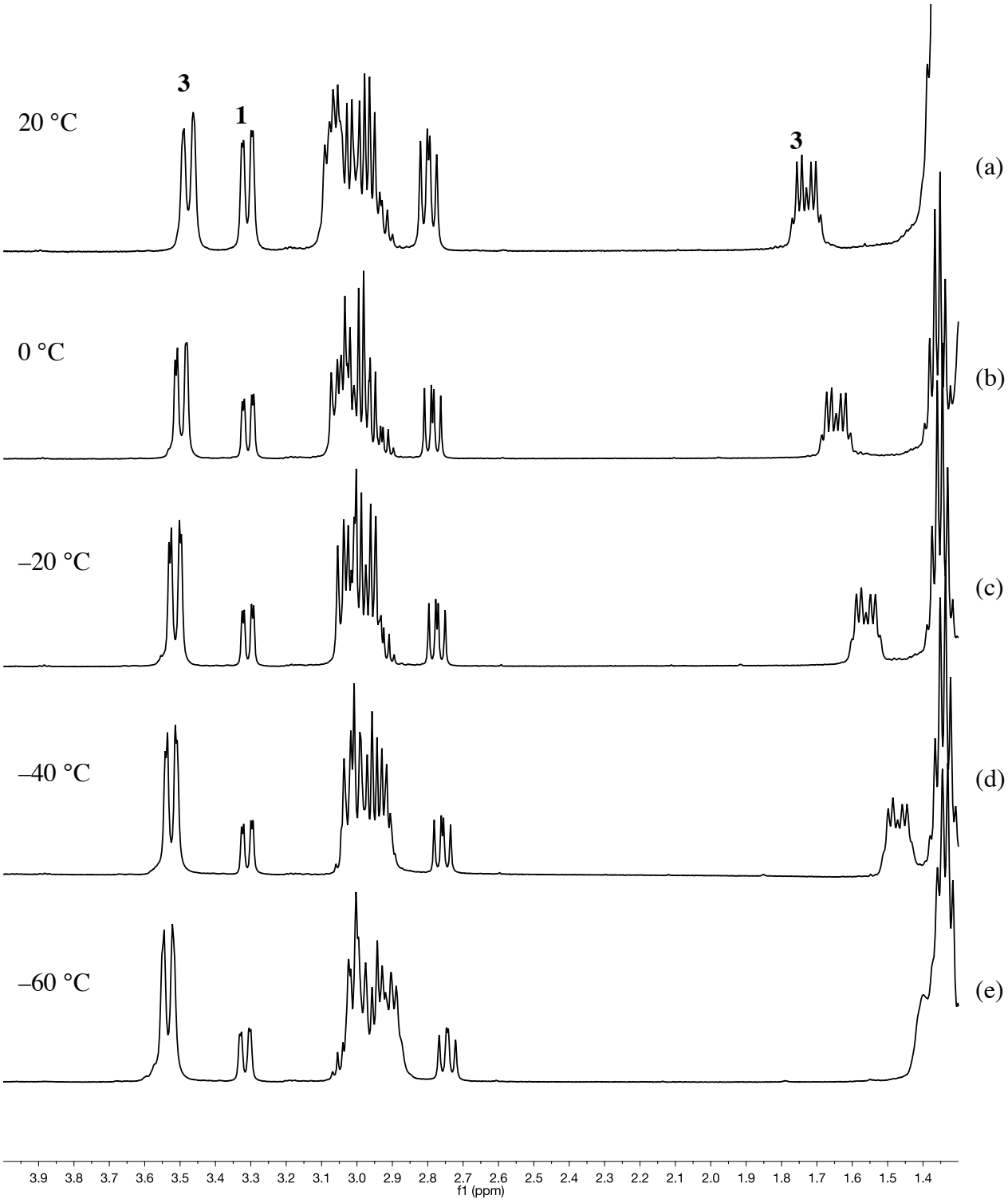

Figure S30. ^{1}H NMR spectra of 0.20 M **1** and 0.15 M Bu_2BOTf in $CDCl_3$ recorded at: (a) 20 °C; (b) 0 °C; (c) –20 °C; (d) –40 °C; (e) –60 °C.

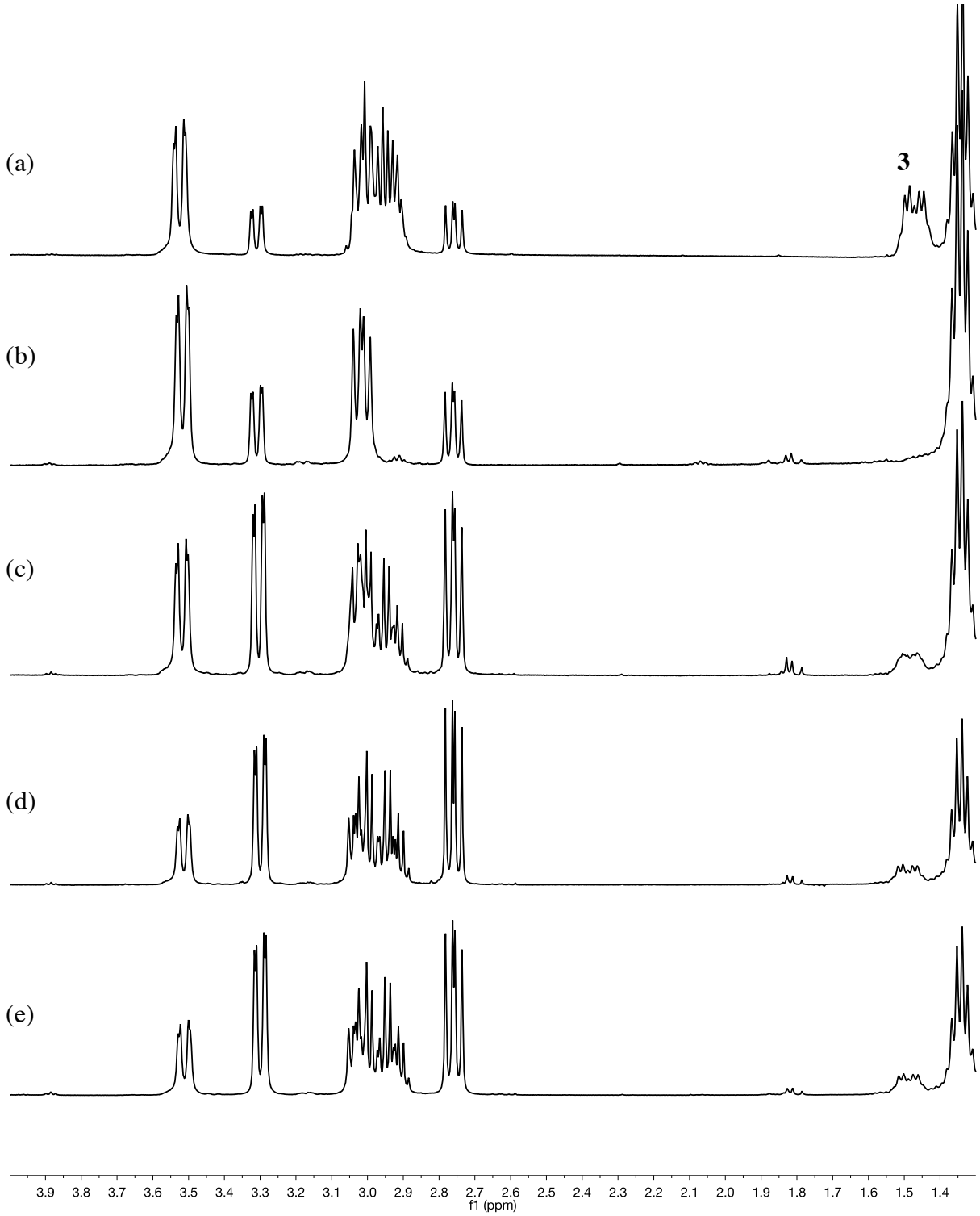

Figure S31. ^{1}H NMR spectra in $CDCl_3$ recorded at –40 °C: (a) 0.20 M **1** and 0.15 M Bu_2BOTf; (b) 0.20 M **1**-d_2 and 0.15 M Bu_2BOTf; (c) injecting 0.20 M **1** into 0.20 M **1**-d_2 and 0.15 M Bu_2BOTf; (d) injecting 0.20 M **1** into 0.20 M **1**-d_2 and 0.15 M Bu_2BOTf after votexing at –40 °C; (e) injecting 0.20 M **1** into 0.20 M **1**-d_2 and 0.15 M Bu_2BOTf after votexing at –40 °C and aging at rt for 10 minutes.

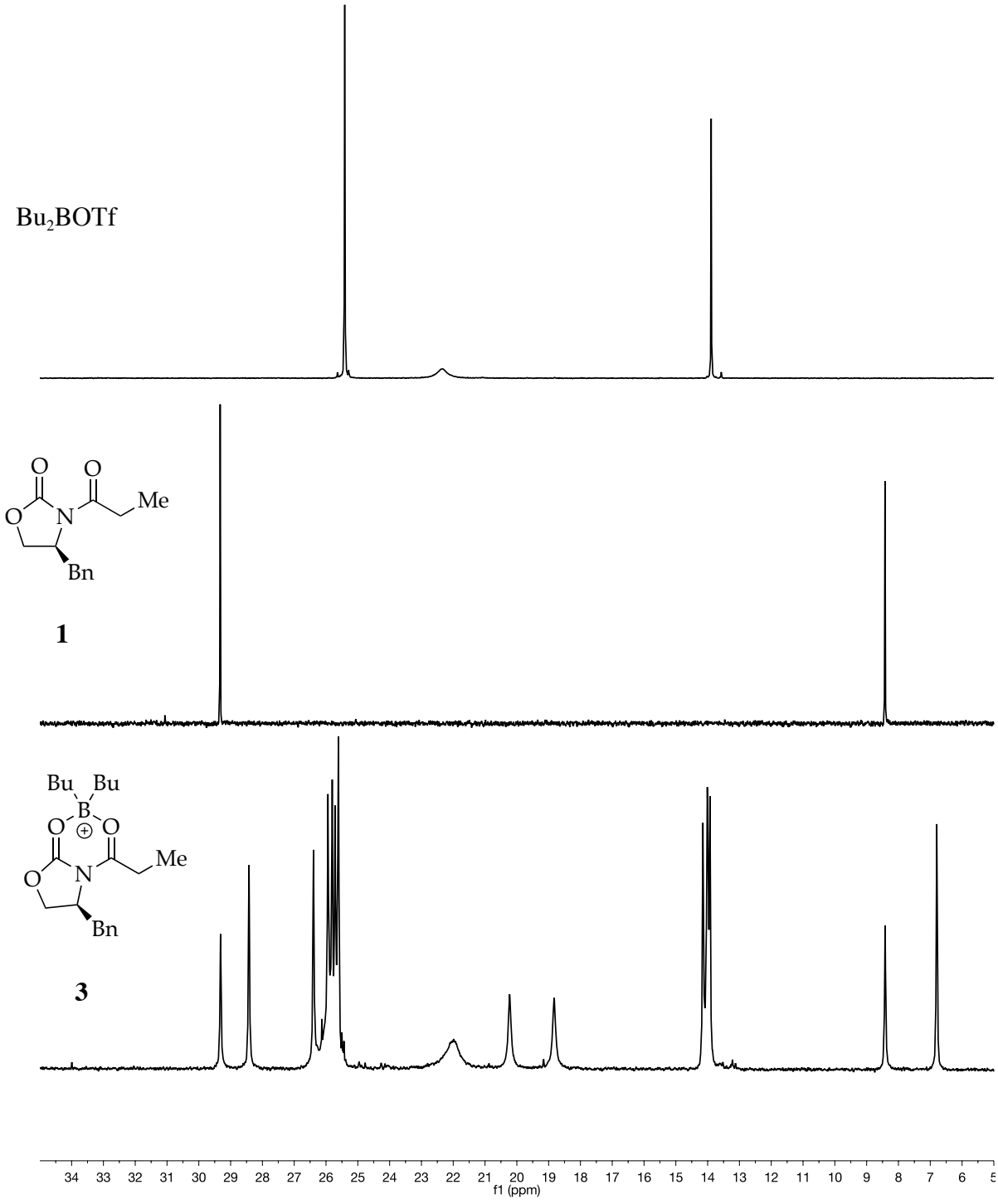

Figure S32. ^{13}C NMR spectra in $CDCl_3$ at rt: (a) 0.20 M Bu_2BOTf; (b) 0.20 M **1**; (c) 0.20 M **1** and 0.20 M Bu_2BOTf.

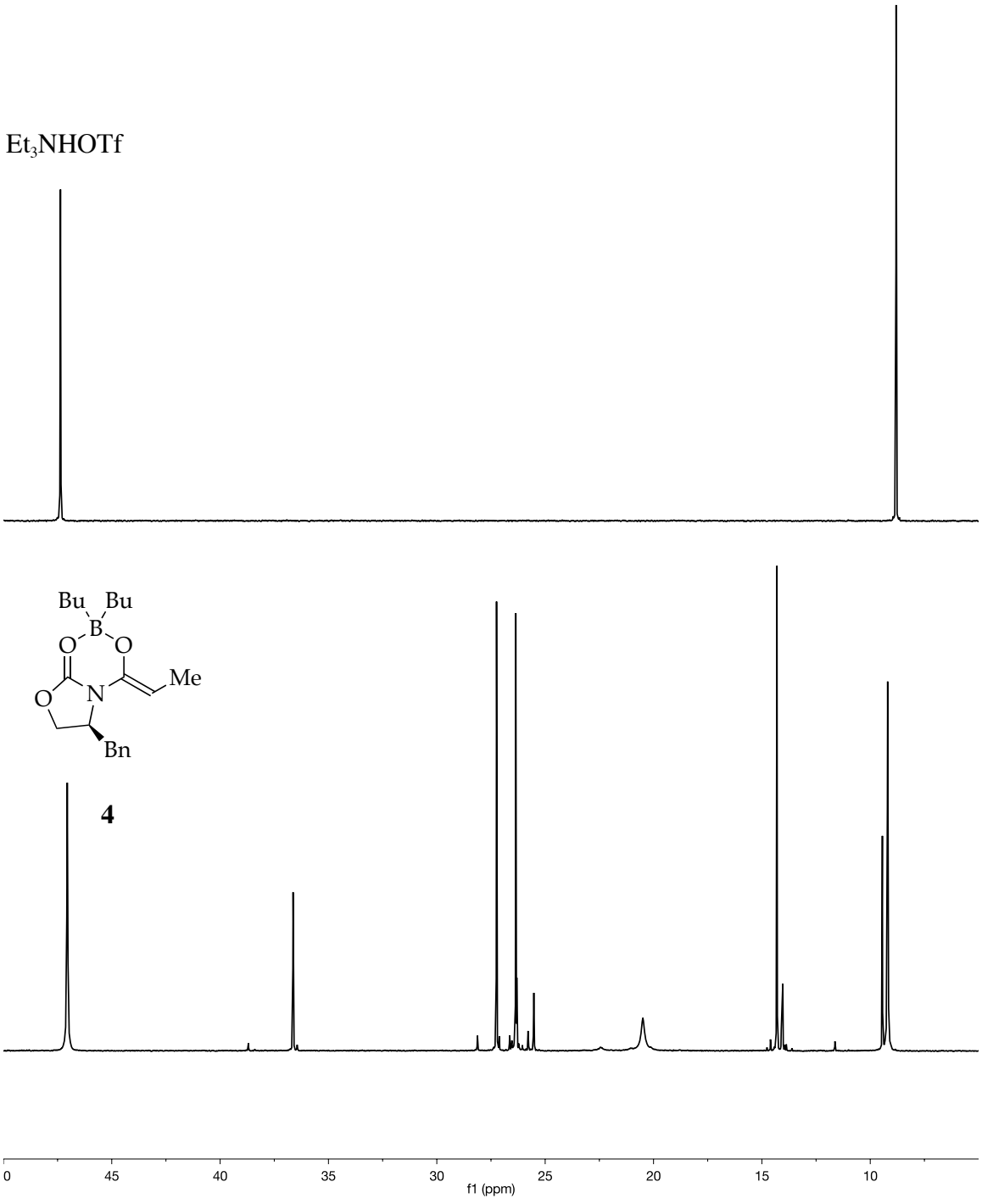

Figure S33. ^{13}C NMR spectra in $CDCl_3$ at rt: (a) 0.20 M Et_3NHOTf; (b) 0.20 M **1**, 0.20 M Bu_2BOTf, and 0.20 M Et_3N.

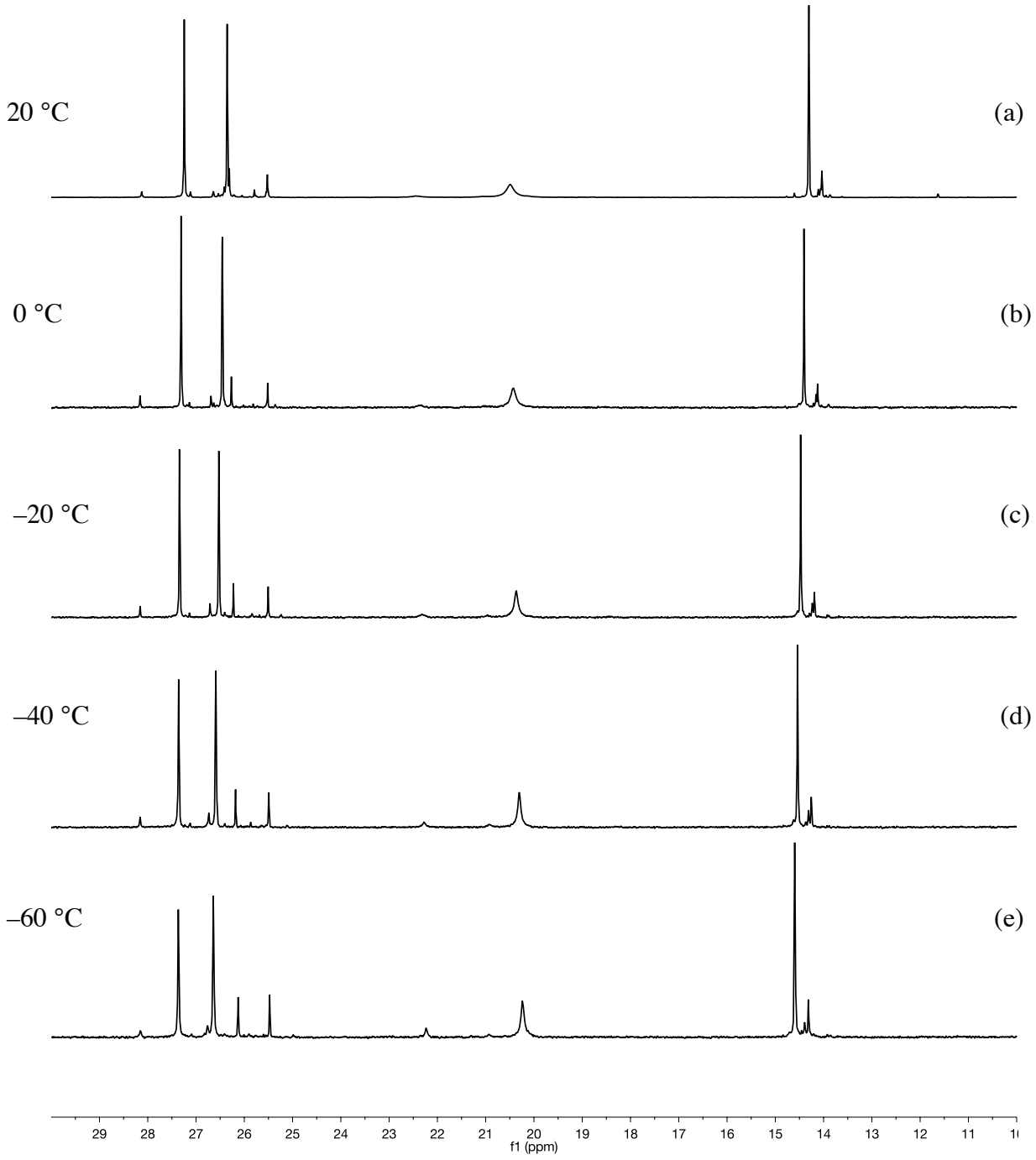

Figure S34. ^{13}C NMR spectra of 0.20 M **1**, 0.20 M Bu_2BOTf and 0.20 M Et_2N in $CDCl_3$ recorded at: (a) 20 °C; (b) 0 °C; (c) –20 °C; (d) –40 °C; (e) –60 °C.

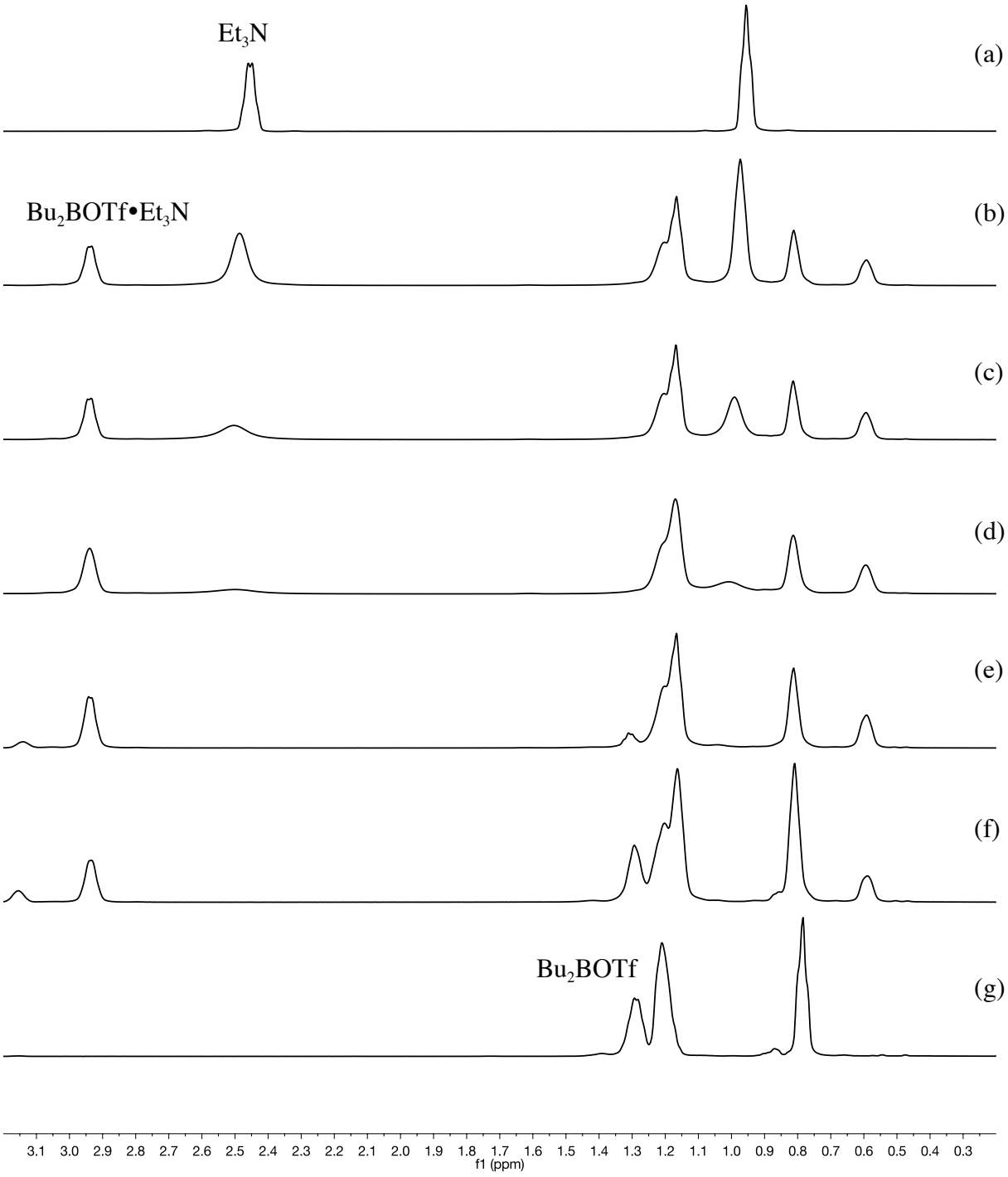

Figure S35. ^{1}H NMR spectra in $CDCl_3$ recorded at –60 °C: (a) 0.10 M Et_3N; (b) 0.10 M Bu_2BOTf and 0.30 M Et_3N; (c) 0.10 M Bu_2BOTf and 0.20 M Et_3N; (d) 0.10 M Bu_2BOTf and 0.15 M Et_3N; (e) 0.10 M Bu_2BOTf and 0.10 M Et_3N; (f) 0.10 M Bu_2BOTf and 0.050 M Et_3N; (g) 0.10 M Bu_2BOTf.

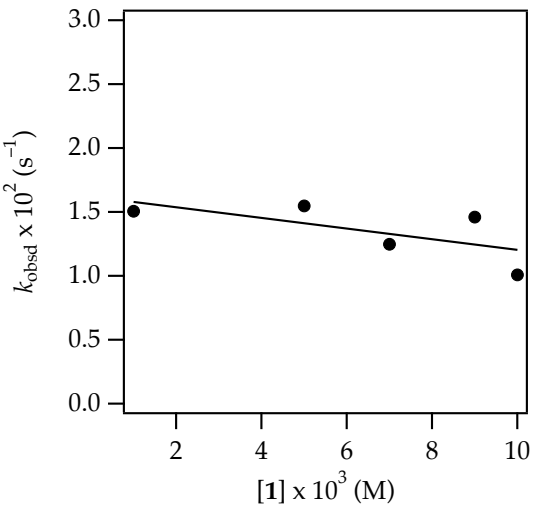

Figure S36. Plot of observed rate vs [**1**] for enolization of [**1**] by Bu_2BOTf and Et_3N in $CHCl_3$ at 0 °C. $y = ax + b$, $a = -0.4 \pm 0.2$, $b = 0.016 \pm 0.002$.

[**1**] (M)	[Bu_2BOTf•Et_3N] (M)	[Et_3N] (M)	k_{obsd} x 10^2 (s^{-1})
0.0010	0.10	0.20	1.51
0.0050	0.10	0.20	1.55
0.0070	0.10	0.20	1.25
0.0090	0.10	0.20	1.46
0.010	0.10	0.20	1.01

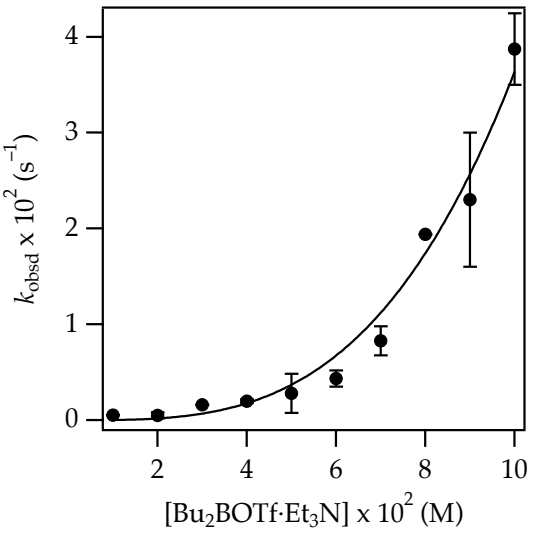

Figure S37. Plot of observed rate vs [$Bu_2BOTf{\bullet}Et_3N$] for enolization of **1** by Bu_2BOTf and Et_3N in $CHCl_3$ at 0 °C. $y = ax^b + c$, $a = 72 \pm 3$, $b = 3.3 \pm 0.3$, c set to 0.0

[**1**] (M)	[$Bu_2BOTf{\bullet}Et_3N$] (M)	[Et_3N] (M)	k_{obsd} x 10^3 (s^{-1})
0.0020	0.010	0.10	0.538
0.0020	0.020	0.10	0.498
0.0020	0.030	0.10	1.59
0.0020	0.040	0.10	1.97
0.0020	0.050	0.10	2.79
0.0020	0.060	0.10	4.34
0.0020	0.070	0.10	8.28
0.0020	0.080	0.10	19.4
0.0020	0.090	0.10	23.0
0.0020	0.10	0.10	38.7

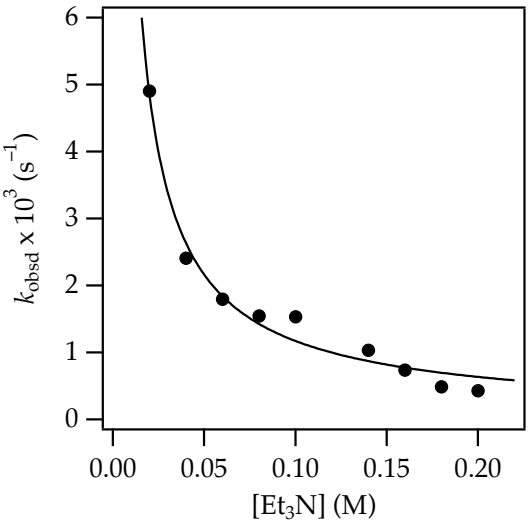

Figure S38. Plot of observed rate vs added [Et_3N] for enolization of **1** by Bu_2BOTf and Et_3N in $CHCl_3$ at 0 °C. $y = ax^b + c$, $a = 0.00015 \pm 0.00003$, b = –0.88 ± 0.05, c set to 0.00

[**1**] (M)	[Bu_2BOTf•Et_3N] (M)	[Et_3N] (M)	k_{obsd} x 10^3 (s^{-1})
0.0020	0.040	0.020	4.91
0.0020	0.040	0.040	2.41
0.0020	0.040	0.060	1.79
0.0020	0.040	0.080	1.55
0.0020	0.040	0.10	1.53
0.0020	0.040	0.14	1.03
0.0020	0.040	0.16	0.737
0.0020	0.040	0.18	0.487
0.0020	0.040	0.20	0.429

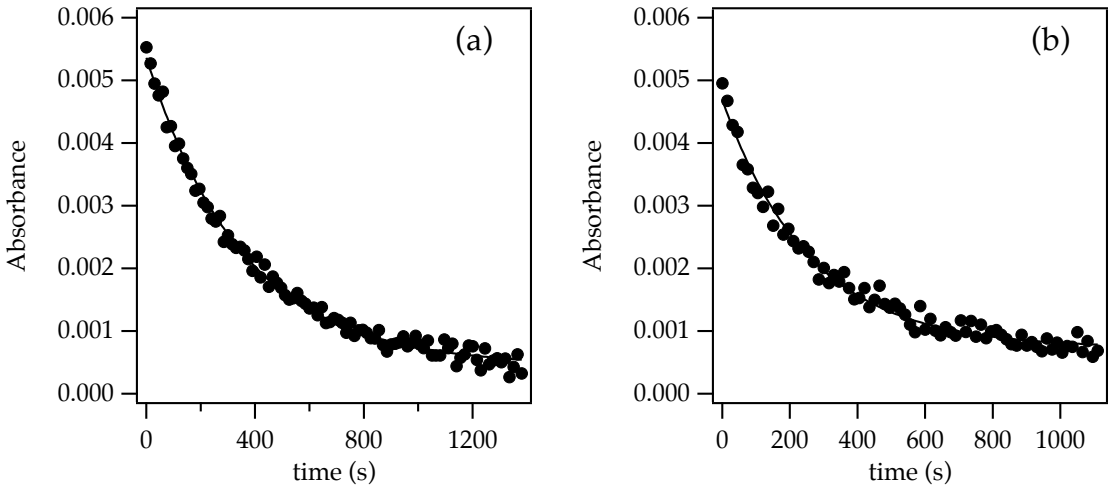

Figure S39. IR spectra in $CHCl_3$ at 0 °C, following loss of **1**: (a) injecting 0.0030 M **1** into pre-mixed 0.050 M Bu_2BOTf and 0.10 M Et_3N, k_{obsd} = 0.003 s^{-1}; (b) injecting 0.0030 M **1**-$\boldsymbol{d}_2$ into pre-mixed 0.050 M Bu_2BOTf and 0.10 M Et_3N, k_{obsd} = 0.003 s^{-1}.

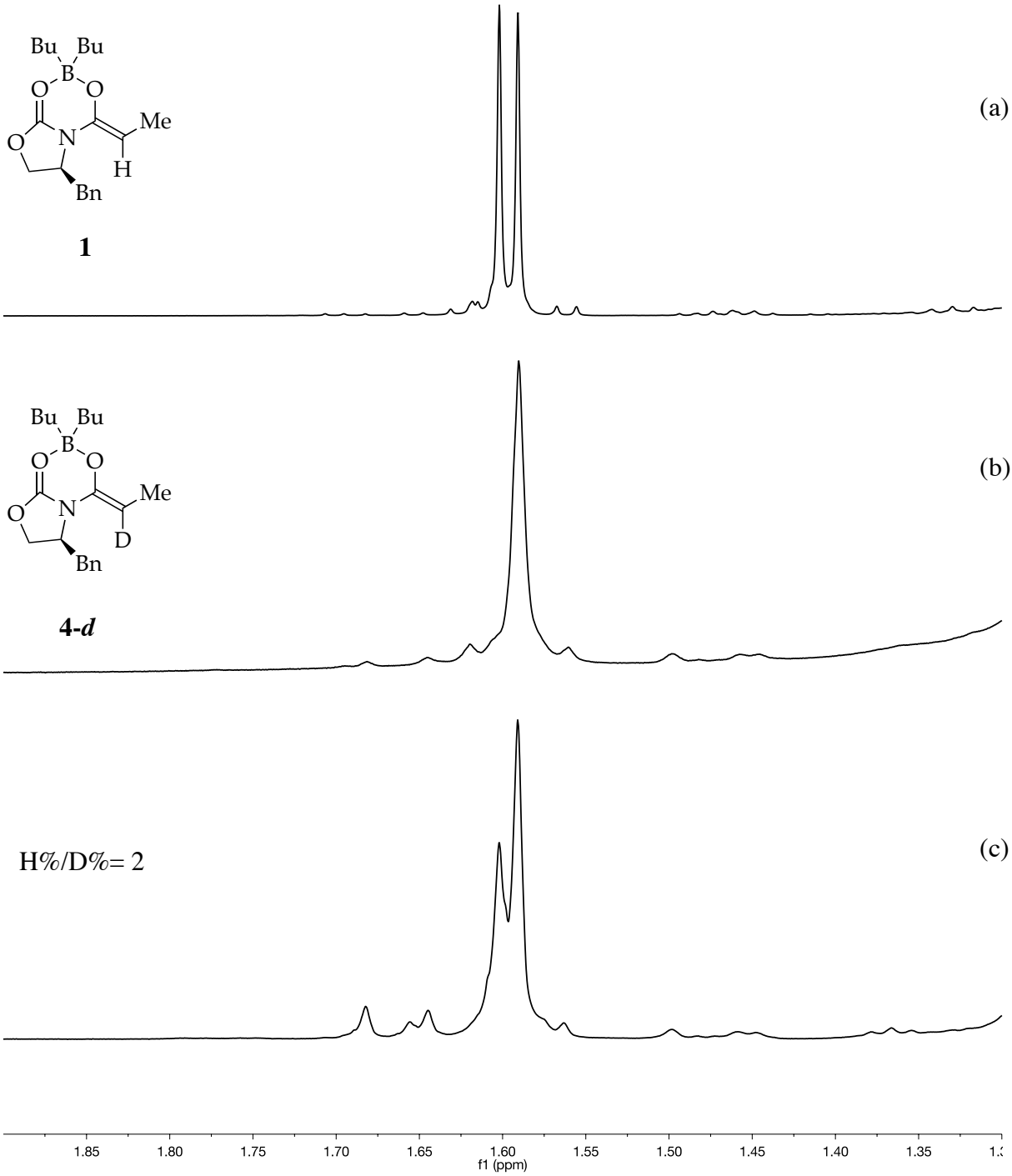

Figure S40. ^{1}H NMR spectra in $CDCl_3$ at rt: (a) 0.10 M **1**, 0.040 M Bu_2BOTf, and 0.040 M Et_3N; (b) 0.10 M **1**-d_2, 0.040 M Bu_2BOTf, and 0.040 M Et_3N; (c) injecting pre-mixed 0.10 M **1** and 0.10 M **1**-d_2 into pre-mixed 0.040 M Bu_2BOTf and 0.040 M Et_3N. $k_H/k_D = 2$

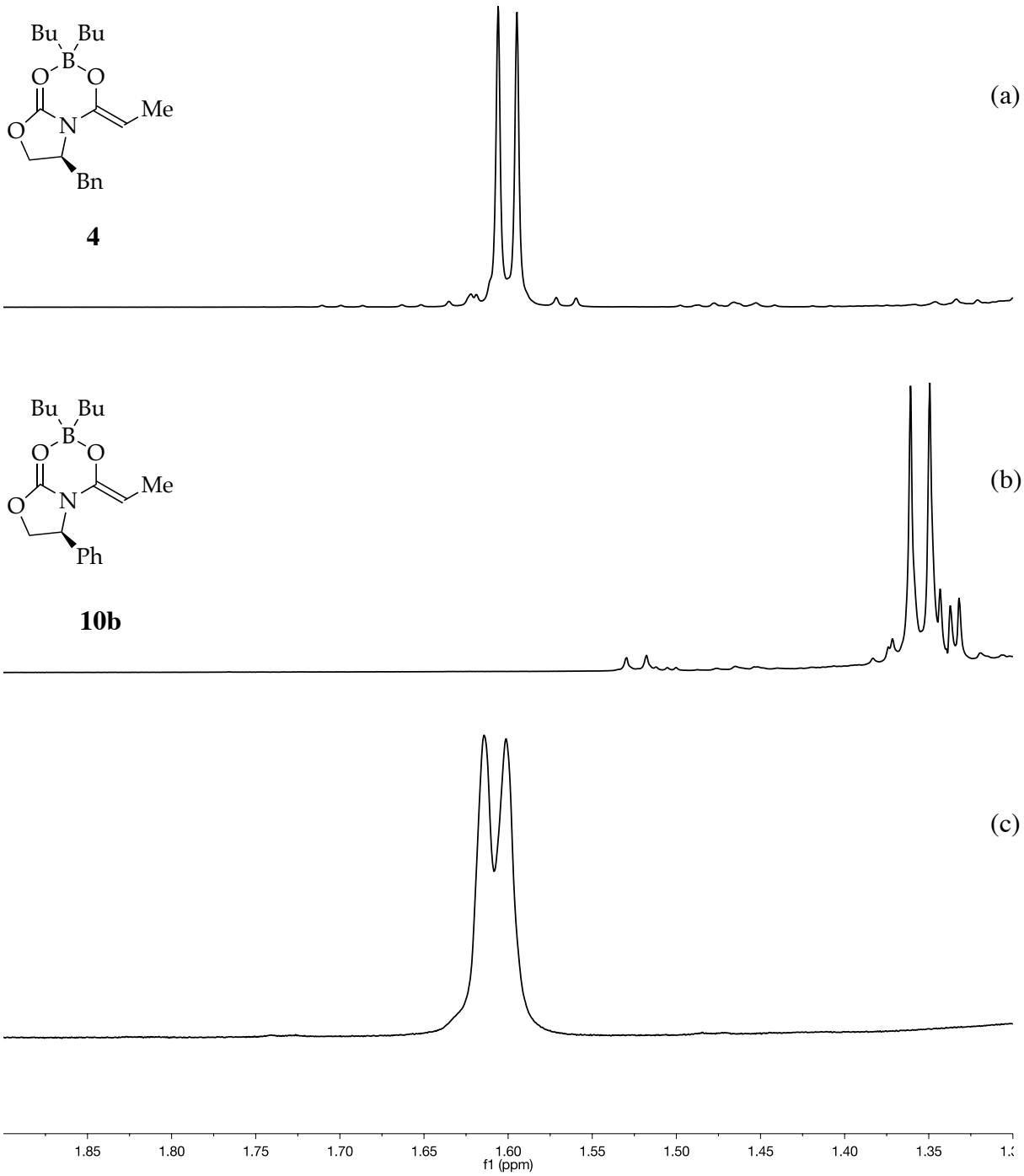

Figure S41. ^{1}H NMR spectra in $CDCl_3$ at rt: (a) 0.10 M **1**, 0.10 M Bu_2BOTf, and 0.10 M Et_3N; (b) 0.10 M **10**, 0.10 M Bu_2BOTf, and 0.10 M Et_3N; (c) injecting 0.10 M **10** into pre-mixed 0.10 M **1**, 0.050 M Bu_2BOTf, and 0.10 M Et_3N.

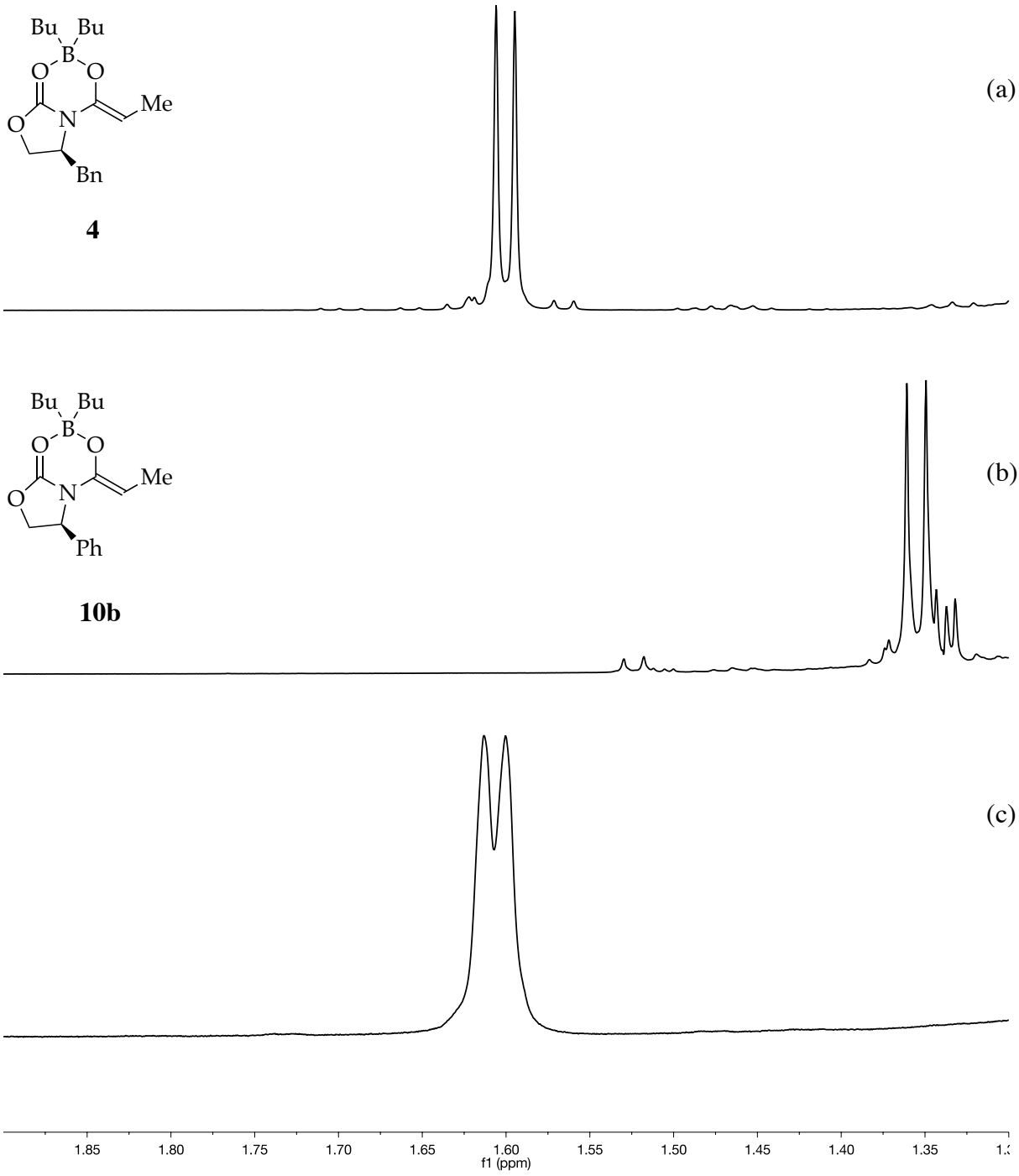

Figure S42. ^{1}H NMR spectra in $CDCl_3$ at rt: (a) 0.10 M **1**, 0.10 M Bu_2BOTf, and 0.10 M Et_3N; (b) 0.10 M **10**, 0.10 M Bu_2BOTf, and 0.10 M Et_3N; (c) injecting pre-mixed 0.10 M **1** and 0.050 M Bu_2BOTf into pre-mixed 0.10 M Et_3N and 0.10 M **10**.

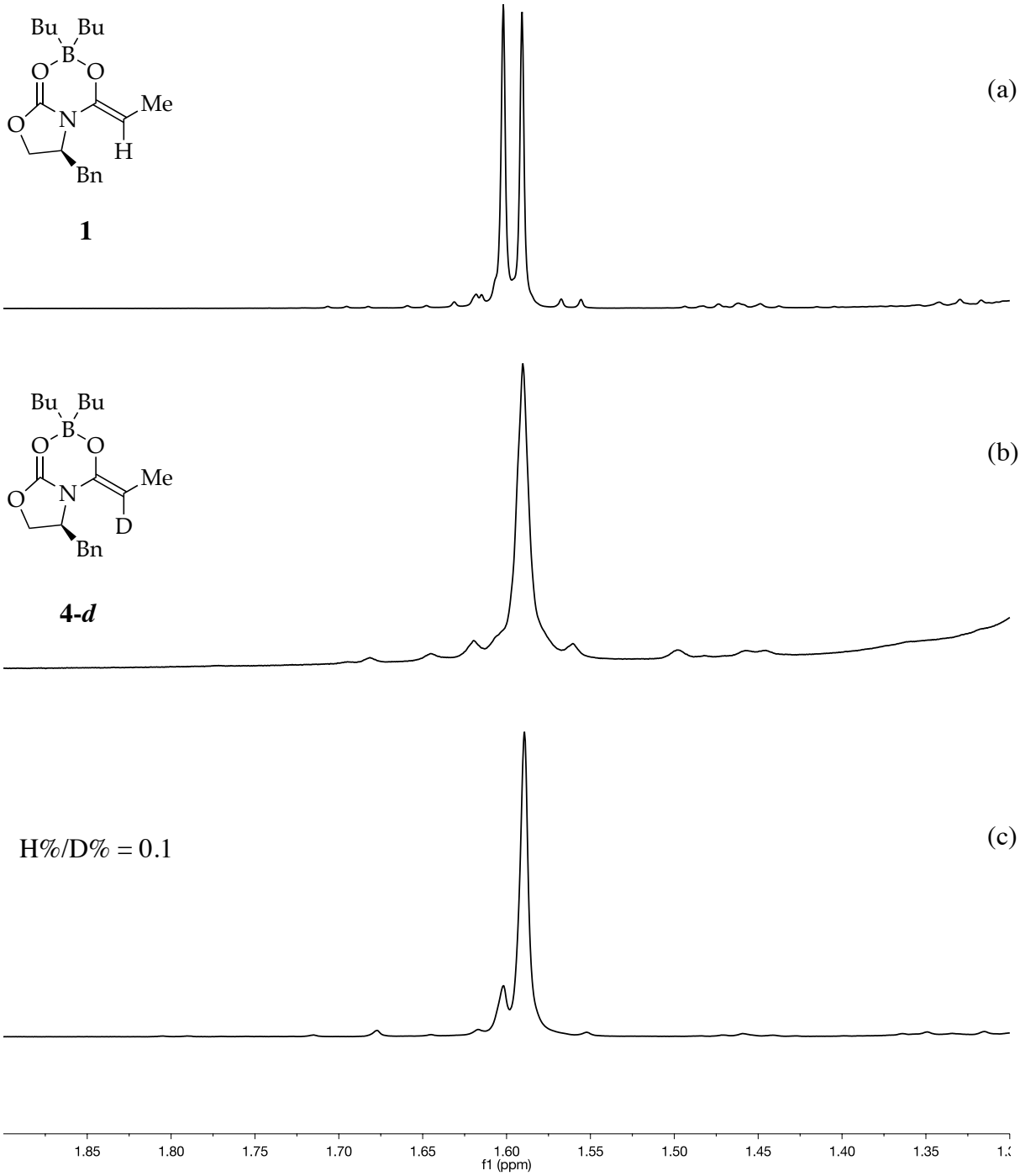

Figure S43. ^{1}H NMR spectra in $CDCl_3$ at rt: (a) 0.10 M **1**, 0.10 M Bu_2BOTf, and 0.10 M Et_3N; (b) 0.10 M **1**-***d***$_2$, 0.10 M Bu_2BOTf, and 0.10 M Et_3N; (c) injecting pre-mixed 0.10 M **1**-***d***$_2$ and 0.050 M Bu_2BOTf into pre-mixed 0.10 M Et_3N and 0.10 M **1**. H%/D% = 0.1.

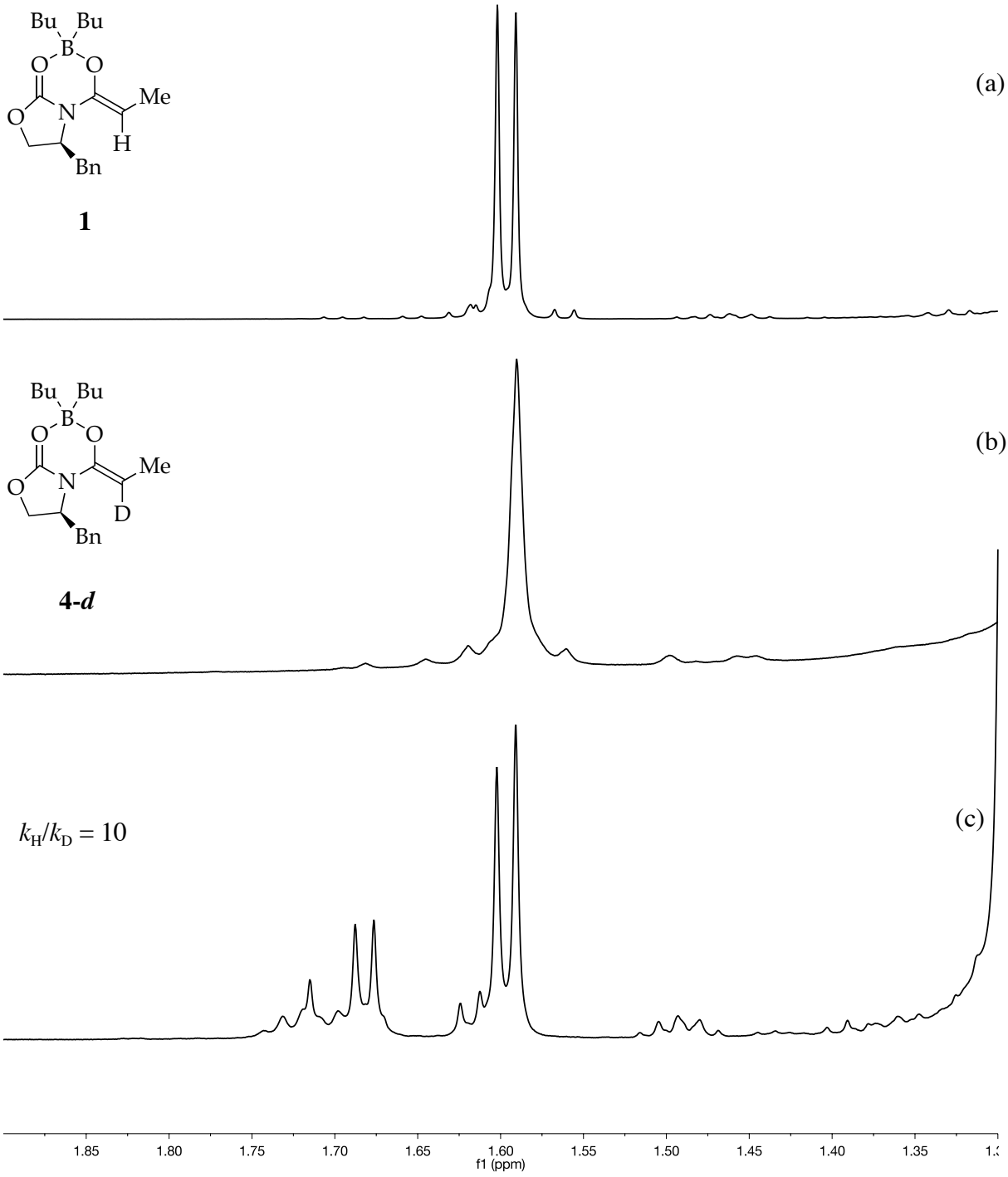

Figure S44. ^{1}H NMR spectra in $CDCl_3$ at rt: (a) 0.10 M **1**, 0.10 M Bu_2BOTf, and 0.10 M Et_3N; (b) 0.10 M **1**-***d***$_2$, 0.10 M Bu_2BOTf, and 0.10 M Et_3N; (c) injecting 0.080 M Et_3N into pre-mixed 0.10 M **1**-***d***$_2$, 0.10 M **1**, and 0.20 M Bu_2BOTf. k_H/k_D= 10.

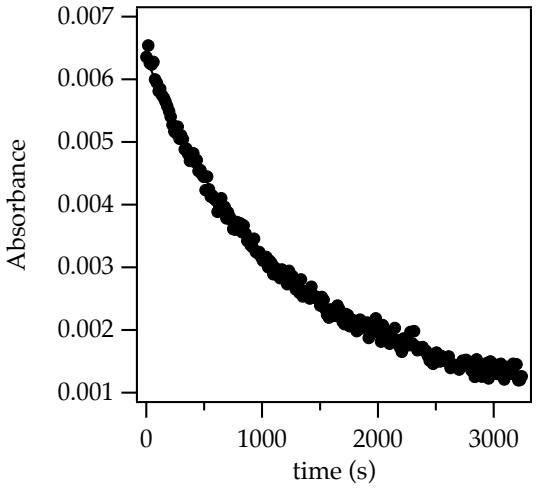

Figure S45. IR spectra of injecting 0.0040 M **1** into pre-mixed 0.050 M Bu_2BOTf and 0.15 M Et_3N in $CHCl_3$ recorded at 0 °C, following loss of **1**. k_{obsd} = 9.9 x 10^{-4} s^{-1}.

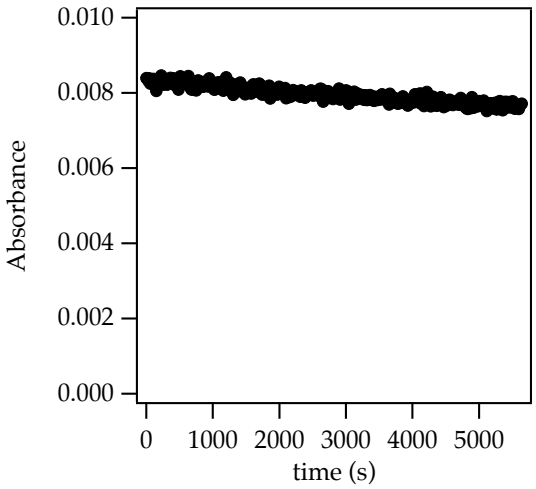

Figure S46. IR spectra of injecting 0.0050 M **1** into pre-mixed 0.050 M Bu_2BOTf and 0.15 M Et_2NMe in $CHCl_3$ recorded at 0 °C, following loss of **1**. $k_{obsd} = 3.1 \times 10^{-5}$ s^{-1}, $k_{rel} = 0.03$.

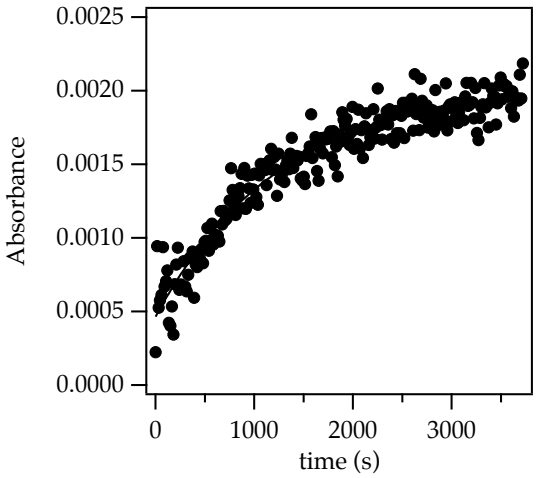

Figure S47. IR spectra of injecting 0.0040 M **1** into pre-mixed 0.050 M Bu_2BOTf and 0.15 M Me_2NCy in $CHCl_3$ recorded at 0 °C, following growth of **4**. k_{obsd}= 8.0 x 10^{-5} s^{-1}, k_{rel} = 0.8.

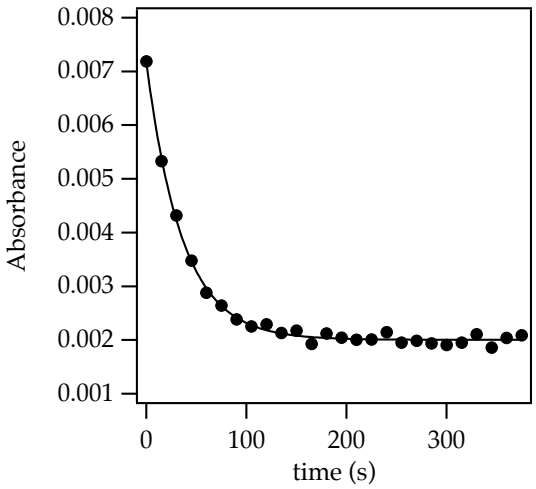

Figure S48. IR spectra of injecting 0.0040 M **1** into pre-mixed 0.050 M Bu_2BOTf and 0.15 M *i*-Pr_2NEt in $CHCl_3$ recorded at 0 °C, following loss of **1**. k_{obsd} = 2.8 x 10^{-2} s^{-1}, k_{rel} = 30.

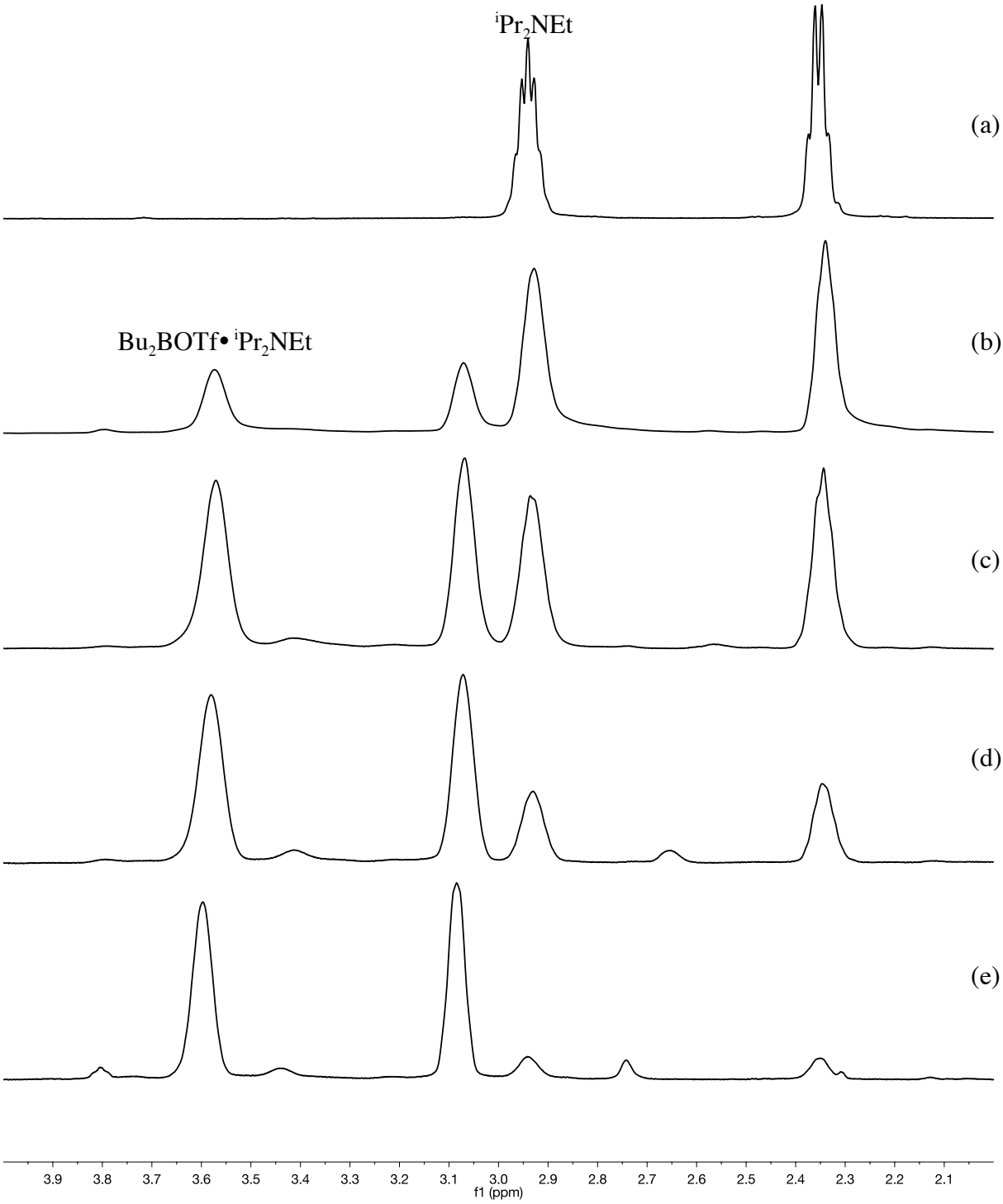

Figure S49. ^{1}H NMR spectra in $CDCl_3$ recorded at –60 °C: (a) 0.10 M $^{i}Pr_2NEt$; (b) 0.10 M Bu_2BOTf and 0.30 M $^{i}Pr_2NEt$; (c) 0.10 M Bu_2BOTf and 0.20 M $^{i}Pr_2NEt$; (d) 0.10 M Bu_2BOTf and 0.15 M $^{i}Pr_2NEt$; (e) 0.10 M Bu_2BOTf and 0.10 M $^{i}Pr_2NEt$.

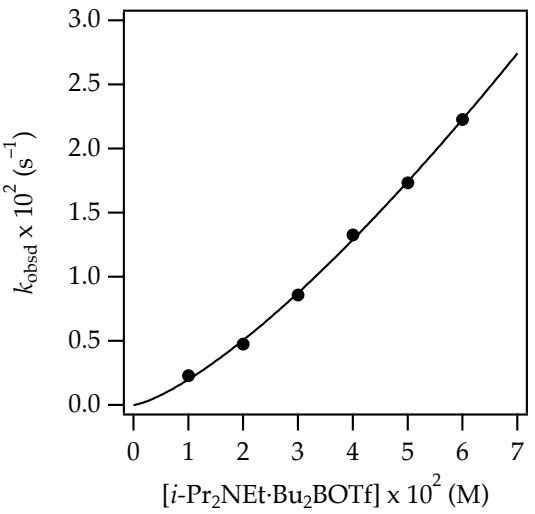

Figure S50. Plot of observed rate vs added [i-Pr_2NEt•Bu_2BOTf] for enolization of **1** by Bu_2BOTf and i-Pr_2NEt in $CHCl_3$ at 0 °C. y = $ax^b + c$, $a = 0.99 \pm 0.10$, $b = 1.35 \pm 0.03$, c set to 0.00.

[**1**] (M)	[i-Pr_2NEt•Bu_2BOTf] (M)	[i-Pr_2NEt] (M)	k_{obsd} x 10^2 (s^{-1})
0.002	0.010	0.20	0.229
0.002	0.020	0.20	0.475
0.002	0.030	0.20	0.859
0.002	0.040	0.20	1.33
0.002	0.050	0.20	1.73
0.002	0.060	0.20	2.23

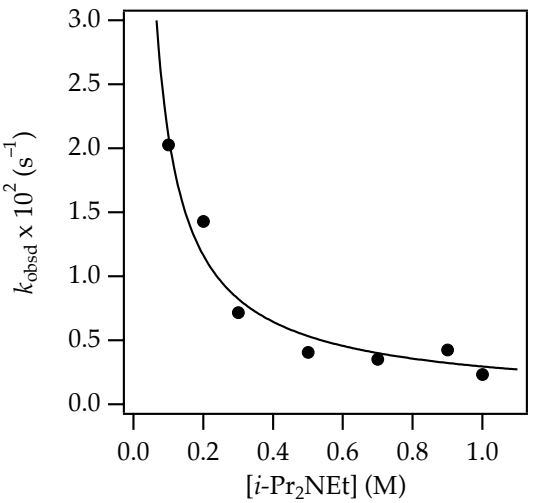

Figure S51. Plot of observed rate vs added [i-Pr_2NEt] for enolization of **1** by Bu_2BOTf and i-Pr_2NEt in $CHCl_3$ at 0 °C. $y = ax^b + c$, $a = 0.0030 \pm 0.0006$, $b = -0.85 \pm 0.09$, c set to 0.00.

[**1**] (M)	[i-Pr_2NEt•Bu_2BOTf] (M)	[i-Pr_2NEt] (M)	k_{obsd} x10^2 (s^{-1})
0.0020	0.040	0.10	2.03
0.0020	0.040	0.20	1.43
0.0020	0.040	0.30	0.716
0.0020	0.040	0.50	0.407
0.0020	0.040	0.70	0.353
0.0020	0.040	0.90	0.426
0.0020	0.040	1.00	0.233

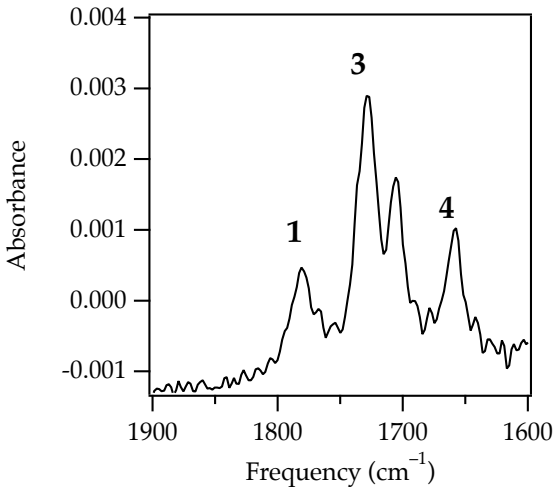

Figure S52. IR spectra of 0.0020 M **1**, 0.050 M Bu_2BOTf, and 0.15 M *i*-Bu_3N in $CHCl_3$ recorded at 0 °C.

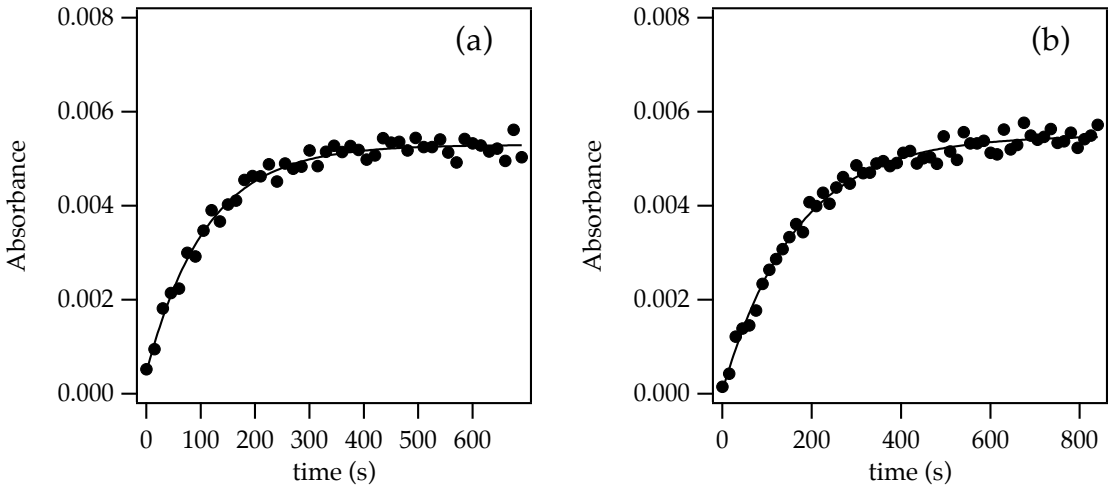

Figure S53. IR spectra in $CHCl_3$ recorded at 0 °C: (a) injecting 0.060 M *i*-Bu_3N into pre-mixed 0.040 M Bu_2BOTf and 0.0020 M **1**, following growth of **4**, $k_{obsd} = 0.009\ s^{-1}$; (b) injecting 0.0020 M **1** into pre-mixed 0.040 M Bu_2BOTf and 0.060 M *i*-Bu_3N, following growth of **4**, $k_{obsd} = 0.009\ s^{-1}$.

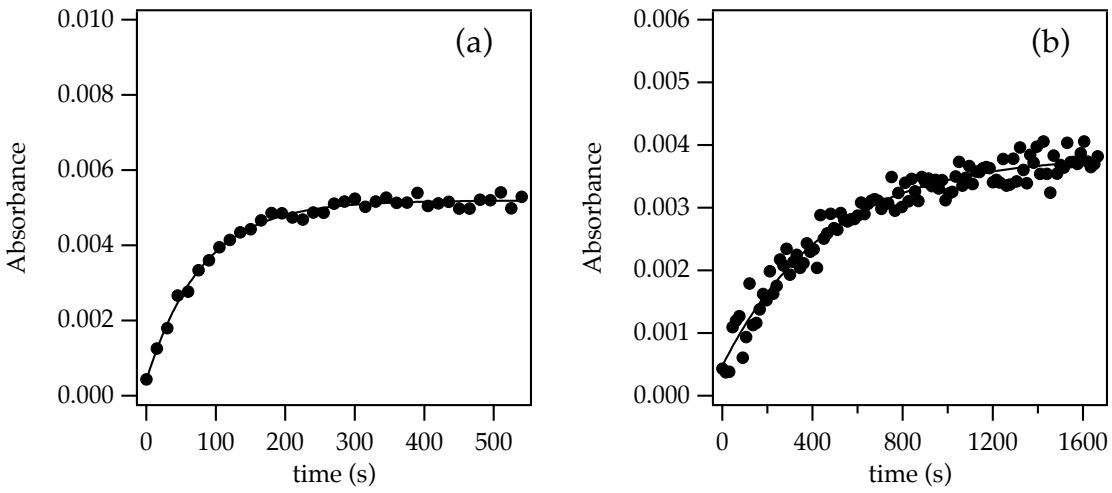

Figure S54. IR spectra in $CHCl_3$ recorded at 0 °C: (a) injecting 0.002 M **1** into pre-mixed 0.040 M Bu_2BOTf and 0.080 M *i*-Bu_3N, following growth of **4**, $k_{obsd} = 0.02\ s^{-1}$; (b) injecting 0.002 M **1**-***d***$_2$ into pre-mixed 0.040 M Bu_2BOTf and 0.080 M *i*-Bu_3N, following growth of **4**-***d***, $k_{obsd} = 0.002\ s^{-1}$. $k_H/k_D = 10$.

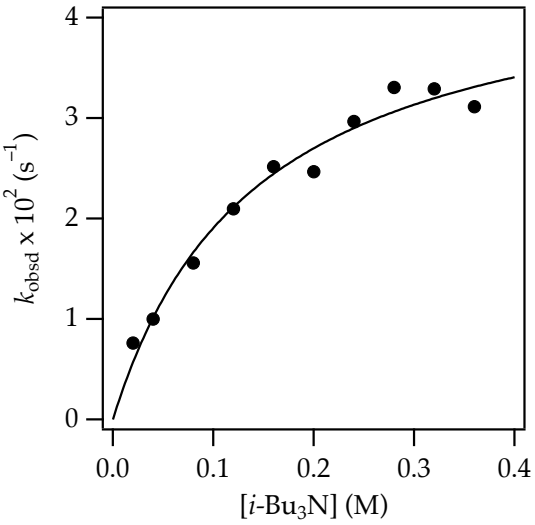

Figure S55. Plot of observed rate vs added [*i*-Bu_3N] for enolization of **1** by Bu_2BOTf and *i*-Bu_3N in $CHCl_3$ at 0 °C. $y = ax / (x + b)$, $a = 0.046 \pm 0.004$, $b = 0.14 \pm 0.03$.
K_{eq} = [**3**][*i*-Bu_3N] / [**1**][*i*-Bu_3N-Bu_2BOTf] = b / [*i*-Bu_3N-Bu_2BOTf] = 3.5

[**1**] (M)	[*i*-Bu_3N-Bu_2BOTf] (M)	[*i*-Bu_3N] (M)	k_{obsd} x 10^2 (s^{-1})
0.0020	0.040	0.020	0.762
0.0020	0.040	0.040	1.00
0.0020	0.040	0.080	1.56
0.0020	0.040	0.12	2.10
0.0020	0.040	0.16	2.55
0.0020	0.040	0.20	2.47
0.0020	0.040	0.24	2.97
0.0020	0.040	0.28	3.30
0.0020	0.040	0.32	3.29
0.0020	0.040	0.36	3.11

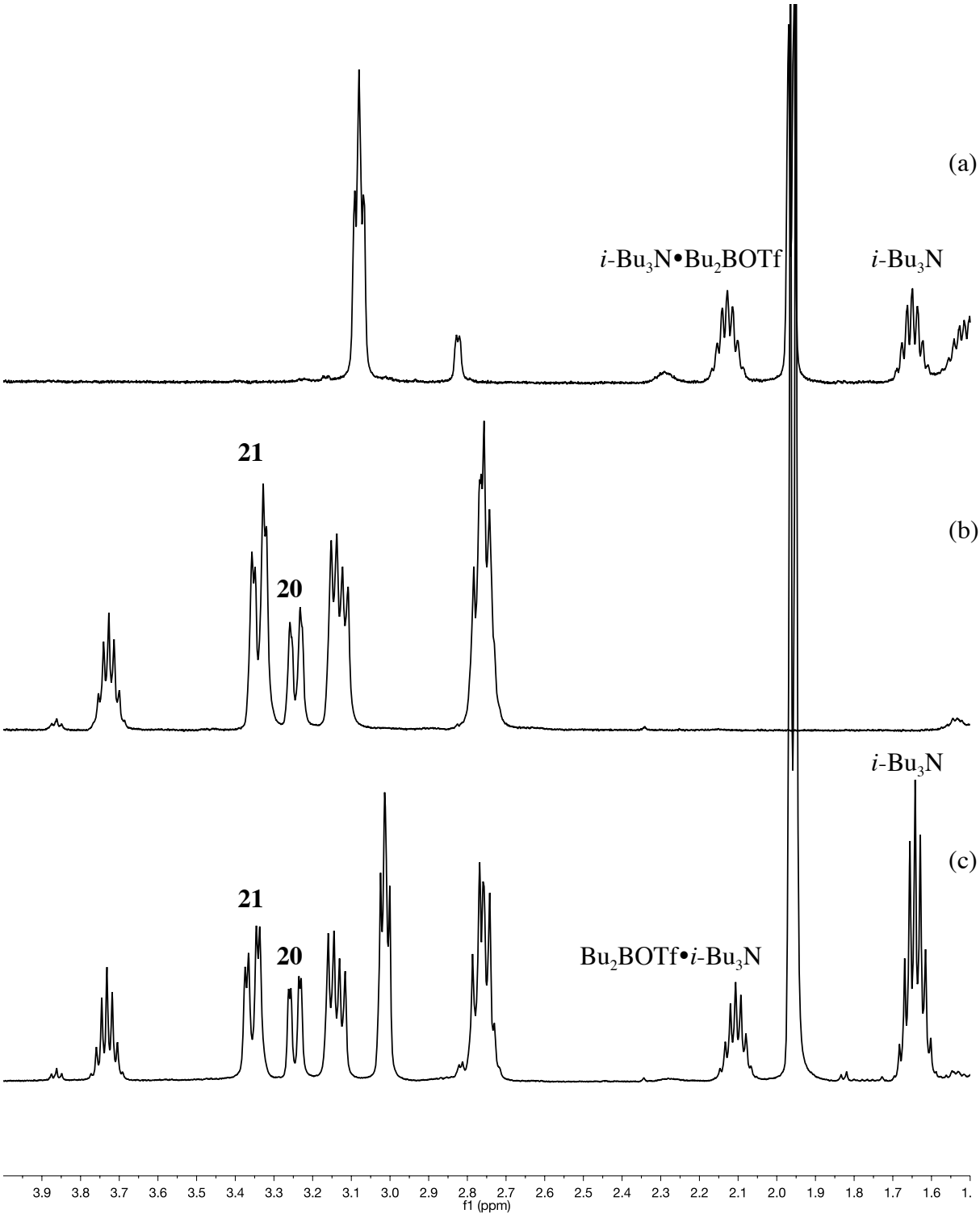

Figure S56. ^{1}H NMR spectra in $CDCl_3$ at 0 °C: (a) 0.10 M Bu_2BOTf and 0.03 M *i*-Bu_3N; (b) 0.10 M Bu_2BOTf, and 0.10 M **20**; (c) 0.10 M Bu_2BOTf, 0.05 M *i*-Bu_3N, and 0.10 M **20**.

K_{eq} = [**21**][*i*-Bu_3N] / [**20**][*i*-Bu_3N•Bu_2BOTf] = 4.

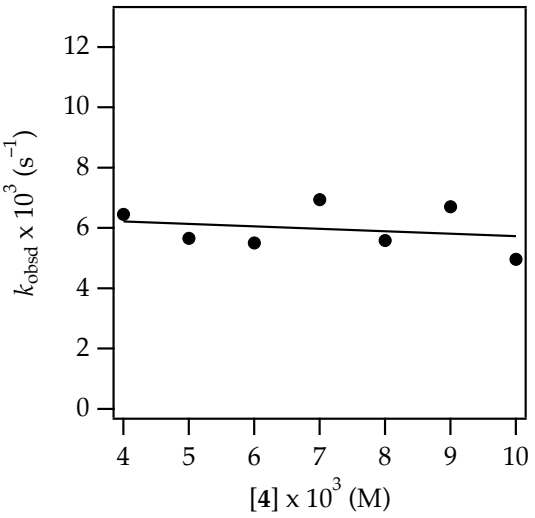

Figure S57. Plot of observed rate vs [**4**] for aldol reaction of **4** and *i*-PrCHO in $CHCl_3$ at –60 °C. $y = ax + b$, $a = -0.1 \pm 0.1$, $b = 0.006 \pm 0.001$.

[**4**] (M)	[*i*-PrCHO] (M)	k_{obsd} x 10^3 (s^{-1})
0.0040	0.10	6.46
0.0050	0.10	5.66
0.0060	0.10	4.89
0.0070	0.10	6.94
0.0080	0.10	4.61
0.0090	0.10	6.71
0.010	0.10	4.97

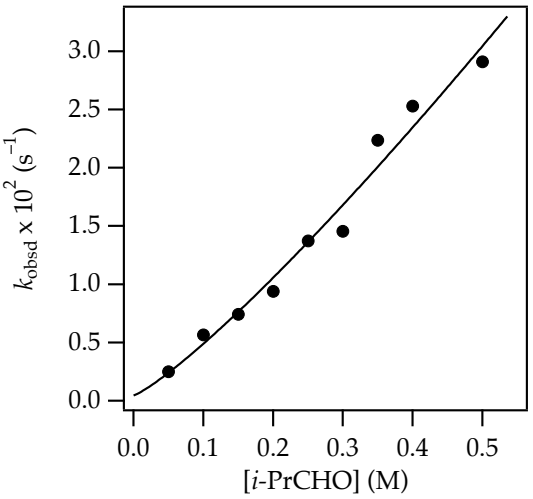

Figure S58. Plot of observed rate vs [*i*-PrCHO] for aldol reaction of **4** and *i*-PrCHO in $CHCl_3$ at –60 °C. $y = ax^b + c$, $a = 0.067 \pm 0.007$, b = 1.09 ± 0.10, c set to 0.00.

[**4**] (M)	[*i*-PrCHO] (M)	k_{obsd} x 10^2 (s^{-1})
0.0050	0.050	0.250
0.0050	0.10	0.566
0.0050	0.15	0.742
0.0050	0.20	0.940
0.0050	0.25	1.37
0.0050	0.30	1.45
0.0050	0.35	2.24
0.0050	0.40	2.53
0.0050	0.50	2.91

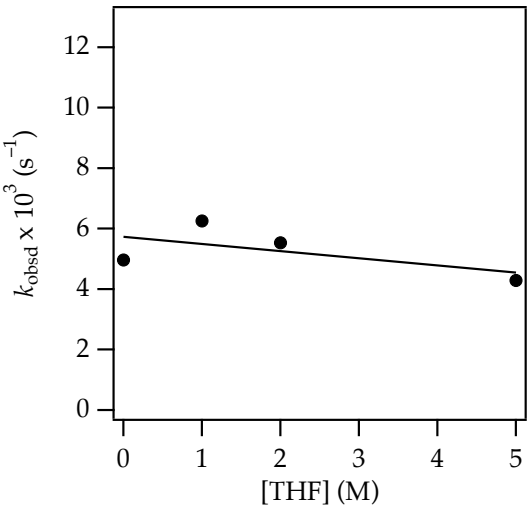

Figure S59. Plot of observed rate vs added [THF] for aldol reaction of **4** and *i*-PrCHO in $CHCl_3$ at –60 °C. $y = ax + b$, $a = -0.0002 \pm 0.0002$, $b = 0.0057 \pm 0.0006$.

[**4**] (M)	[*i*-PrCHO] (M)	[THF] (M)	k_{obsd} x 10^3 (s^{-1})
0.0050	0.10	0	4.9691
0.0050	0.10	1.0	6.2526
0.0050	0.10	2.0	5.5373
0.0050	0.10	5.0	4.2908

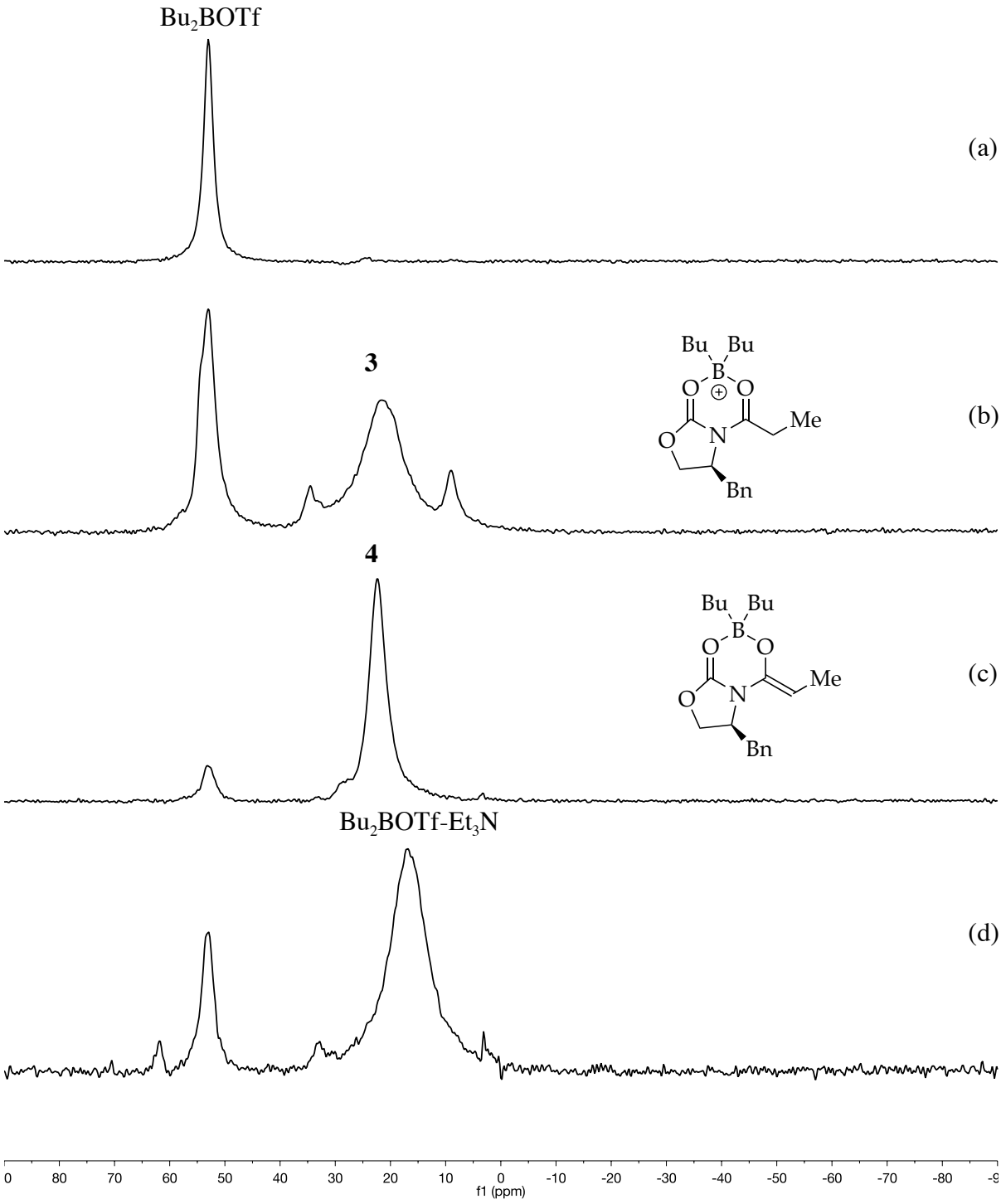

Figure S60. ^{11}B NMR spectra in $CHCl_3$ at rt: (a) 0.10 M Bu_2BOTf; (b) 0.10 M Bu_2BOTf and 0.10 M **1**; (c) 0.10 M Bu_2BOTf, 0.10 M Et_3N, and 0.10 M **1**; (d) 0.10 M Bu_2BOTf and 0.10 M Et_3N.

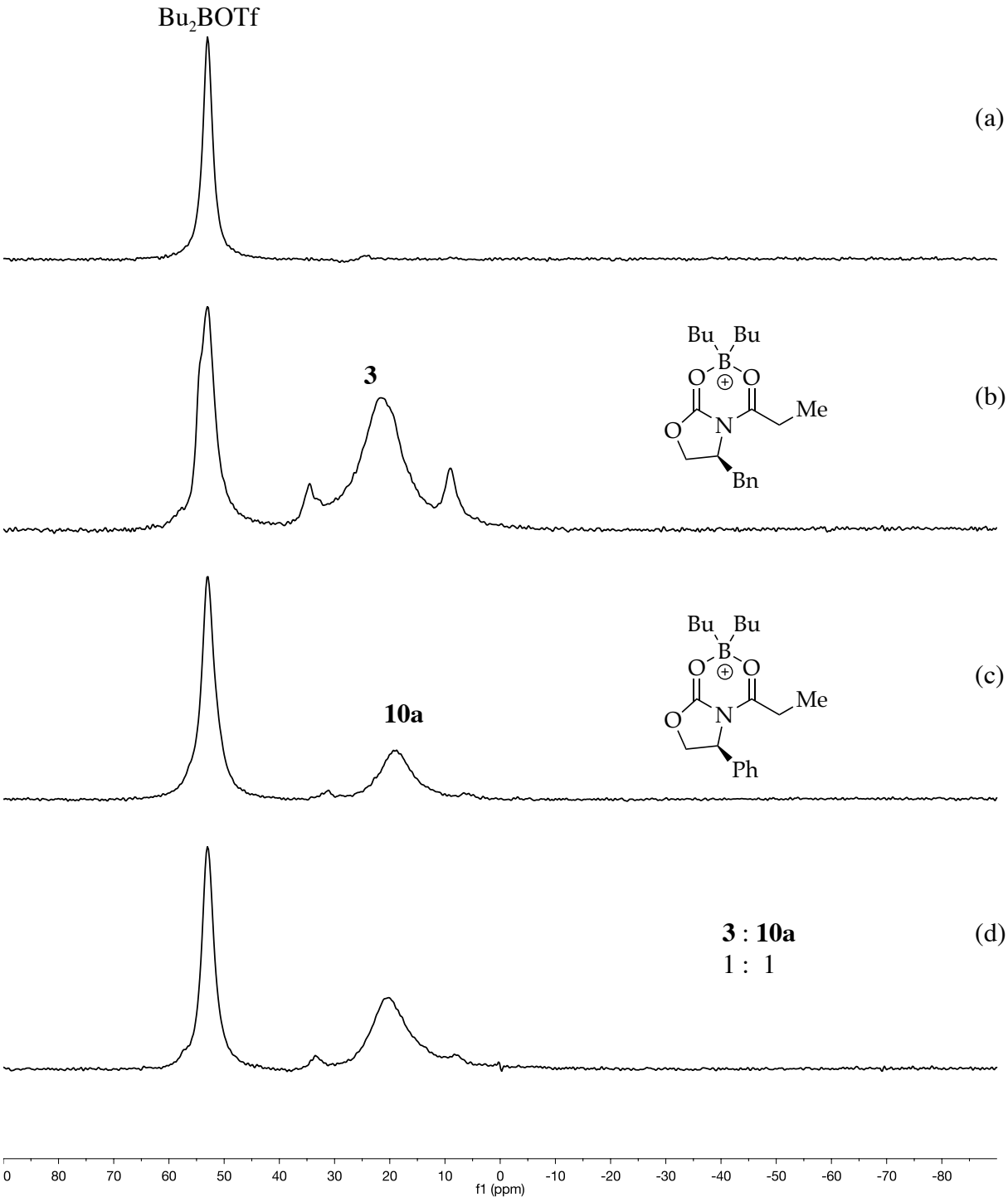

Figure S61. ^{11}B NMR spectra in $CHCl_3$ at rt: (a) 0.10 M Bu_2BOTf; (b) 0.11 M Bu_2BOTf and 0.10 M **1**; (c) 0.11 M Bu_2BOTf and 0.10 M **10**; (d) 0.11 M Bu_2BOTf, 0.050 M **1** and 0.050 M **10**.

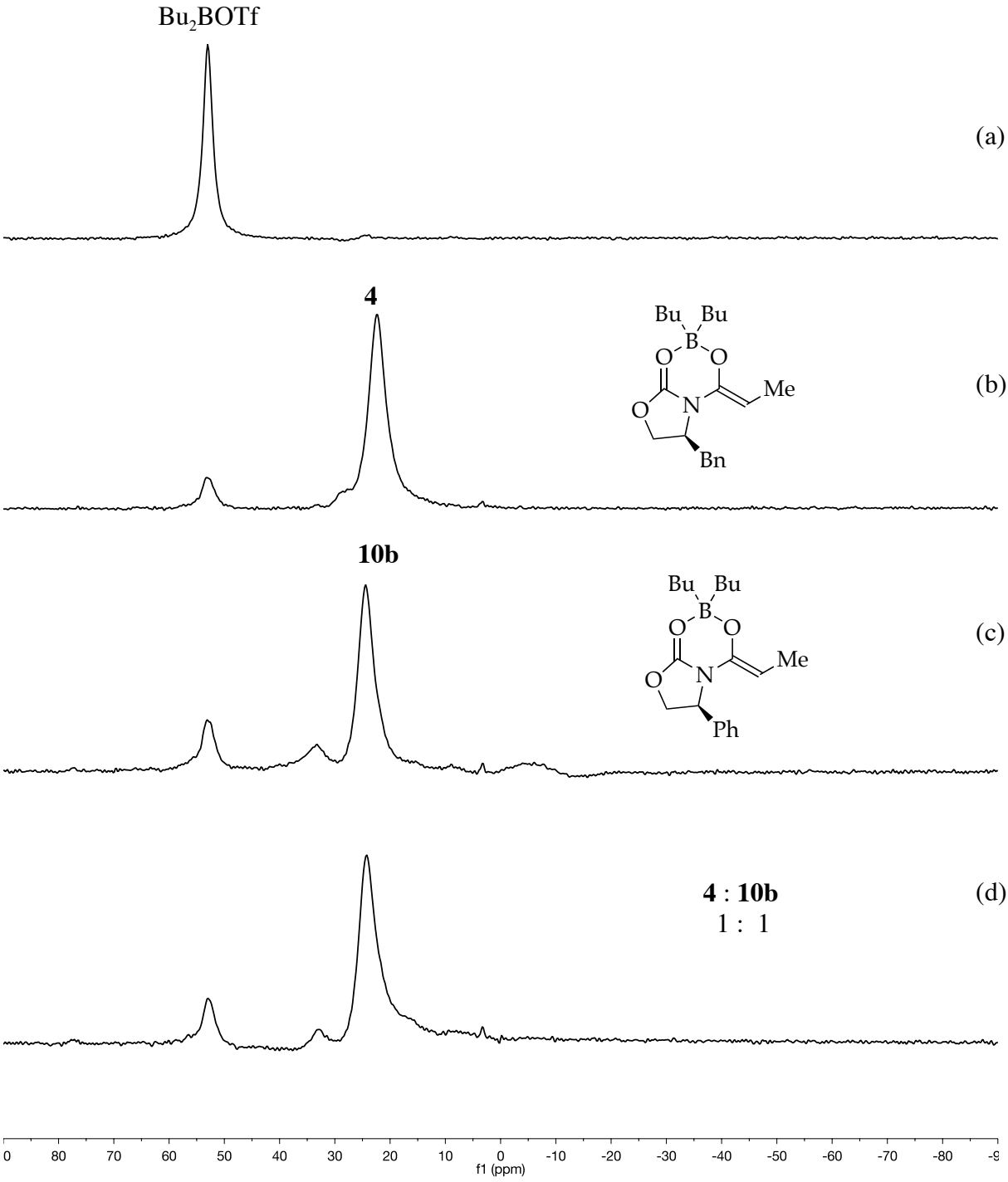

Figure S62. ^{11}B NMR spectra in $CHCl_3$ at rt: (a) 0.10 M Bu_2BOTf; (b) 0.10 M Bu_2BOTf, 0.10 M Et_3N, and 0.10 M **1**; (c) 0.10 M Bu_2BOTf, 0.10 M Et_3N, and 0.10 M **10**; (d) 0.10 M Bu_2BOTf, 0.10 M Et_3N, 0.050 M **1**, and 0.050 M **10**.

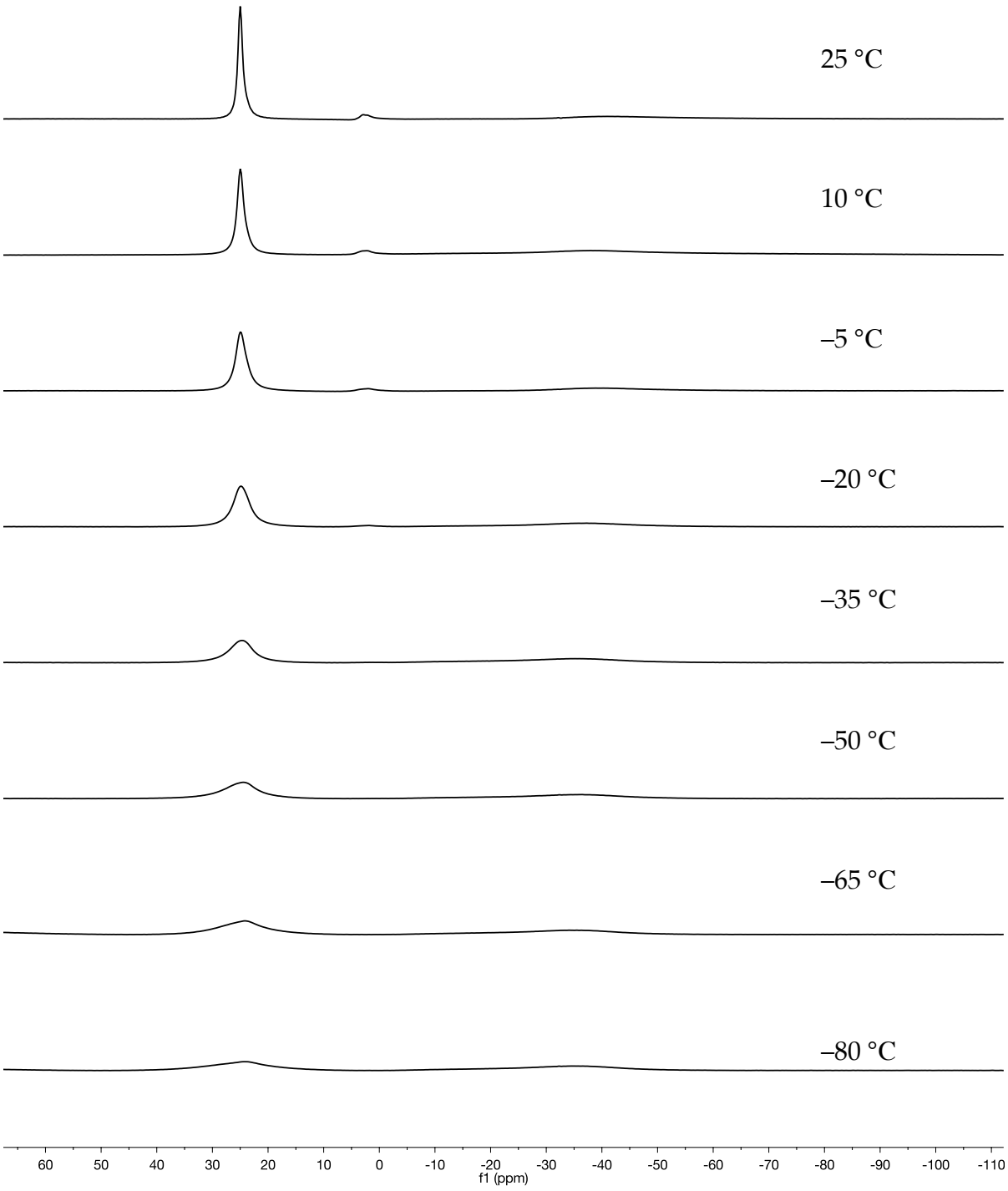

Figure S63. ^{11}B NMR spectra of 0.05 M **1**, 0.05 M **10**, 0.10 M Bu_2BOTf, and 0.10 M Et_3N in CH_2Cl_2 recorded at: (a) 25 °C; (b) 10 °C; (c) –5 °C; (d) –20 °C; (e) –35 °C; (f) –50 °C; (g) –65 °C; (h) –80 °C.

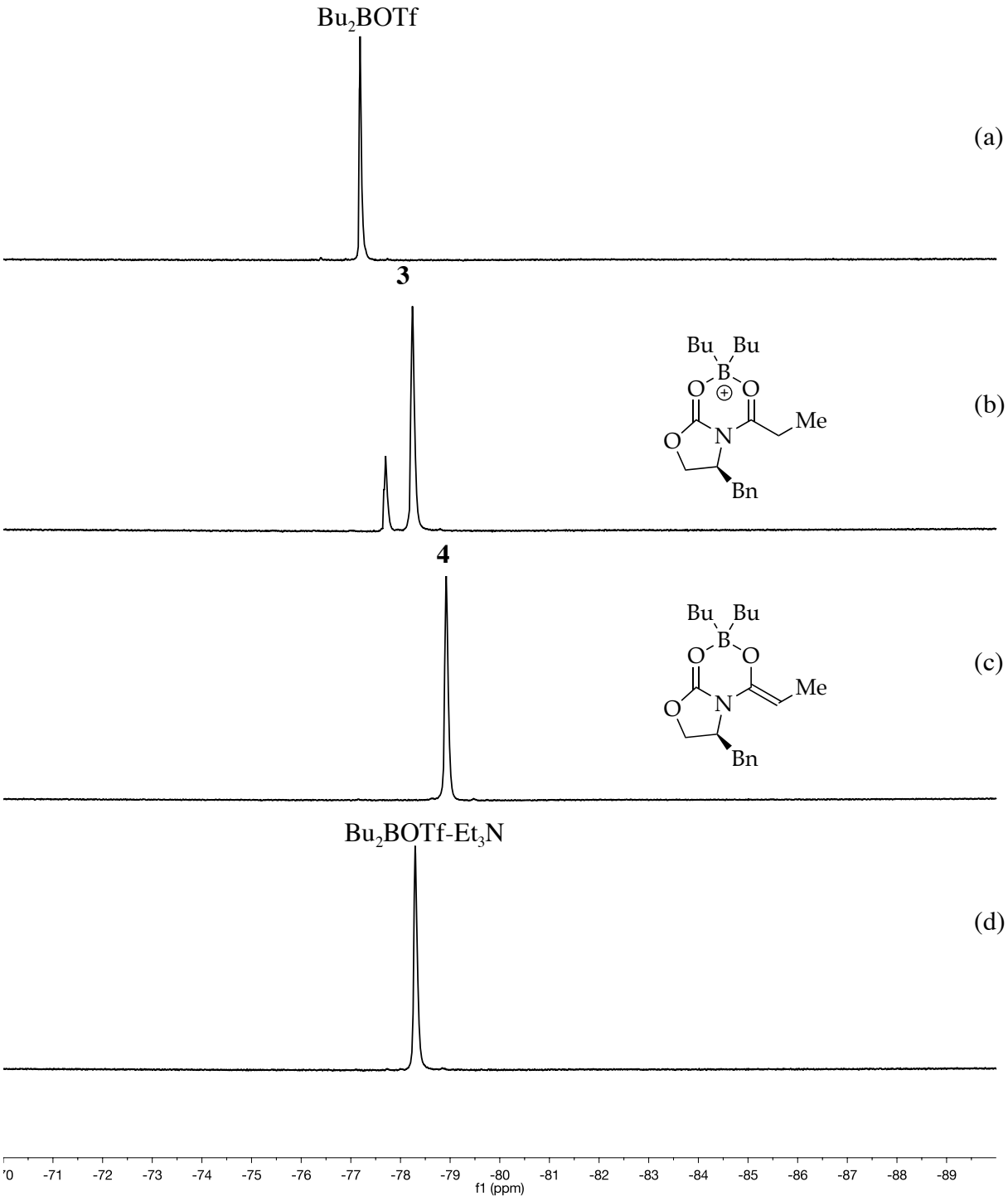

Figure S64. ^{19}F NMR spectra in $CHCl_3$ at rt: (a) 0.10 M Bu_2BOTf; (b) 0.10 M Bu_2BOTf and 0.10 M **1**; (c) 0.10 M Bu_2BOTf, 0.10 M Et_3N, and 0.10 M **1**; (d) 0.10 M Bu_2BOTf and 0.10 M Et_3N in $CHCl_3$.

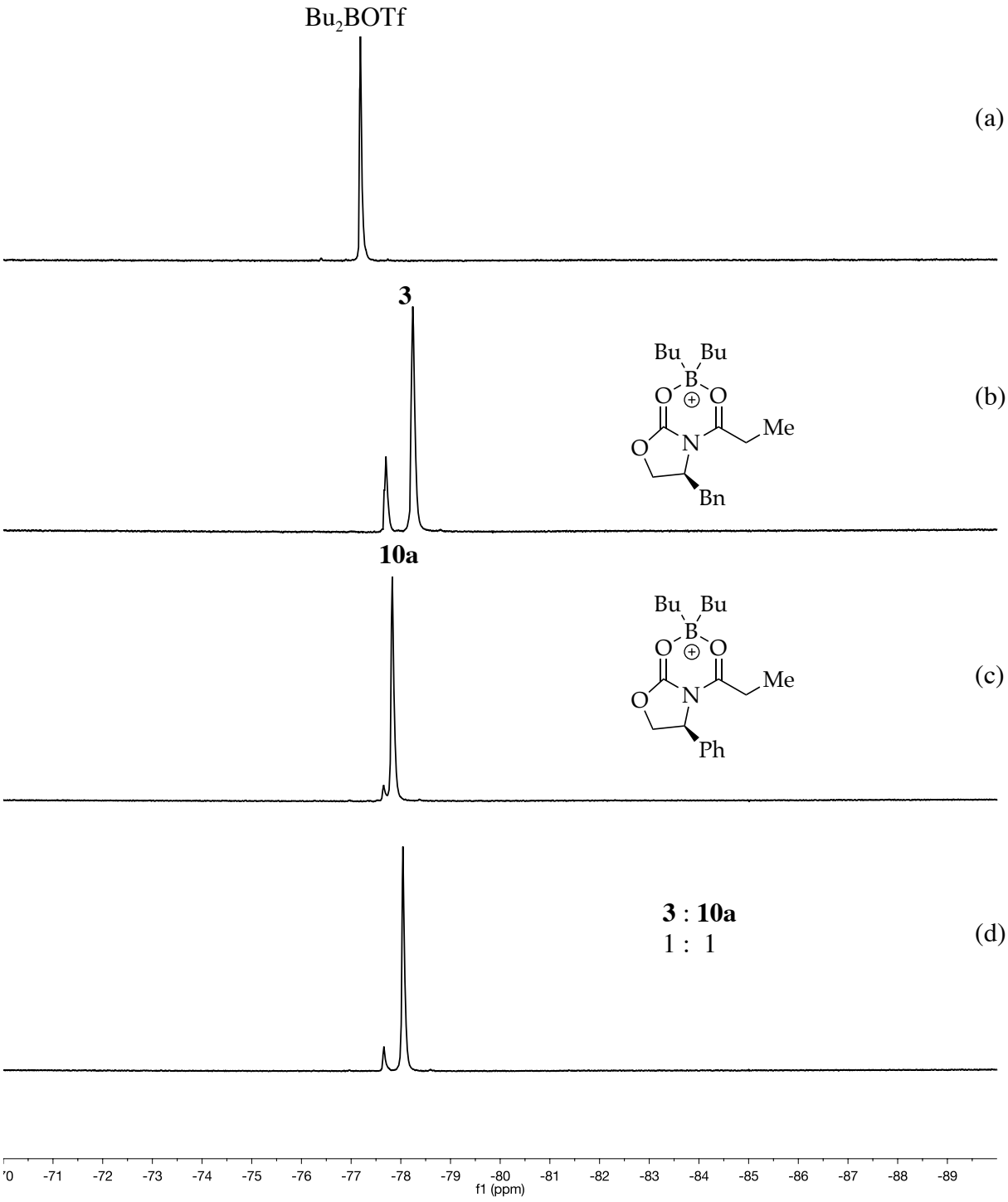

Figure S65. ^{19}F NMR spectra in $CHCl_3$ at rt: (a) 0.10 M Bu_2BOTf; (b) 0.10 M Bu_2BOTf and 0.10 M **1**; (c) 0.10 M Bu_2BOTf and 0.10 M **10**; (d) 0.10 M Bu_2BOTf, 0.050 M **1**, and 0.050 M **10**.

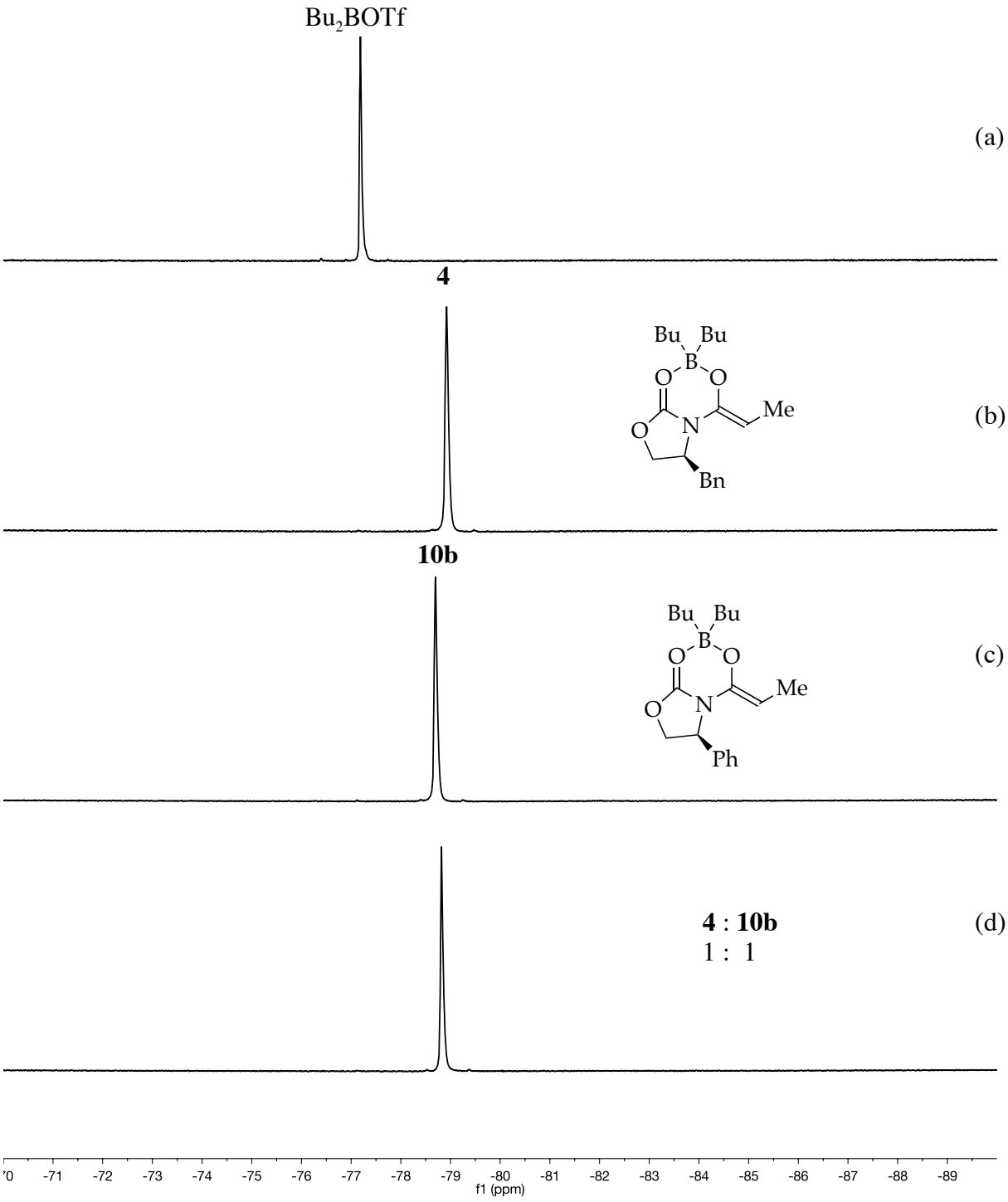

Figure S66. ^{19}F NMR spectra in $CHCl_3$ at rt: (a) 0.10 M Bu_2BOTf; (b) 0.10 M Bu_2BOTf, 0.10 M Et_3N, and 0.10 M **1**; (c) 0.10 M Bu_2BOTf, 0.10 M Et_3N, and 0.10 M **10**; (d) 0.10 M Bu_2BOTf, 0.10 M Et_3N, 0.050 M **1**, and 0.050 M **10**.

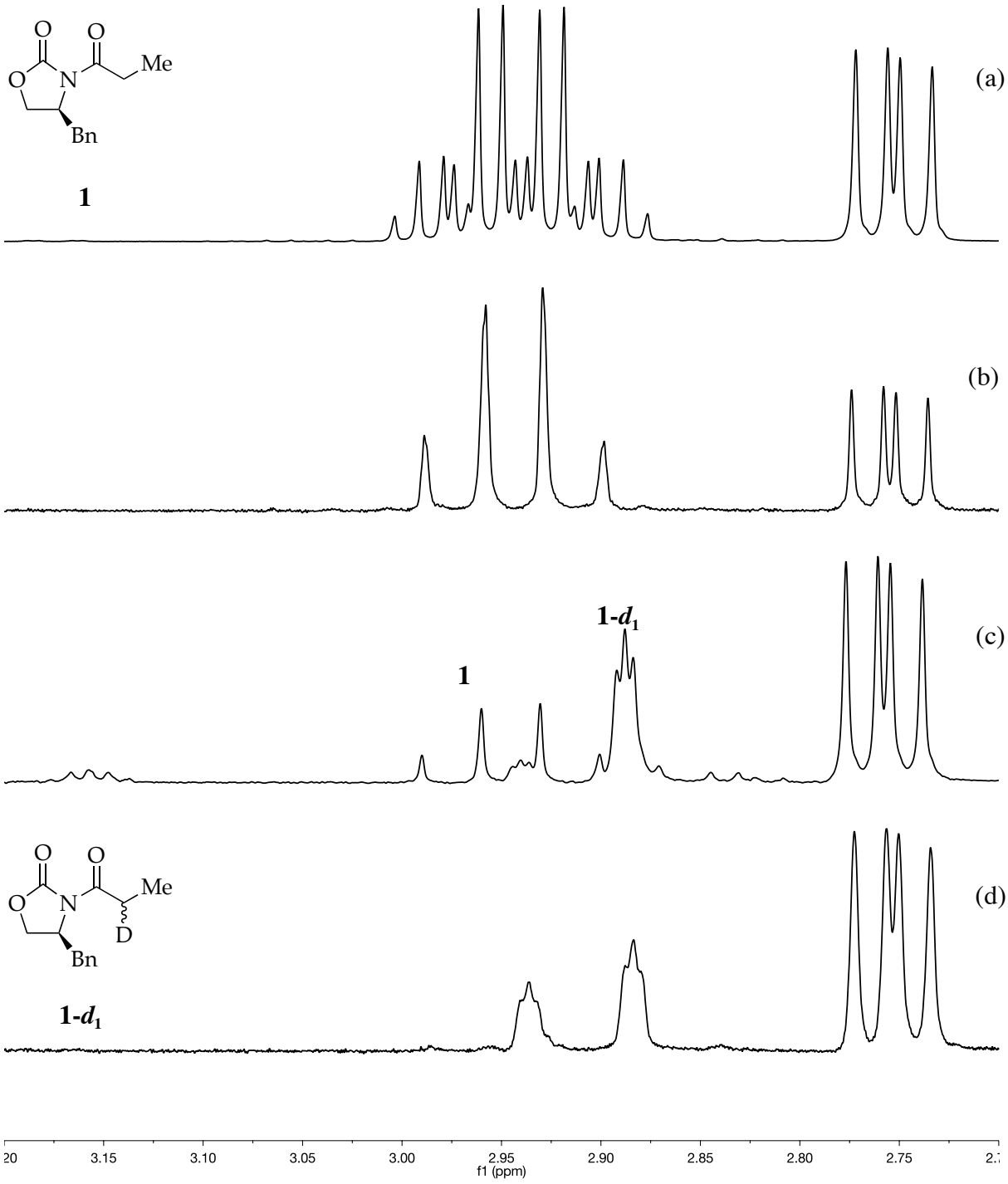

Figure S67. ^{1}H NMR spectra in $CDCl_3$ at rt: (a) 0.10 M **1**; (b) 0.10 M **1** single frequency irradiated at 1.2 ppm; (c) 0.10 M **1**-d_1 single frequency irradiated at 1.2 ppm, **1**-d_1 prepared by enolizing **1** and quenching with MeOD; (c) 0.10 M **1**-d_1 single frequency irradiated at 1.2 ppm, **1**-d_1 prepared by enolizing **1**-d_2 and quenching with MeOH.

Geometries are optimized at the B3LYP level of theory using the 6-31G(d) basis set. Energies are defined as follows: G is the sum of electronic and thermal free energies calculated at the B3LYP level of theory (T = 195 K). GMP2 is derived from an MP2 SP calculation corresponding to the DFT-optimized geometry and includes a thermal correction from the DFT calculation.

Table S1. Optimized geometries at B3LYP level of theory with 6–31G(d) basis set for **3** at –78 °C with free energies (Hartrees) and Cartesian coordinates (X, Y, Z) (Note: GMP2 includes single point MP2 corrections to B3LYP/6–31G(d) optimized structures).

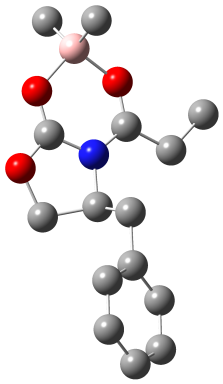

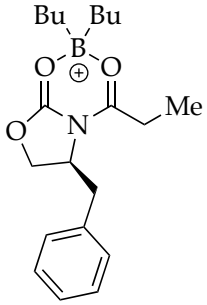

G = –889.064536
G_{MP2} = –886.2253287

C	0.00000000	0.00000000	0.00000000	C	–0.48732100	–1.41496800	0.10895100
N	0.38016100	–2.45702000	–0.11871500	C	–0.09693500	–3.75911200	–0.20012400
O	0.82970100	–4.58525800	–0.59899000	C	2.02567500	–3.83066600	–0.99729600
H	2.89179500	–4.38173500	–0.63593600	H	2.02451800	–3.79413300	–2.08831300
C	1.85930100	–2.44914500	–0.32849800	H	2.12408400	–1.64921500	–1.02250300
C	2.63961200	–2.30806200	0.99696700	H	2.34630000	–1.37073100	1.48433900
H	2.34344500	–3.12190000	1.66979600	C	4.13676100	–2.33617400	0.75902500
C	4.78360800	–1.23720700	0.17527300	C	6.15628700	–1.26957800	–0.06703000
C	6.90027700	–2.40224400	0.27289700	C	6.26759300	–3.49843700	0.85973800
C	4.89241100	–3.46555200	1.10074600	H	4.41038900	–4.31565800	1.57940900
H	6.84253200	–4.37652300	1.13824200	H	7.97005900	–2.42528800	0.08856600
H	6.64654100	–0.40897800	–0.51236400	H	4.21817600	–0.34119500	–0.07573700
O	–1.25525800	–4.11170100	0.04809200	B	–2.38877500	–3.08719400	0.63632600
O	–1.68344800	–1.66079400	0.37005600	C	–2.46566600	–3.30024300	2.20259600
H	–3.16510700	–2.58742400	2.65558100	H	–2.84581100	–4.30358300	2.42963800
H	–1.50446200	–3.19106700	2.72326000	C	–3.64863000	–3.19126100	–0.30729400
H	–4.41721000	–2.46892900	–0.00724700	H	–3.42381000	–3.01374200	–1.36633400
H	–4.10161800	–4.18689100	–0.23100800	H	0.84143800	0.12081500	0.69556400
H	0.42965100	0.12207400	–1.00530000	C	–1.08580800	1.04576800	0.26525000
H	–1.49450700	0.94735800	1.27407500	H	–0.65211700	2.04380500	0.16583600
H	–1.90830400	0.95510600	–0.44839600				

Table S2. Optimized geometries at B3LYP level of theory with 6–31G(d) basis set for **4** at –78 °C with free energies (Hartrees) and Cartesian coordinates (X, Y, Z) (Note: GMP2 includes single point MP2 corrections to B3LYP/6–31G(d) optimized structures).

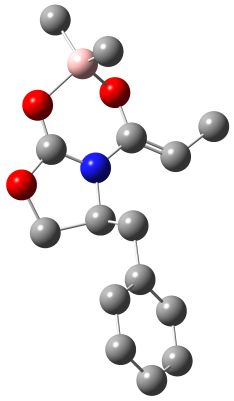

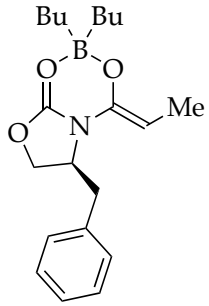

G = –888.683863
G_{MP2} = –885.8517903

C	0.00000000	0.00000000	0.00000000	H	0.86194600	–0.55053500	0.37634100
H	0.01345200	0.00976800	–1.09379900	C	–0.14084700	1.41226200	0.60276500
H	0.16546300	2.17521000	–0.11782500	C	0.61447000	1.60492700	1.93914000
H	0.26852700	2.54210700	2.38764200	H	0.32010900	0.79881800	2.62191700
C	2.11725700	1.61928000	1.75816500	C	2.75673300	2.73175300	1.19066000
C	4.13729100	2.74040100	0.99477300	C	4.90509700	1.63394600	1.36573800
C	4.28311000	0.52318600	1.93596200	C	2.89998600	0.51779800	2.12923800
H	2.42426100	–0.34640400	2.58822300	H	4.87276800	–0.33878400	2.23617300
H	5.98125200	1.64148400	1.21669500	H	4.61491500	3.61354900	0.55845700
H	2.17017300	3.60467200	0.91063600	N	–1.59755100	1.45758700	0.78049100
C	–2.11284100	0.21244300	0.76572400	O	–1.19809100	–0.70368800	0.42389200
O	–3.27853100	–0.12083700	1.04827000	B	–4.22791400	1.09766000	1.72922100
O	–3.71868600	2.32173200	1.04747100	C	–2.42492900	2.61558900	0.97813700
C	–1.90445800	3.85546700	0.99084200	H	–0.83758200	3.98140000	0.83625400
C	–2.73962600	5.08872000	1.17369100	H	–2.38226500	5.69353000	2.01823100
H	–2.70883200	5.73440100	0.28481000	H	–3.78271400	4.82299900	1.36061400
C	–3.88860100	1.03585000	3.29955100	H	–2.83148200	1.22726000	3.53786100
H	–4.47126200	1.79557300	3.83807900	H	–4.14974800	0.06399300	3.73727800
C	–5.71782500	0.78280600	1.25521300	H	–6.41363400	1.53470600	1.65126700
H	–5.81954500	0.79223300	0.16234300	H	–6.06358500	–0.19472000	1.61472200

Table S3. Optimized geometries at B3LYP level of theory with 6–31G(d) basis set for **6** at –78 °C with free energies (Hartrees) and Cartesian coordinates (X, Y, Z) (Note: GMP2 includes single point MP2 corrections to B3LYP/6–31G(d) optimized structures).

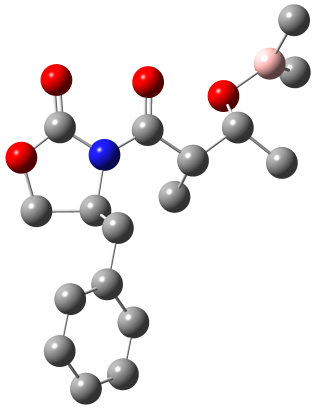

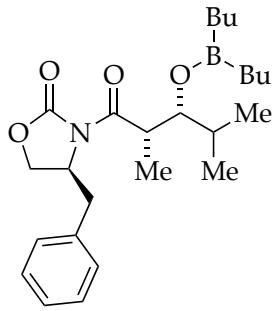

G = –1042.491306
G_{MP2} = –1039.186804

C	0.00000000	0.00000000	0.00000000	C	0.06915800	1.46054400	–0.46807000
N	1.30876700	2.11094400	–0.28573900	C	1.48947800	3.50414400	–0.48621800
O	2.76919300	3.81322000	–0.10796700	C	3.37166200	2.68777900	0.54621800
H	4.43538600	2.67399700	0.30535600	H	3.24322800	2.79442800	1.62972000
C	2.60730800	1.47594800	–0.00349700	H	2.51008900	0.70362000	0.76152800
C	3.25000700	0.88215300	–1.28220600	H	2.53739800	0.18232400	–1.73515900
H	3.39145900	1.69563000	–2.00346100	C	4.56517400	0.18283800	–1.01050900
C	4.58811300	–1.08195200	–0.40399900	C	5.79571700	–1.72108100	–0.12515600
C	7.00599700	–1.10450200	–0.45070400	C	6.99823900	0.15083800	–1.05913800
C	5.78660700	0.78768900	–1.33588700	H	5.78883200	1.76102500	–1.82177100
H	7.93427300	0.63502300	–1.32404500	H	7.94746700	–1.60271300	–0.23663900
H	5.79217300	–2.70284200	0.34080500	H	3.65076100	–1.57727100	–0.15704000
O	0.71598700	4.31475500	–0.90533900	O	–0.89593100	2.04448300	–0.91415100
H	0.93252000	–0.50992700	–0.26964100	C	–1.14146400	–0.74982300	–0.73502000
H	–1.14844900	–0.41600400	–1.77783400	C	–0.95144200	–2.26732100	–0.69811800
H	–1.76965200	–2.75673300	–1.23595700	H	–0.00783400	–2.55893100	–1.17412600
H	–0.95613400	–2.64310200	0.33036800	O	–2.38595500	–0.43657100	–0.11745000
B	–3.48556000	0.06750600	–0.76120500	C	–4.72066700	0.40330500	0.16714500
H	–4.98767800	1.46539800	0.06868000	H	–5.61250800	–0.15570900	–0.15020200
H	–4.54006200	0.19293600	1.22661700	C	–3.53355400	0.29834800	–2.32974900
H	–4.54326900	0.53583600	–2.68163400	H	–2.88615500	1.14629400	–2.59231400
H	–3.17469200	–0.56230600	–2.91073600	C	–0.15699100	–0.03881500	1.53578500
H	–1.07736300	0.46828300	1.83185300	H	–0.20974400	–1.07224000	1.89180300
H	0.68517200	0.44783100	2.03874700				

Table S4. Optimized geometries at B3LYP level of theory with 6–31G(d) basis set for **6** dimer at –78 °C with free energies (Hartrees) and Cartesian coordinates (X, Y, Z) (Note: GMP2 includes single point MP2 corrections to B3LYP/6–31G(d) optimized structures).

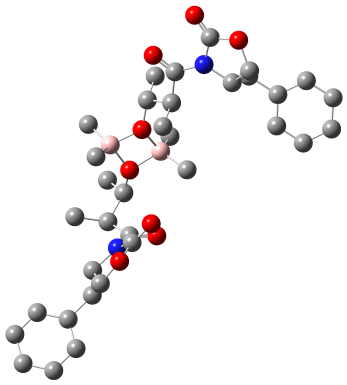

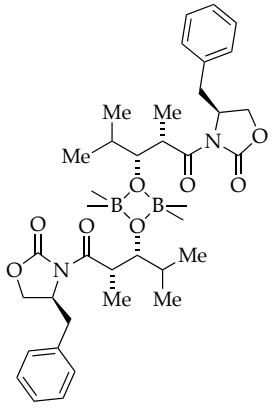

G = –2084.931299
G_{MP2} = –2078.355277

C	0.00000000	0.00000000	0.00000000	B	–0.18424700	–1.53080300	0.42597700
O	0.20300400	–2.55330800	–0.70750100	C	1.44412400	–3.06769100	–1.23151600
C	2.16192000	–1.96063300	–2.04084600	C	3.41604400	–2.55487100	–2.69367600
N	4.51433300	–1.69178400	–2.85493500	C	4.62469000	–0.29120200	–2.40790100
C	5.67602300	0.21093900	–3.40766900	H	6.33678400	0.97304900	–2.99332900
H	5.21715700	0.58420400	–4.33047600	O	6.45859700	–0.95343800	–3.71343100
C	5.71394900	–2.08233600	–3.50734000	O	6.07763900	–3.17729400	–3.82420800
H	3.67960300	0.23753100	–2.54545400	C	5.09092300	–0.18355200	–0.93517200
H	4.38104600	–0.73339300	–0.30592500	H	6.05512700	–0.69749000	–0.84355200
C	5.21251800	1.24955200	–0.45979000	C	6.46857300	1.84986700	–0.29920800
C	6.58066400	3.17967700	0.11207300	C	5.43355700	3.93093100	0.36866200
C	4.17548300	3.34357700	0.21640400	C	4.06729300	2.01484100	–0.19309300
H	3.08059400	1.56767600	–0.29712200	H	3.27628100	3.91816100	0.42150200
H	5.51787300	4.96541500	0.69018200	H	7.56440600	3.62494600	0.23454400
H	7.36767800	1.26692000	–0.48747700	O	3.42549400	–3.69345700	–3.11764300
H	2.42377000	–1.15705600	–1.34659500	C	1.28241800	–1.38478700	–3.17170700
H	0.36268200	–0.95656400	–2.77119300	H	1.81094300	–0.59857400	–3.72257000
H	1.02267500	–2.17338200	–3.88527500	H	1.15765800	–3.85769400	–1.92959600
C	2.31277900	–3.67103800	–0.12836300	H	2.68985100	–2.90461600	0.55627500
H	1.73740300	–4.39438800	0.45477600	H	3.16221900	–4.19327100	–0.57627000
B	–1.20376300	–3.23723400	–0.80804700	O	–1.66668900	–2.06149700	0.17140800
C	–2.74904200	–1.83439500	1.09640500	H	–2.44941700	–0.93492400	1.63721200
C	–2.93610200	–2.97027500	2.10242500	H	–3.19886100	–3.91863800	1.62984000
H	–2.01695600	–3.12171400	2.67172700	H	–3.73255600	–2.70435200	2.80760400
C	–4.06994200	–1.45516700	0.36073700	H	–4.74813500	–1.17743100	1.18218700
C	–4.71754100	–2.59969500	–0.42934000	H	–5.78404700	–2.42288100	–0.59219600
H	–4.23977100	–2.74421100	–1.39871200	H	–4.64174900	–3.53885400	0.12434800
C	–3.81522000	–0.14309500	–0.41059200	O	–3.11886800	0.72710600	0.06171800
N	–4.37596800	0.02953000	–1.71030000	C	–5.78156800	–0.14699400	–2.11525500
C	–5.81576900	0.74638600	–3.37548800	H	–6.37113500	0.29790700	–4.20010900

H	–6.23390800	1.73580100 –3.15690000	O	–4.45066300	0.90278800 –3.77830900
C	–3.61697000	0.61490400 –2.73908900	O	–2.42847100	0.78638300 –2.77986300
H	–5.97144700	–1.18894500 –2.39438300	C	–6.80046600	0.29633300 –1.04716600
H	–6.68127600	–0.32585600 –0.15212900	H	–6.56611800	1.32574800 –0.75180800
C	–8.23045900	0.20356700 –1.54335200	C	–8.85433000	–1.04363900 –1.69678400
C	–10.1611100	–1.13621500 –2.17464300	C	–10.8698840	0.02097700 –2.50510600
C	–10.2637160	1.26789700 –2.35114700	C	–8.95446900	1.35649300 –1.87389600
H	–8.49406000	2.33359500 –1.74582300	H	–10.8096150	2.17446400 –2.59787100
H	–11.8892210	–0.04963700 –2.87428500	H	–10.6279940	–2.11144100 –2.28319500
H	–8.31701800	–1.95175400 –1.43041000	C	–1.78316100	–3.10618800 –2.29884400
H	–1.95920400	–2.06787400 –2.60535900	H	–1.06155100	–3.52920900 –3.01257300
H	–2.70784500	–3.67618200 –2.45437200	C	–1.22600200	–4.70924300 –0.16605200
H	–0.62205400	–5.39158700 –0.78175000	H	–0.83712300	–4.76842200 0.85736500
H	–2.23707900	–5.13872000 –0.16198300	C	0.36254000	–1.91099400 1.89117700
H	1.40220500	–1.58269700 2.02242400	H	–0.20807300	–1.37559600 2.66381300
H	0.32613400	–2.97911100 2.13691600	H	–0.45234700	0.25595000 –0.96320100
H	–0.45040600	0.66988400 0.74353700	H	1.06752800	0.26656300 –0.03716700

Geometries are optimized at the B3LYP level of theory using the 6-31G(d) basis set. Energies are defined as follows: G is the sum of electronic and thermal free energies calculated at the B3LYP level of theory (T = 195 K). GMP2 is derived from an MP2 SP calculation corresponding to the DFT-optimized geometry and includes a thermal correction from the DFT calculation.

Table S5. Optimized geometries at B3LYP level of theory with 6–31G(d) basis set for **5a** at –78 °C with free energies (Hartrees) and Cartesian coordinates (X, Y, Z) (Note: GMP2 includes single point MP2 corrections to B3LYP/6–31G(d) optimized structures).

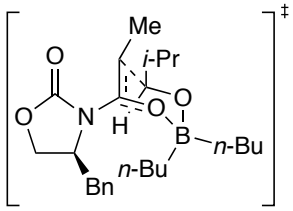

5

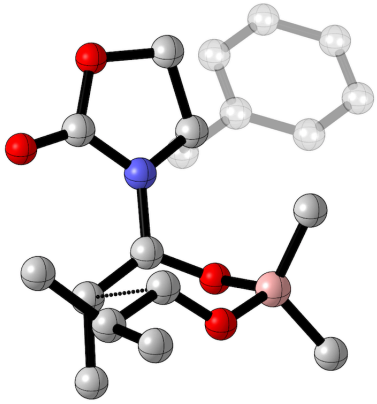

G = –1121.025373
G_{MP2} = –1117.4267

C	0.00000000	0.00000000	0.00000000
C	2.17546600	-0.46286400	1.18951100
H	3.33829400	1.06690800	2.03864900
H	3.95071000	-1.92044700	2.65555500
H	4.92933500	-0.51966800	3.15581300
B	2.60353000	-2.63926500	0.01775100
C	4.40294200	-0.92231500	-0.07898300
H	6.07452200	-0.70364200	1.19477400
H	7.79184600	-0.92852600	-0.58748700
H	6.67308000	-2.31175800	-0.59134000
H	5.77020300	1.32956600	-1.10551900
H	5.21516100	1.63234500	0.54450300
C	2.08662900	-2.40680600	-1.49579600
H	1.05411300	-2.76542300	-1.60615700
C	2.57357000	-4.14894100	0.54648000
H	1.54307600	-4.52520200	0.59880400
C	1.57111700	1.75054800	0.17819000
C	-0.33053700	1.15906700	-0.95209700
H	-0.08697300	0.91849400	-1.99287200
C	-0.95249300	-0.11605100	1.21362200
H	-1.00860300	0.85826100	1.71471000
C	-3.41568900	0.30290100	0.75293000
C	-4.88604800	-1.47182600	0.01951600
N	1.35954500	0.39397900	0.40479600
C	3.20126000	-0.00479200	1.97501300
C	3.90854100	-0.87643100	2.97353800
H	3.38884900	-0.84759400	3.94184900
O	1.88995200	-1.74484200	1.06504100
O	4.10334500	-2.13400800	0.13753500
C	5.80903000	-0.44301100	0.16292700
C	6.75689700	-1.23646300	-0.77015500
H	6.52911200	-1.04140700	-1.82472400
C	5.93805500	1.07010400	-0.05289700
H	6.94609400	1.40530100	0.21189700
H	3.76054600	-0.32202200	-0.73014500
H	2.68907200	-2.99314900	-2.20279700
H	2.10018100	-1.36729900	-1.85380400
H	3.00484300	-4.25176000	1.55086900
H	3.12478100	-4.82534200	-0.12022000
O	0.51577100	2.24485000	-0.52597000
H	-1.36904800	1.48694700	-0.88961400
O	2.51583100	2.43095800	0.50861700
H	-0.50238900	-0.82263700	1.91930200
C	-2.33529100	-0.58686700	0.81775500
C	-4.68194900	-0.13384600	0.35738800
C	-3.81821100	-2.37034400	0.08375300

C	-2.55561500	-1.93098700	0.48032000
H	-3.97018000	-3.41614100	-0.17001000
H	-5.50796800	0.57141100	0.31827200
H	0.02936600	-0.94941400	-0.53278900
H	-1.73114200	-2.63856000	0.53875800
H	-5.87076700	-1.81449400	-0.28653200
H	-3.26726900	1.34536400	1.02719200

Table S6. Optimized geometries at B3LYP level of theory with 6–31G(d) basis set for **5b** at –78 °C with free energies (Hartrees) and Cartesian coordinates (X, Y, Z) (Note: GMP2 includes single point MP2 corrections to B3LYP/6–31G(d) optimized structures).

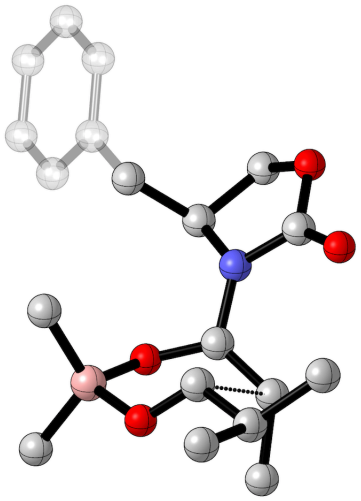

G = –1121.019933
G_{MP2} = –1117.419194

B	0.00000000	0.00000000	0.00000000
H	1.67706900	-0.50908600	-1.41753400
H	0.77150400	0.89472800	-1.98242900
H	-0.68060200	-2.14045500	0.16554800
H	-0.67834000	-1.30832600	1.72741700
C	-1.65175800	1.78077700	-0.55368100
C	-3.05081000	2.32651200	-0.61795600
C	-3.07363100	3.82556200	-0.93850300
H	-2.68319000	4.01554700	-1.94555600
C	-3.83529800	1.50359500	-1.67134900
H	-4.87045100	1.85846100	-1.71194500
O	0.70311000	1.01731400	0.93923400
N	1.35750900	3.18746500	0.53038400
O	0.05367200	5.01323800	-0.13126500
C	3.31604600	4.37813200	0.73890200
H	3.01081700	2.36843200	1.55073700
H	2.82189900	1.23613500	-0.67708800
C	4.86083400	1.87715800	-0.42790500
C	6.65960400	0.61194800	0.61515500
C	7.18595400	2.34475400	-0.97883100
H	5.50206500	3.37442000	-1.83964100
H	8.66772500	1.14288900	0.02766400
H	4.56721000	0.28586700	0.99864800
H	3.40978600	4.71274300	1.77842100
H	-0.87584000	3.82928300	1.72713700
H	-2.70322900	2.16208500	2.39293400
H	-1.42360300	2.09918400	3.59674800
C	0.67192100	-0.07062900	-1.46619200
H	0.08412700	-0.72633900	-2.12313600
C	-0.14606500	-1.39629700	0.77088600
H	0.84267400	-1.81906400	0.99355500
O	-1.46059400	0.59314900	-0.16816800
H	-0.86048300	2.30846300	-1.09387100
H	-3.51910500	2.13787700	0.35629500
H	-2.46373300	4.40194700	-0.23954000
H	-4.10218600	4.19963900	-0.90556400
H	-3.83747700	0.43990200	-1.41843700
H	-3.39968800	1.62255600	-2.67031400
C	0.38721800	2.28933000	1.06687500
C	1.11320300	4.49961800	0.14844800
O	2.29913400	5.16945500	0.09345500
C	2.80627200	2.92979200	0.63552200
C	3.38213700	2.16705100	-0.57663900
H	3.19814000	2.75902100	-1.48183600
C	5.29995100	0.87384900	0.44963600
C	7.60820500	1.34879100	-0.09806700
C	5.82323500	2.60499000	-1.14042800
H	7.91533900	2.91786600	-1.54526300
H	6.97885500	-0.17260400	1.29623100
H	4.25984000	4.54252300	0.21801800
C	-0.74654100	2.75419200	1.67710500
C	-1.64413500	1.91140200	2.53611000
H	-1.51156000	0.84414800	2.35479300

Reference S1. Gaussian 03, Revision B.04, Frisch, M. J.; Trucks, G. W.; Schlegel, H. B.; Scuseria, G. E.; Robb, M. A.; Cheeseman, J. R.; Montgomery, Jr., J. A.; Vreven, T.; Kudin, K. N.; Burant, J. C.; Millam, J. M.; Iyengar, S. S.; Tomasi, J.; Barone, V.; Mennucci, B.; Cossi, M.; Scalmani, G.; Rega, N.; Petersson, G. A.; Nakatsuji, H.; Hada, M.; Ehara, M.; Toyota, K.; Fukuda, R.; Hasegawa, J.; Ishida, M.; Nakajima, T.; Honda, Y.; Kitao, O.; Nakai, H.; Klene, M.; Li, X.; Knox, J. E.; Hratchian, H. P.; Cross, J. B.; Bakken, V.; Adamo, C.; Jaramillo, J.; Gomperts, R.; Stratmann, R. E.; Yazyev, O.; Austin, A. J.; Cammi, R.; Pomelli, C.; Ochterski, J. W.; Ayala, P. Y.; Morokuma, K.; Voth, G. A.; Salvador, P.; Dannenberg, J. J.; Zakrzewski, V. G.; Dapprich, S.;Daniels, A. D.; Strain, M. C.; Farkas, O.; Malick, D. K.; Rabuck, A. D.; Raghavachari, K.; Foresman, J. B.; Ortiz, J. V.; Cui, Q.; Baboul, A. G.; Clifford, S.; Cioslowski, J.; Stefanov, B. B.; Liu, G.; Liashenko, A.; Piskorz, P.; Komaromi, I.; Martin, R. L.; Fox, D. J.; Keith, T.; Al-Laham, M. A.; Peng, C. Y.; Nanayakkara, A.; Challacombe, M.; Gill, P. M. W.; Johnson, B.; Chen, W.; Wong, M. W.; Gonzalez, C.; and Pople, J. A. Gaussian, Inc., Wallingford CT, 2004.